Supplementary Information for

Rational guide RNA engineering for small-molecule control of CRISPR/Cas9 and gene editing.

Xingyu Liu, Wei Xiong, Qianqian Qi, Yutong Zhang, Huimin Ji, Shuangyu Cui, Jing An, Xiaoming Sun, Hao Yin, Tian Tian*, Xiang Zhou

Tian Tian
Email: ttian@whu.edu.cn

This PDF file includes:

Supplementary text

Chemical synthesis.

All reactions in anhydrous solvents were performed in flame-dried glassware under a nitrogen (N_2) atmosphere. Unless otherwise indicated, commercially available reagents were used without further purification. Chromatographic purification was performed on silica gel (100-200 mesh). Analytical thin layer chromatography (TLC) was performed on silica gel 60-F_{254} (Yantai, China) using UV-detection at 230 nm. ^{1}H NMR and ^{13}C NMR were recorded on 400 MHz ^{1}H (101 MHz. ^{13}C) spectrometer in deuterochloroform ($CDCl_3$). The peaks around δ 7.26 (^{1}H NMR) and 77.16 (^{13}C NMR) correspond to $CDCl_3$. Multiplicities are indicated as follows: s (singlet), d (doublet), t (triplet), m (multiplet), dd (doublet of doublets), etc. Coupling constants (*J*) are given in hertz. Chemical shifts (δ) are reported in parts per million relative to TMS as an internal standard. The ESI-HRMS was performed on a Bruker Bio TOF IIIQ (quadrupole time of flight) mass spectrometer.

The NMR spectra of the selected synthesized compounds are given in the appendix sections (**Appendix A**), and HRMS spectra of the tested compounds are also given (**Appendix B**).

The synthesis of NCD

The **NCD** was synthesized according to the Scheme 1.

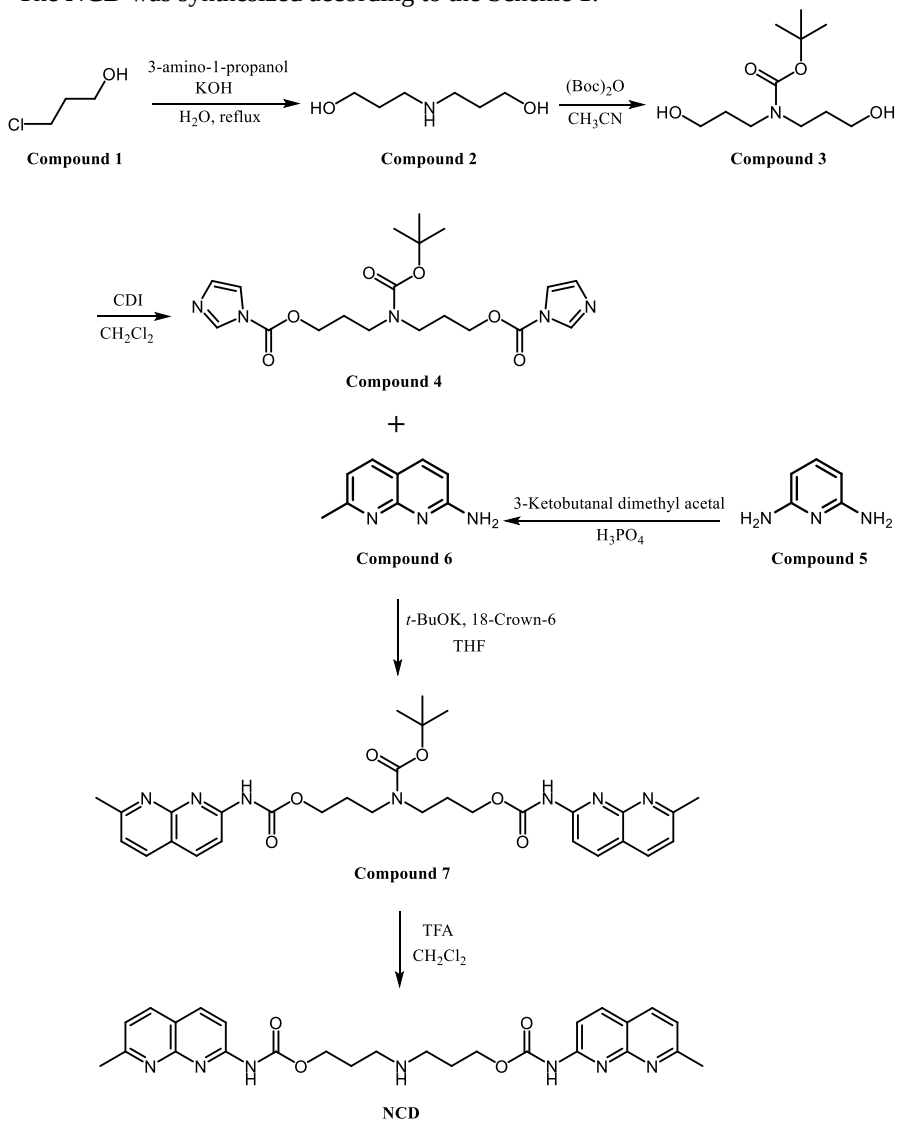

Scheme 1. The synthetic route for **NCD**

3,3'-azanediylbis(propan-1-ol) (Compound 2)[1]

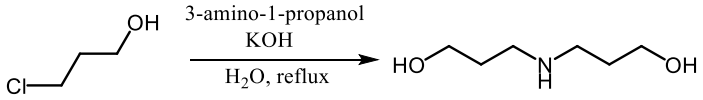

Compound 1 **Compound 2**

3-Chloro-1-propanol (Compound **1**, 4.72 g, 50 mmol) and 3-amino-1-propanol (7.51 g, 100 mmol) were dissolved in water (30 mL), and the reaction mixture was refluxed for 24 hr. After cooling to room temperature, KOH (2.8 g, 50 mmol) was added and the resulting mixture was filtered. Subsequently, the filtrate was concentrated in vacuo to give the crude product as a yellow oil. The desired product (compound **2**, Dipropanolamine) was obtained by distillation (180 °C, 1 mbar) as a colorless oil (2.66 g, 40%).
^{1}H NMR (400 MHz, $CDCl_3$) δ 3.79-3.74 (m, 4H), 2.82 (t, *J* = 6.2 Hz, 4H), 1.75-1.67 (m, 4H).
^{13}C NMR (101 MHz, $CDCl_3$) δ 62.8, 48.5, 31.4.
HRMS (ESI) m/z calcd for $C_6H_{16}NO_2$ [$(M+H)^+$] 134.1176, found 134.1175.

Bis-(3-hydroxypropyl)-carbamic acid *tert*-butyl ester (Compound **3)**[2]

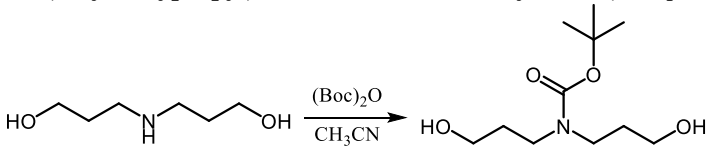

Compound 2 **Compound 3**

Compound **2** (2.0 g, 15 mmol) was dissolved in acetonitrile (60 mL) in a dried flask under argon atmosphere. Di-*tert*-butyl-dicarbonate (4.0 g, 18.4 mmol) was separately dissolved in acetonitrile (40 mL) and added dropwise via syringe to the reaction flask over 10 min. After 3 hr, the solution was concentrated in vacuo to yield a pale yellow oil. Then the crude product was purified by column chromatography on silica gel (CH_2Cl_2/MeOH=10/1) to give product (compound **3**) as a colorless oil (3.2 g, 92 %).
^{1}H NMR (400 MHz, $CDCl_3$) δ 3.50-3.72 (m, 4H), 321-3.45 (m, 4H), 1.64-1.82 (m, 4H), 1.48 (s, 9H).
^{13}C NMR (101 MHz, $CDCl_3$) δ 157.04, 80.55, 59.75, 58.28, 43.53, 42.55, 31.31, 30.47, 28.37.
HRMS (ESI) m/z calcd for $C_{11}H_{23}NO_4Na$ [$(M+Na)^+$] 256.1519, found 256.1517.

((*tert*-Butoxycarbonyl)azanediyl)bis(propane-3,1-diyl) bis(1H-imidazole-1-carboxylate) (compound **4)**

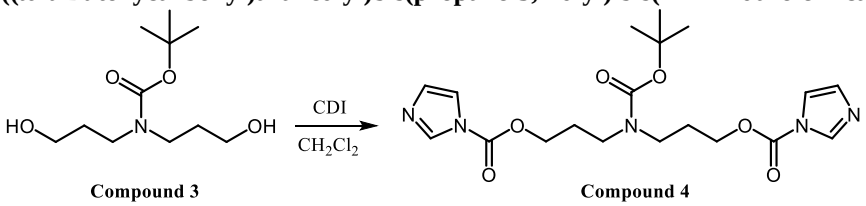

Compound 3 **Compound 4**

Compound **3** (2.33 g, 10 mmol) was dissolved in anhydrous CH_2Cl_2 (100 mL) in a dried flask. Carbonyldiimidazole (CDI) (4.86 g, 30 mmol) was added and the reaction solution was stirred at room temperature for 1 hr. The mixture was diluted into CH_2Cl_2 (400 mL) and then washed with water (2 × 400 mL) and brine (1 × 400 mL). The organic phase was dried over Na_2SO_4 and concentrated in vacuo to obtain the compound **4** as a colorless oil (3.83 g, 91%).
^{1}H NMR (400 MHz, $CDCl_3$) δ 8.13-8.15 (m, 2H), 7.42 (t, *J* = 1.4 Hz, 2H), 7.06-7.09 (m, *J* = 0.7 Hz, 2H), 4.45 (t, *J* = 6.5 Hz, 4H), 3.38 (t, *J* = 6.0 Hz, 4H), 2.05 (m, 4H), 1.43 (s, 9H).
^{13}C NMR (101 MHz, $CDCl_3$) δ 155.3, 148.6, 137.1, 130.8, 117.1, 80.4, 66.1, 44.0, 28.3, 27.8.
HRMS (ESI) m/z calcd for $C_{19}H_{28}N_5O_6$ [$(M+H)^+$] 422.2034, found 422.2020.

7-methyl-1,8-naphthyridin-2-amine (Compound **6)**[3]

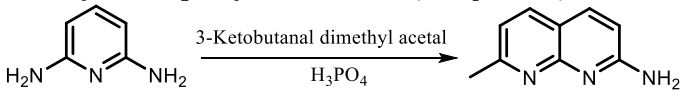

Compound 5 **Compound 6**

2,6-Diaminopyridine (compound **5**, 5.0 g, 45.8 mmol) and 85% H_3PO_4 (50 mL) were added to a 100 mL round-bottomed flask and heated to 90 °C until melted. 3-Ketobutanal dimethyl acetal (6.5 g, 49.2 mmol) was then added dropwise over 15 min and the reaction mixture was then refluxed at 115 °C for 3 hr. After

cooling to room temperature, ammonium hydroxide was added dropwise until pH > 10. The resulting mixture was extracted with CH_2Cl_2 (5 × 100 mL) and the combined organic phase was washed with brine (2 × 300 mL), dried (Na_2SO_4) and concentrated in vacuo to give the desired compound **6** (5.0 g, 69%) as a brown solid.

^{1}H NMR (400 MHz, $CDCl_3$) δ 7.83 (d, *J* = 2.6 Hz, 1H), 7.81 (d, *J* = 3.2 Hz, 1H), 7.08 (d, *J* = 8.0 Hz, 1H), 6.71 (d, *J* = 8.6 Hz, 1H), 5.02 (br, 2H), 2.69 (s, 3H).

^{13}C NMR (101 MHz, $CDCl_3$) δ 162.1, 159.4, 156.3, 138.0, 136.2, 118.9, 115.3, 111.3, 25.4.

HRMS (ESI) m/z calcd for $C_9H_{10}N_3$ [$(M+H)^+$] 160.0869, found 160.0867.

***tert*-Butyl bis(3-(((7-methyl-1,8-naphthyridin-2-yl)carbamoyl)oxy)propyl)carbamate** (Compound **7**)

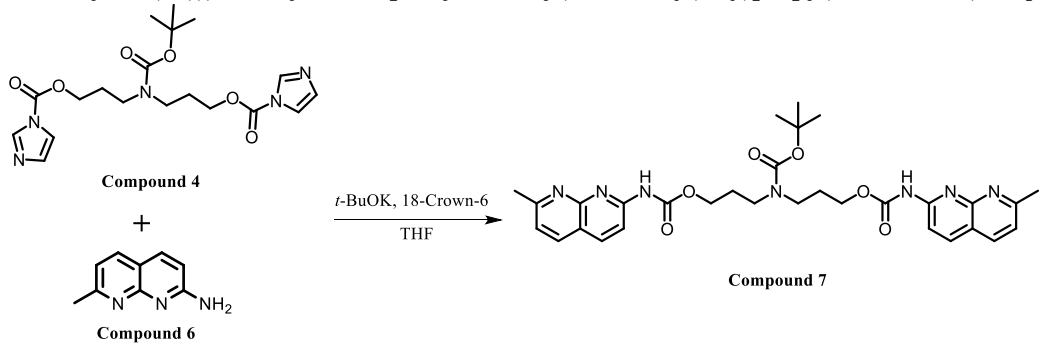

To a stirred solution of compound **6** (1.59 g, 10 mmol) in dry THF (60 mL) was added *t*-BuOK (1.68 g, 15 mmol) and 18-crown-6-ether (264 mg, 1 mmol) at 0 °C under argon atmosphere. The reaction mixture was stirred at 0 °C for 30 min, followed by drop wise addition of a solution of compound **4** (1.95 g, 5 mmol) in dry THF (20 mL). The resulting mixture was then stirred at 0 °C to room temperature during 1 hr. After completion, the reaction solution was diluted with CH_2Cl_2 (300 mL) and then washed with water (2 × 200 mL) and brine (1 × 200 mL). The organic phase was dried over Na_2SO_4 and concentrated in vacuo to get crude product. The crude material was purified by column chromatography on silica gel (CH_2Cl_2/MeOH = 6/1) to obtain compound **7** as a pale white solid (2.35 g, 78%).

^{1}H NMR (400 MHz, $CDCl_3$) δ 8.27 (d, *J* = 8.8 Hz, 2H), 8.12 (d, *J* = 8.8 Hz, 2H), 7.98 (d, *J* = 8.1 Hz, 2H), 7.79 (br, 2H), 7.26 (d, *J* = 8.4 Hz, 2H), 4.27 (t, *J* = 6.3 Hz, 4H), 3.30-3.41 (m, 4H), 2.75 (s, 6H), 1.96-2.04 (m, 4H), 1.47 (s, 9H).

^{13}C NMR (101 MHz, $CDCl_3$) δ 163.2, 155.5, 154.7, 153.3, 153.1, 139.0, 136.4, 121.3, 118.0, 112.6, 79.9, 63.6, 44.4, 28.43, 27.8, 25.6.

HRMS (ESI) m/z calcd for $C_{31}H_{38}N_7O_6$ [$(M+H)^+$] 604.2878, found 604.2873.

NCD

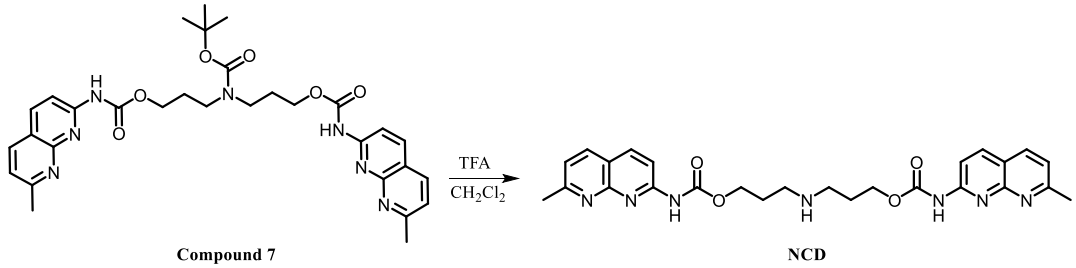

Compound **7** (1.81 g, 3.0 mmol) was dissolved in anhydrous CH_2Cl_2 (50 mL) and trifluoroacetic acid (TFA, 30 mL) was added dropwise via syringe at 0 °C under argon atmosphere. The resulting mixture was vigorously stirred for 30 min and monitored by TLC. All the solvent was removed under reduced pressure and the crude product was dissolved in CH_2Cl_2 (100 mL) and neutralized by ammonia in methanol solution followed by column chromatography purification using silica gel (CH_2Cl_2/MeOH = 3/1) to give **NCD** as an off-white solid (1.3 g, 86%).

^{1}H NMR (400 MHz, $CDCl_3$) δ 8.24 (d, *J* = 8.8 Hz, 2H), 8.10 (d, *J* = 8.9 Hz, 2H), 7.98 (d, *J* = 8.2 Hz, 2H), 7.25 (d, *J* = 8.2 Hz, 2H), 4.32 (t, *J* = 6.2 Hz, 4H), 2.91 (m, 4H), 2.75 (s, 6H), 1.99 (dt, *J* = 12.8, 6.3 Hz, 4H).

^{13}C NMR (101 MHz, $CDCl_3$) δ 163.1, 154.7, 153.5, 153.3, 139.0, 136.5, 121.3, 118.0, 112.8, 63.9, 46.2, 28.8, 25.6.

HRMS (ESI) m/z calcd for $C_{26}H_{29}N_7O_4Na$ [$(M+Na)^+$] 526.2173, found 526.2166.

The synthesis of *Z*-NCTS

The ***Z*-NCTS** was synthesized according to the Scheme 2.

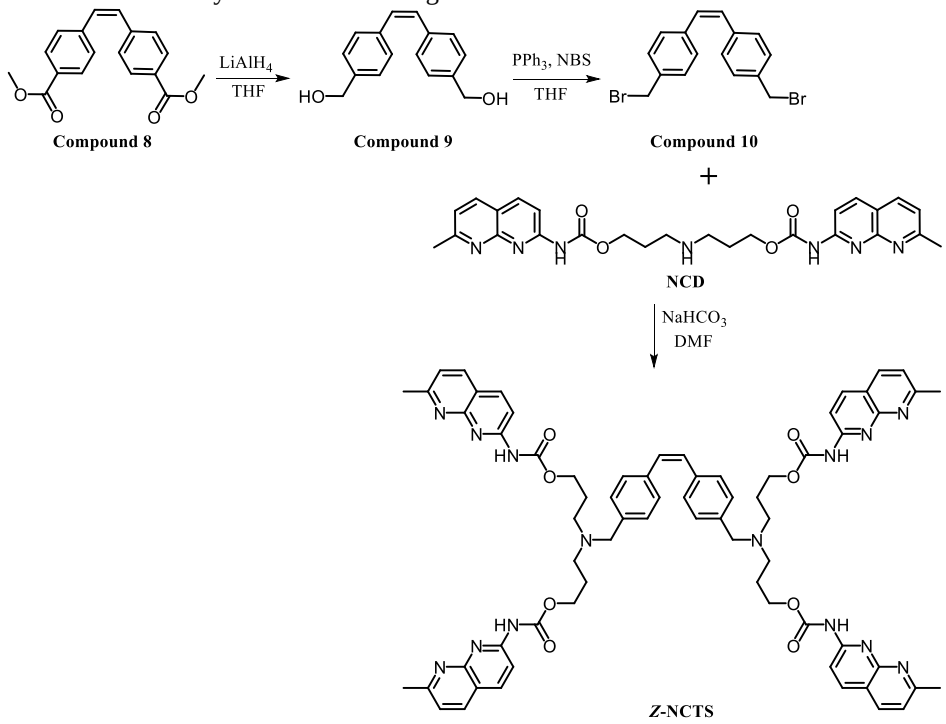

Scheme 2. The synthetic route for ***Z*-NCTS**

***Cis*-stilbene diol (**compound **9)**[4]

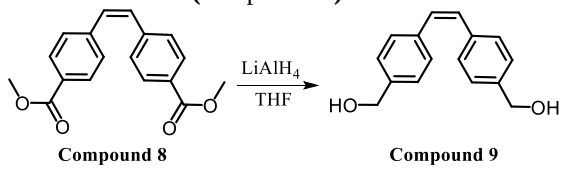

$LiAlH_4$ (228 mg, 6.0 mmol) and dimethyl *cis*-stilbene-4,4′-dicarboxylate (compound **8**, 593 mg, 2.0 mmol) was added to a 100 mL round bottom. Anhydrous THF (20 mL) was added slowly to the reaction mixture via syringe at 0 °C and the resulting mixture was stirred for 5 hr at room temperature. After completion, the reaction was quenched by H_2O (1.0 mL) and 1 N NaOH (1.0 mL). Subsequently, the mixture was diluted with CH_2Cl_2 (100 mL) and filtered to remove precipitate. The filtrate was dried over Na_2SO_4 and then concentrated in vacuo to give compound **9** as a white solid (466 mg, 97%).

^{1}H NMR (400 MHz, DMSO-d_6) δ 7.22-7.17 (m, 8H), 6.59 (s, 2H), 4.46 (s, 4H).

^{13}C NMR (101 MHz, DMSO-d_6) δ 142.1, 135.7, 130.1, 128.7, 126.9, 63.1.

***Cis*-stilbene dibromide (**compound **10)**[4]

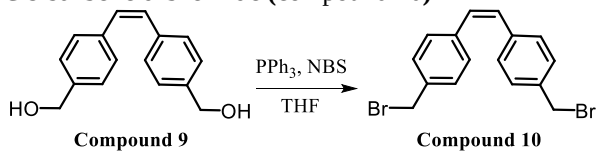

Cis-stilbene diol (compound **9**, 240 mg, 1.0 mmol), PPh_3 (577 mg, 2.2 mmol), and NBS (392 mg, 2.2 mmol) were dissolved in anhydrous THF (20 mL) at 0 °C under argon atmosphere. The resulting mixture was stirred overnight at room temperature and then was quenched with saturated sodium bicarbonate (10 mL) and diluted with H_2O (150 mL). The solution was extracted with CH_2Cl_2 (2 × 100 mL). The combined organic phase was dried over Na_2SO_4 and concentrated in vacuo. The crude product was purified by column chromatography on silica gel (EtOAc/petroleum ether = 1/10) to afford the *cis*-stilbene dibromide as a pale white solid (compound **10**, 263 mg, 68%).

^{1}H NMR (400 MHz, $CDCl_3$) δ 7.28-7.19 (m, 8H), 6.58 (s, 2H), 4.47 (s, 4H).
^{13}C NMR (101 MHz, $CDCl_3$) δ 137.3, 136.7, 130.2, 129.3, 129.1, 33.4.

***Z*-NCTS**[5]

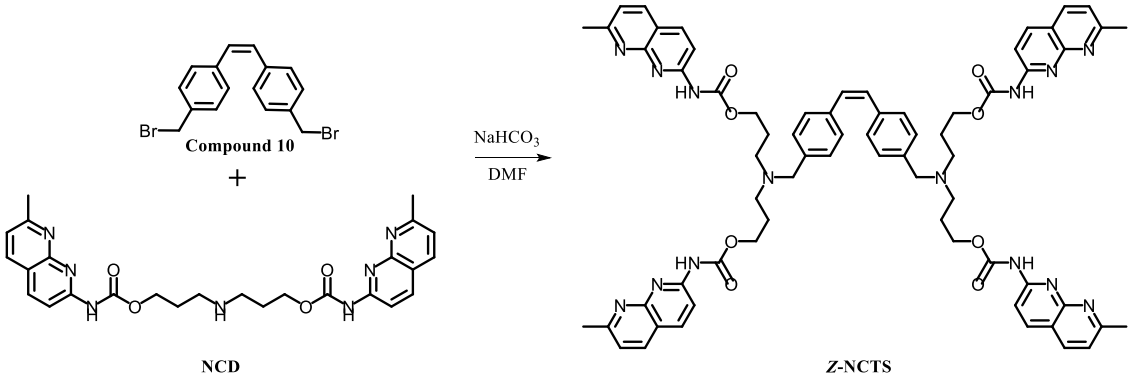

NCD (151 mg, 0.3 mmol), *cis*-stilbene dibromide (compound **10**, 55 mg, 0.15 mmol) and anhydrous $NaHCO_3$ (30 mg, 0.36 mmol) were dissolved in anhydrous DMF (5 ml) under argon atmosphere. The reaction mixture was stirred at room temperature for overnight. The reaction solution was diluted with CH_2Cl_2 (100 mL) and washed with H_2O (2 × 120 mL) and brine (1 × 120 mL). The organic phase was dried over Na_2SO_4 and concentrated in vacuo to get crude material. The crude product was purified by column chromatography on silica gel (CH_2Cl_2/methanol = 30:1) to give ***Z*-NCTS** (50 mg, 28%) as a white solid.
^{1}H NMR (400 MHz, $CDCl_3$) δ 8.28 (d, *J* = 8.8 Hz, 4H), 8.11 (d, *J* = 8.9 Hz, 4H), 7.95 (d, *J* = 8.2 Hz, 4H), 7.75 (br, 4H), 7.23 (d, *J* = 8.2 Hz, 4H), 7.16-7.10 (m, 8H), 6.29 (s, 2H), 4.27 (t, *J* = 6.5 Hz, 8H), 3.51 (s, 4H), 2.74 (s, 12H), 2.54 (t, *J* = 6.4 Hz, 8H), 1.89-1.85 (m, 8H).
^{13}C NMR (101 MHz, $CDCl_3$) δ 163.0, 154.7, 153.5, 153.2, 139.0, 136.4, 136.1, 129.6, 128.9, 128.8, 128.6, 121.2, 118.0, 112.8, 64.1, 58.6, 50.0, 26.6, 25.6. **HRMS** (ESI) m/z calcd for $C_{68}H_{71}N_{14}O_8$ $[(M+H)^+]$ 1211.5574, found 1211.5588.
HRMS (ESI) m/z calcd for $C_{68}H_{70}N_{14}NaO_8$ $[(M+Na)^+]$ 1233.5393, found 1233.5404.

General methods of biological assay
MALDI-TOF Mass measurements
10 μM oligos were incubated with 80 μM NCD in a total reaction volume of 50 μL at 37 °C for 30 min. The whole mixture was dried by a vacuum concentrator. Prior to the MALDI-TOF Mass measurements, the oligos were freshly diluted with autoclaved deionized water. The stainless steel MALDI sample plate was cleaned by rinsing the plate with deionized water and followed by methanol washing. For measurements 3-HPA Matrix solution was used (8:1 mixture of 20 mg/mL 3-hydroxy picolinic acid in MeCN/H_2O, 1:1 and 20 mg/mL diammonium citrate in MeCN/H_2O, 1:1). The 0.3 μL of 3-HPA matrix solution was spotted on the MALDI sample plate, then allowed to air dry. The 0.3 μL of oligo sample was then spotted over the dried matrix, and the solution was allowed to air dry. RNA mass spectra were obtained using an autoflex maX MALDI-TOF/TOF mass spectrometer (Bruker, Germany), with detection in the linear, positive ion mode at a laser frequency of 50 Hz and within a mass range of 3,150 to 5,250 Da. The acceleration voltage was +20.0 kV and grid voltage was +18.2 kV. And the extraction delay time was 450 ns to achieve the highest mass resolution. The linear detector voltage was +1.92 kV. The pressure inside the instrument was maintained at the level of 10^{-8} Torr. Each spectrum was automatically acquired with random edge-biased positioning of laser shots.

Melting studies
UV melting assay was performed using a Jasco-810 spectropolarimeter equipped with a water bath temperature-control accessory. The measurements are performed using a 1.0 mm path length cell and samples containing each model RNA (5 μM) in 10 mM Tris-HCl (pH 7.4) and 50 mM NaCl. UV melting profiles were recorded by using a heating rate of 0.2 °C/min and the absorbance values were collected every 1 °C. The melting point (Tm) corresponds to the midtransition temperature, which was determined by the maximum of the first derivative of the absorbance as a function of temperature.

Sequencing of each gRNA

Reverse transcription of each gRNA was carried out using the *Bst* DNA pol. PCR amplification was performed using the PrimeSTAR HS DNA Polymerase. The PCR products were cloned into plasmid vectors using pClone007 Versatile Simple Vector Kit for Sequencing (Tsingke Biotechnology Co., Ltd.), following manufacturer's instructions. Competent bacteria were transformed with 2 μL ligation mixture and spread onto Luria-Bertani agar plates containing 150 μg/mL ampicillin. Plasmid DNAs were purified and Sanger sequenced using a M13F primer (5'-TGTAAAACGACGGCCAGT-3').

Cell culture

HeLa cells were obtained from ATCC (the American Type Culture Collection). The HeLa-OC cell line containing stably integrated Cas9 gene was used for sgRNAs targeted to different genes[6]. This HeLa-derived cell line was a kind gift from Prof. Wen-Sheng Wei, School of Life Sciences, Peking University, Beijing, China. HeLa and HeLa-OC cells were maintained in complete media, Gibco™ DMEM, High Glucose medium (Thermo Fisher Scientific), 10% (v/v) Gibco™ fetal bovine serum (FBS, Thermo Fisher Scientific) and 1% penicillin/streptomycin (Invitrogen), at 37 °C in a 5% CO_2 incubator[6].

R-SL1: calculated 3811.4, found 3811.4

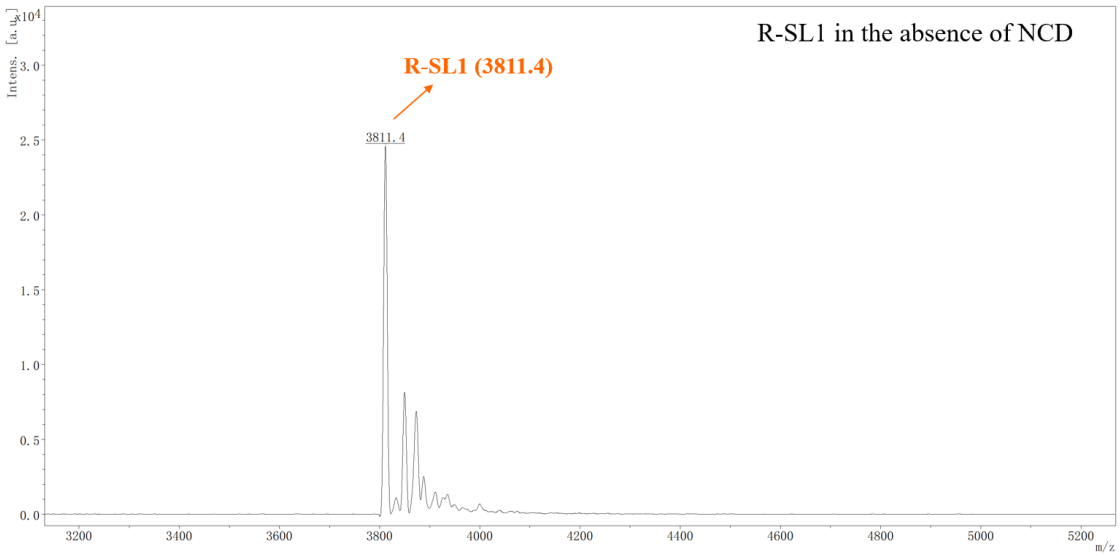

R-SL1: calculated 3811.4, found 3811.3

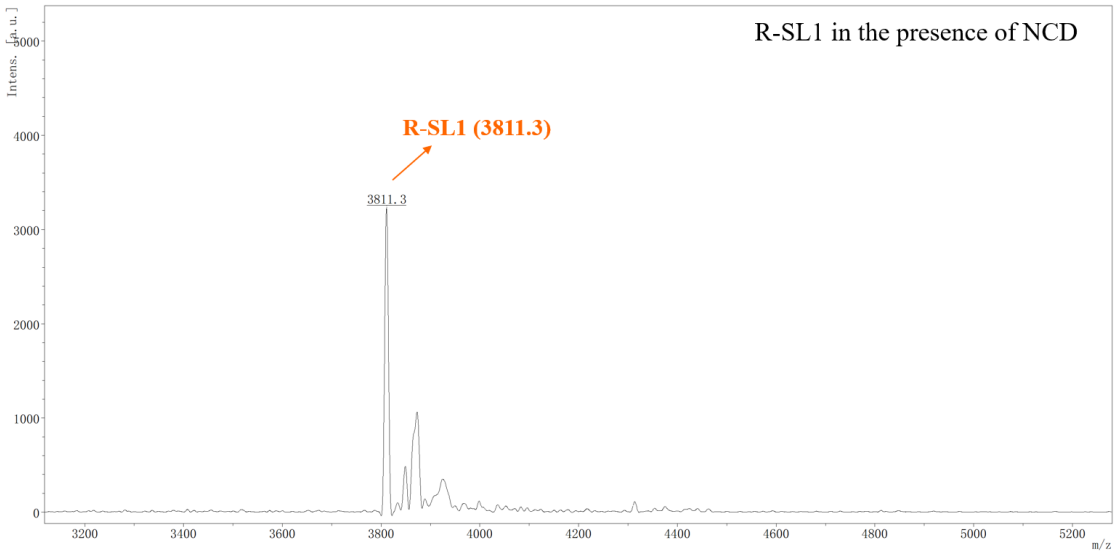

Figure S1. MALDI-TOF Mass Spectra of model RNA (R-SL1) with different treatments.

Representative MALDI-TOF Mass Spectra of R-SL1 in the absence or presence of NCD are demonstrated here. The mass spectrum of the NCD-treated R-SL1 shows no additional peaks for the addition of NCD molecules.

R-SL1-S1a: calculated 3851.4, found 3851.4

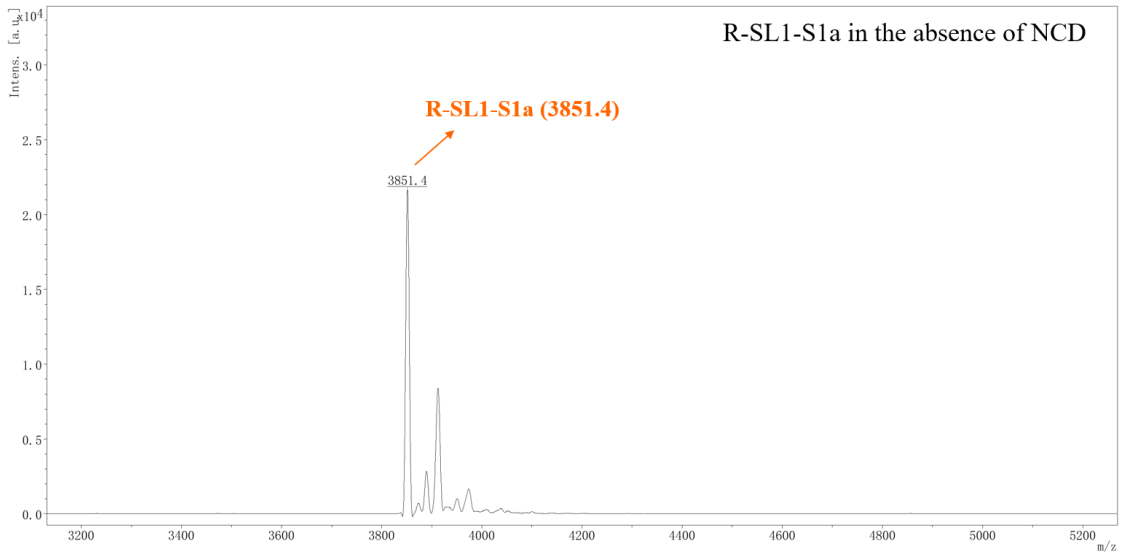

R-SL1-S1a: calculated 3851.4, found 3851.4

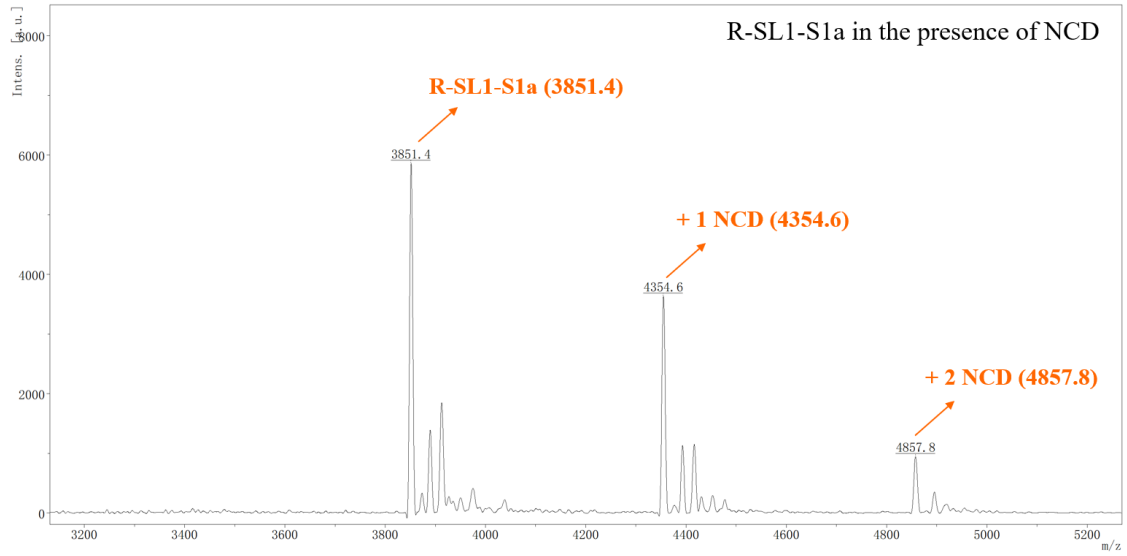

Figure S2. MALDI-TOF Mass Spectra of model RNA (R-SL1-S1a) with different treatments.

Representative MALDI-TOF Mass Spectra of R-SL1-S1a in the absence or presence of NCD are demonstrated here. The mass spectrum of the NCD-treated R-SL1-S1a shows several peaks for the addition of one and two NCD molecules. The peak at 3851.4 corresponds to unreacted R-SL1-S1a, whereas the peaks at 4354.6 (3851.4 + 503.2), 4857.8 (3851.4 + 503.2 × 2) are ascribed to the mono-adducts and bis-adducts.

A

>20 dna:chromosome chromosome:GRCh38:20:10435305:10636829:1

TTATCCGGCACTGTGAAAGCTACCTTTCCTTTCTCACAATCTTTCGCACCGAATATATGTTCCA
TTCTTGAGCTAGTCATTTTCCAATGTTAAGAAAACACACCACAGAAAAGCGTTTTTTTTTCTCT
CGGTCAGTTCAACTGCCTAGCACCGTGAGTTACCATGATACGTTATTTGCTAATGAGAGTCAT
TGGGGTCCCAGCCTTTAAAAATAGCCTGCGTCCGGCGCCATTTTTGTTTTGGGCCCACTTTGAA
AGCCGCGATATTCTGAACAGAGGCCATTTTTCTTTTGGGCAGATTCCACGGGCCATCGAAGTG
TTTCGCTGCCA**TCT^TAAATCCTGGCTGTGGC**CTCAATCCTGCAGCGAAGCTGCCCAGATCA
TTTTGTGTTTGGGCGGCGGCTGAGTTCCCAAACGCGCGCGGAGACCCTGGGAAGGAGGAAGT
AAGCGCGAAAGTGCTTCCCTTAAGCTTCTGAAGGTTGGCTGCAGTTCCGGCTACCTGTGTAGT
CCGAGTTTCCACAGCCAGGTACTACTCCGCCAGTGACCCTGGACAGTAACAAAACATATAAA
GCCCGAGCCCAAACCCCGCCACCATCATAGGTAAGCACATGGACCTCTGACAACCTCAGATGT
TCCTTCAAGTGAACTGAACTGTTTGCCCATCTCCTCCCTCCTGGTTTTTGGCTTTGATTTTTTGA
GACTTTTCCGAATCCTTCTCCCTGTACTTCCACCTTTCTTCATTGTTTTCAAAAAGCCAAAAAG
TTGCTAAACATCAGG

B

>X dna:chromosome chromosome:GRCh38:X:134460165:134520513:1

GTTGTGATAAAAGGTGATGCTCACCTCTCCCACACCCTTTTATAGTTTAGGGATTGTATTTCCA
AGGTTTCTAGACTGAGAGCCCTTTTCATCTTTGCTCATTGACACTCTGTACCCATTAATCCTCC
TTATTAGCTCCCCTTCAATGGACACATGGGTAGTCAGGGTGCAGGTCTCAGAACTGTCCTTCA
GGTTCCAGGTGATCAACCAAGTGCCTTGTCTGTAGTGTCAACTCATTGCTGCCCCTTCCTAGTA
ATCCCCATAATTTAGCTCTCCA**TTT^CATAGTCTTTCCTTGGG**TGTGTTAAAAGTGACCATGG
TACACTCAGCACGGATGAAATGAAACAGTGTTTAGAAACGTCAGTCTTCTCTTTTGTAATGCC
CTGTAGTCTCTCTGTATGTTATATGTCACATTTTGTAATTAACAGCTTGCTGGTGAAAAGGACC
CCACGAAGTGTTGGATATAAGCCAGACTGTAAGTGAATTACTTTTTTTGTCAATCATTTAACCA
TCTTTAACCTAAAAGAGTTTTATGTGAAATGGCTTATAATTGCTTAGAGAATATTTGTAGAGA
GGCACATTTGCCAGTATTAGATTTAAAAGTGATGTTTTCTTTATCTAAATGATGAATTATGATT
CTTTTTAGTTGTTGGATTTGAAATTCCAGACAAGTTTGTTGTAGGATATGCCCTTGACTATAAT
GAATACTTCAGGGATTTGAATGTAAGTAATTGCTTCTTTTTCTCACTCATTTTTCAAAACACGC
ATAAAAATTTAGGAAAGAGAATTGTTTTCTCCTTCCAGCACCTCATAATTTGAACAGACTGAT
GGTTCCCATTAGTCACATAAAGCTGTAGTCTAGTACAGACGTCCTTAGAACTGGAACCTGGCC
AGGCTAGGGTGACACTTCTTGTTGGCTGAAATAGTTGAACAGCTTTAATATACAATAATTGTT
GCATTATTATTTCAGATGATAAATGTGGTCATAAGTAAGAAATAAATGATCGAGTTTAGTCTT
TTAATTCACTGTCCTTTGAATACCTGCCTCTTACTCTGGAGGCAGAAGTCCCATGGATGTGTTT
ATGA

C

>gi|74230048|gb|CH471062.2|:13429990-13430610 Homo sapiens 211000035832302 genomic scaffold, whole genome shotgun sequence

GCCGCTTCGAAAGTGACTGGTGCCTCGCCGCCTCCTCTCGGTGCGGGACCATGAAGCTGCTGC
CGTCGGTGGTGCTGAAGCTCTTTCTGGCTGCAGGTAAGAGGGCTGCCGACGCCCCCGGAGATC
GGGGGGATGGGGGCGTTGTGCTGGGGGCATGGGGGAAGGTCGCCGCAGCGCACCCGGCACG
GGCCACTTGGTGGGGCCCTTGCGCTCTGGCGGACGGGCGTCGGCATCGGTGCGTGTTGGTCAG
GGGTCTGGGCGGGTGTCTGATGCGGCCTGGCCTCTCGCCCGCA**GTTCTCTCGGCACTGGT^G**
ACTGGCGAGAGCCTGGAGCGGCTTCGGAGAGGGCTAGCTGCTGGAACCAGCAACCCGGACCC
TCCCACTGTATCCACGGACCAGCTGCTACCCCTAGGAGGCGGCCGGGACCGGAAAGTCCGTG
ACTTGCAAGAGGCAGATCTGGACCTTTTGAGAGGTGGGTGTGGAGGCCCCCCATCCTTGGACC
TTGGTGGGCTGTTGAAGAATAAGCAGATCCAAGATTCTTGCTGTTTGGGCAATACTGTGGGTT
GAGGGTATTCATGGAGAACCTCGGGGAAAAGCTGATCGGCCTGATGGGCACTGGGGGATC

D

GFP sequences around target loci

GAGGAGCTGTTCACCGGGGTGGTGCCCATCCTGGTCGAGCTGGACGGCGACGTAAACGGCCA
CAAGTTCAGCGTGTCCGGCGAGGGCGAGGGCGATGCCACCTACGGCAAGCTGACCCTGAAGT
TCATCTGCACCACCGGCAAGCTGCCCGTGCCCTGGCCCACCCTCGTGACCACCCTGACCTACG

GCGTGCAGTGCTTCAGCCGCTACCCCGACCACATGAAGCAGCACGACTTCTTCAAGTCCGCCA
TGCCCGAAGGCTACGTCCAGGAGCGCACCATCTTCTTCAAGGACGACGGCAACTACAAGACC
CGCGCCGAGGTGAAGTTCGAGGGCGACACCCTGGTGAACCGCATCGAGCTGAAGGGCATCGA
CTTCAAGGAGGACGGCAACATCCTGGGGCACAAGCTGGAGTACAACTACAACAGCCACAACG
TCTATATCATGGCCG**ACAAGCAGAAGAACGGCA^TC**AAGGTGAACTTCAAGATCCGCCACA
ACATCGAGGACGGCAGCGTGCAGCTCGCCGACCACTACCAGCAGAACACCCCCATCGGCGAC
GGCCCCGTGCTGCTGCCCGACAACCACTACCTGAGCACCCAGTCCGCCCTGAGCAAAGACCCC
AACGAGAAGCGCGATCACATGGTCCTGCTGGAGTTCGTGACCGCCGCCGGGATCACTCTCGGC
ATGGACGAGCTGTACAAG

Figure S3. Location of sequences recognised by gRNAs and PCR primers.

The target loci and PCR primer loci were indicated by blue color and underlining, respectively. Red caret showed the cleavage sites by Cas9 nuclease. PCR primers flanking the target regions were designed by BLAST search and procedures. (**A**) Schematic illustration of the sequence of *SLX4IP* gene around target loci. The SLX4IP gene is located on the short arm (p) of chromosome 20 at position 12.2 (20p12.2). We generated target SLX4IP DNA (t-SLX4IP) carrying the target loci from HeLa-OC genomic DNA. The 20-nt sequence was the exact same sequence as the target sequence. (**B**) Schematic illustration of the sequence of *HPRT1* gene around target loci. We generated target HPRT1 DNA (t-HPRT1) carrying the target loci from HeLa-OC genomic DNA. The 20-nt sequence was the exact same sequence as the target sequence. (**C**) Schematic illustration of the 5'-UTR sequence of *HBEGF* gene around target loci. We generated target HBEGF DNA (t-HBEGF) carrying the target loci from HeLa-OC genomic DNA. The 20-nt sequence was the exact same sequence as the target sequence. (**D**) Schematic illustration of GFP sequences around target loci. We generated target GFP DNA (t-GFP) carrying the target loci from pEGFP-C1 vector. The 20-nt sequence was the exact same sequence as the target sequence.

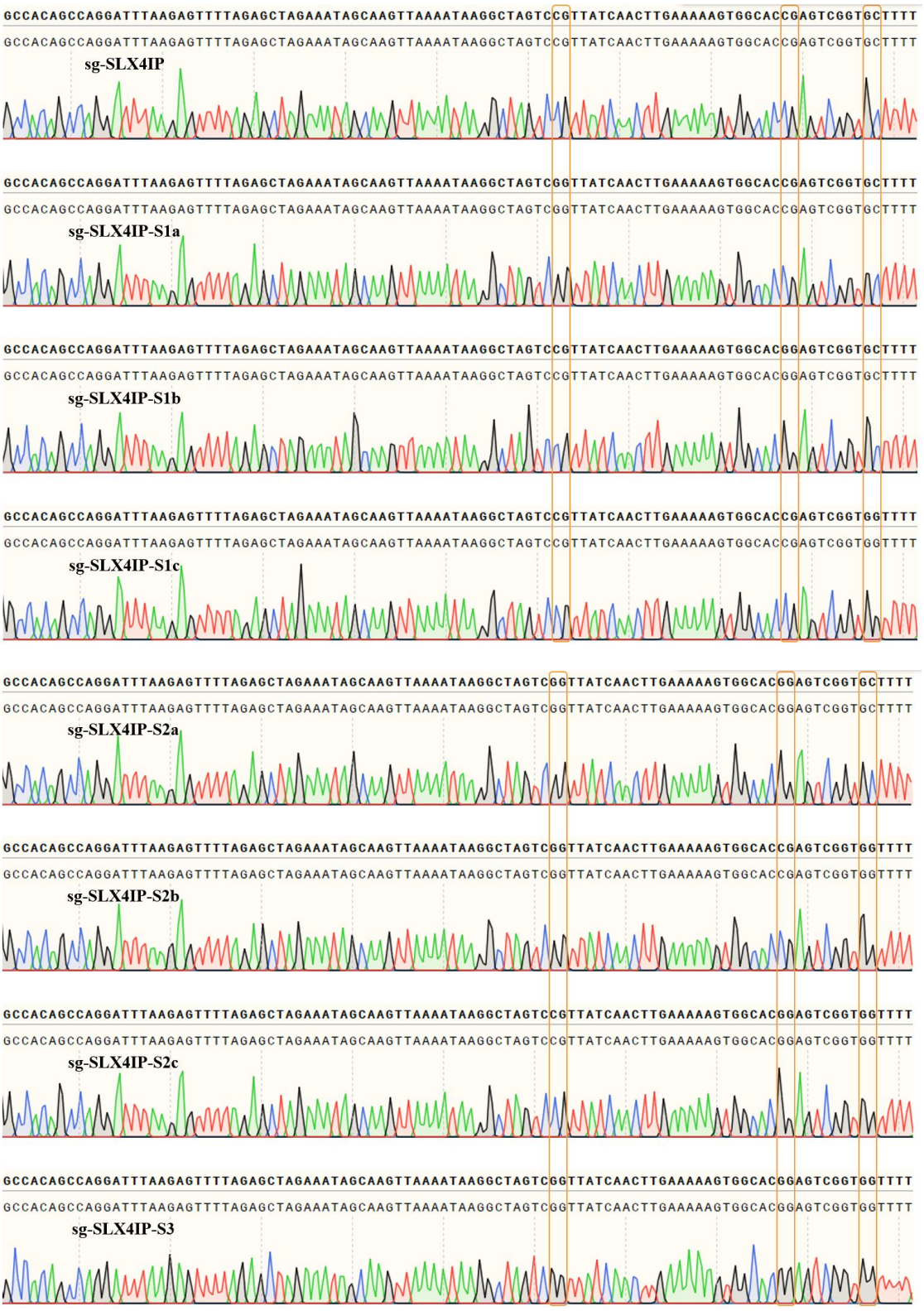

Figure S4. Sanger sequencing analysis of each variant of sg-SLX4IP.
The sites for engineering are indicated.

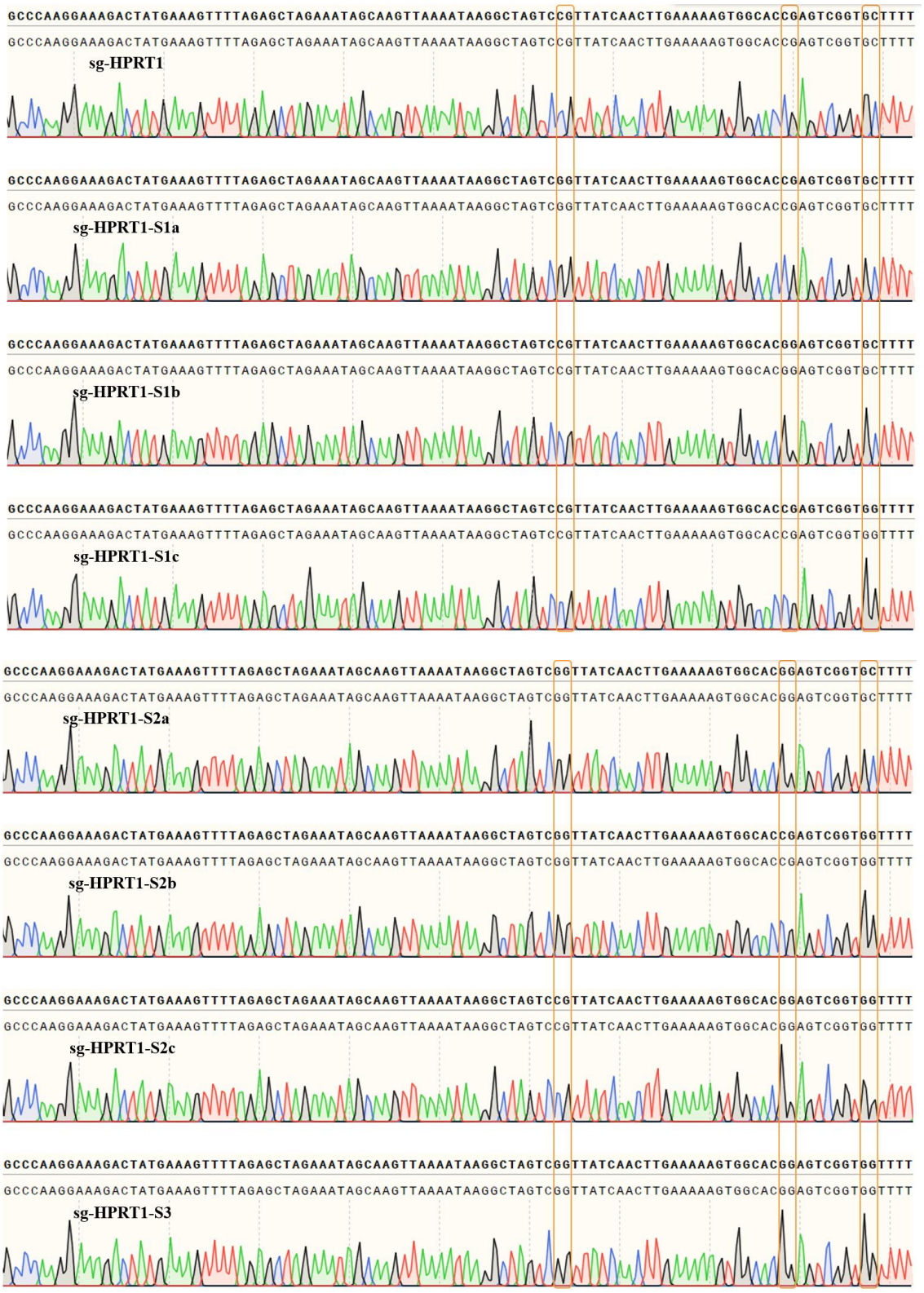

Figure S5. Sanger sequencing analysis of each variant of sg-HPRT1.
The sites for engineering are indicated.

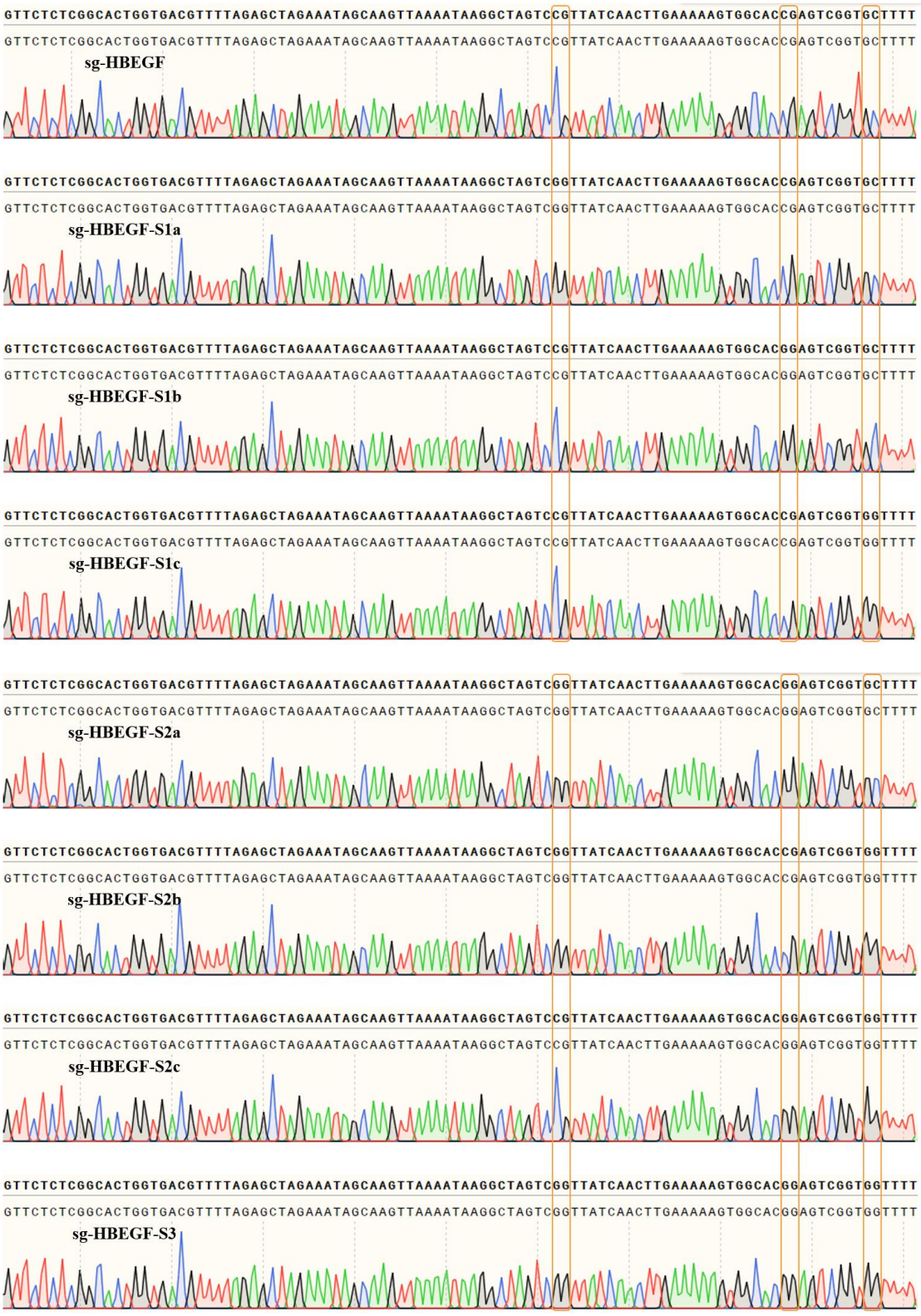

Figure S6. Sanger sequencing analysis of each variant of sg-HBEGF.
The sites for engineering are indicated.

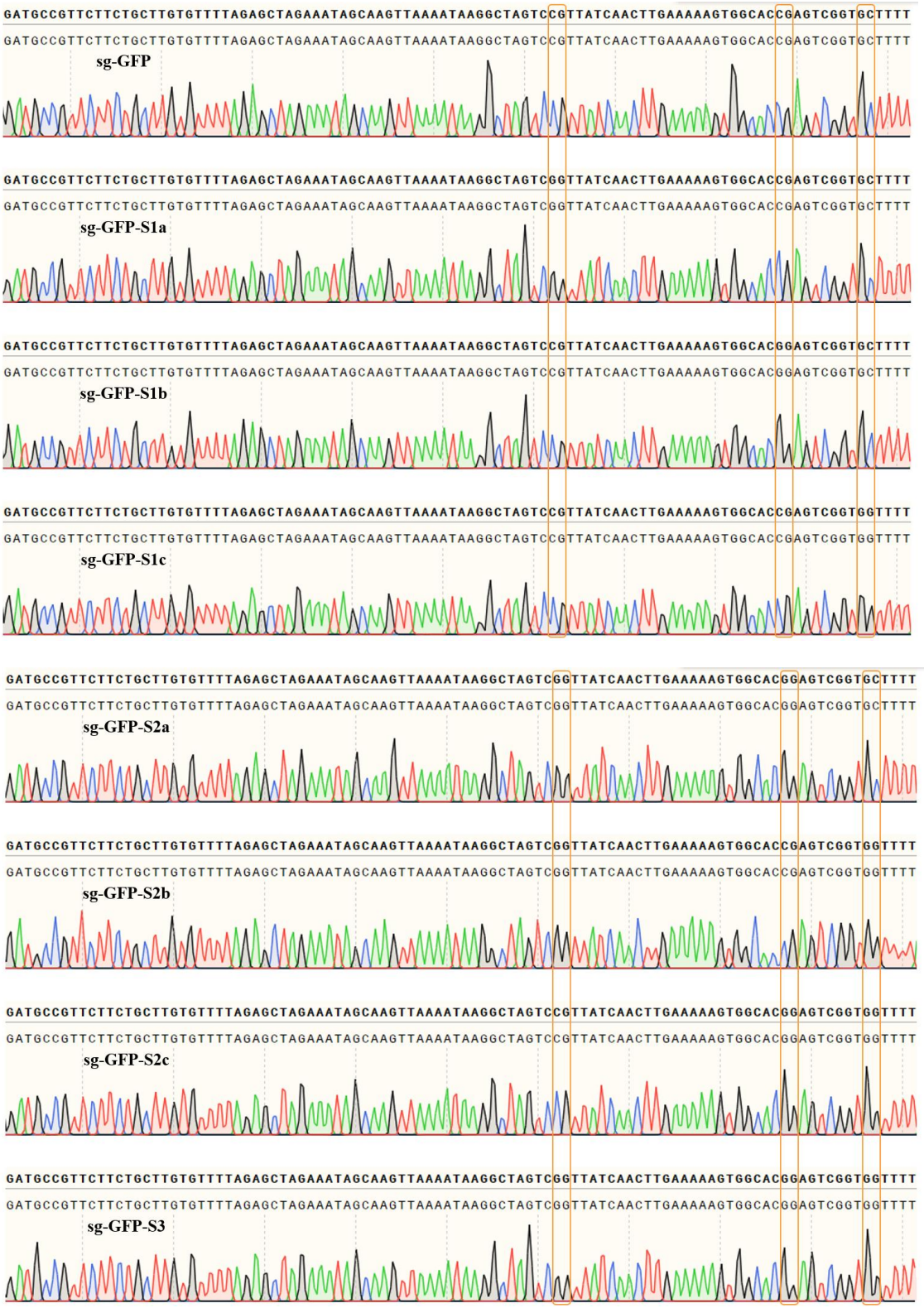

Figure S7. Sanger sequencing analysis of each variant of sg-GFP.
The sites for engineering are indicated.

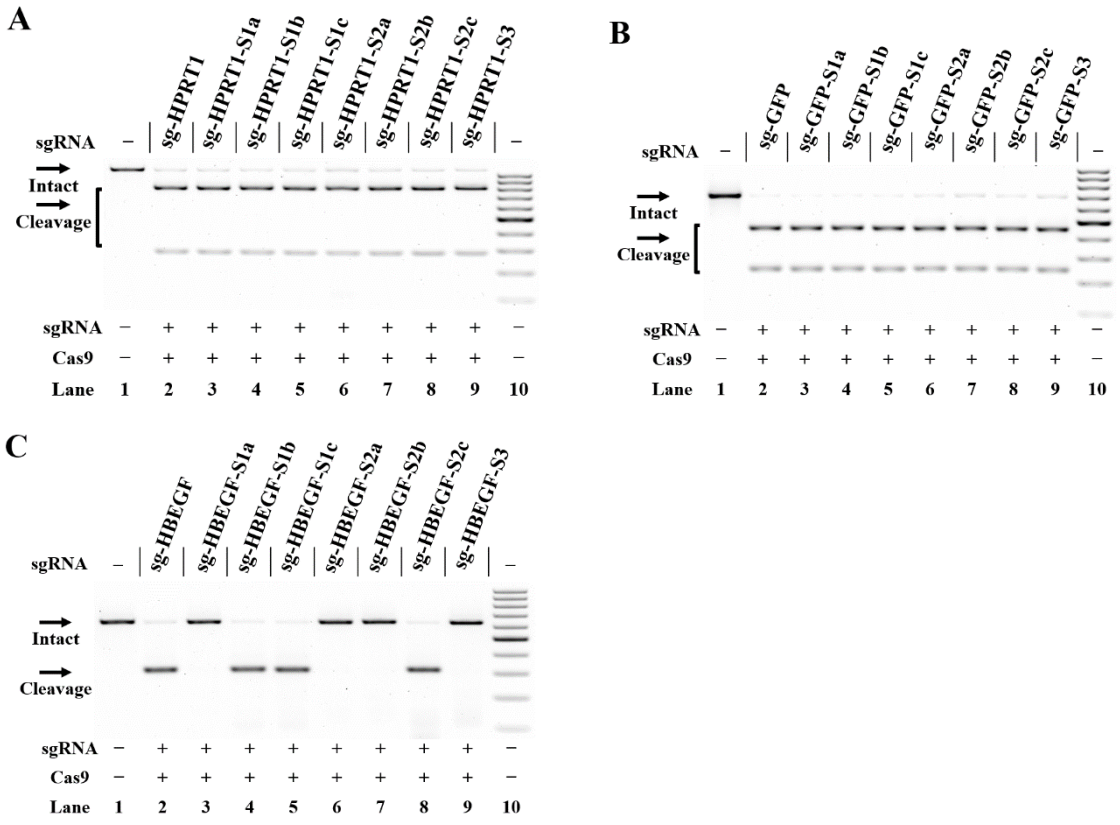

Figure S8. The tolerance of Cas9 to each designer sgRNA.

Reactions were performed as described in the Experimental Section. All samples were tested in three biological replicates. Image of representative data is shown here. (**A**) Uncleaved HPRT1 DNA (1083 bp) cut to shorter cleavage fragments (803 bp and 280 bp) are demonstrated. (**B**) Uncleaved GFP DNA (702 bp) cut to shorter cleavage fragments (469 bp and 233 bp) are demonstrated. (**C**) Uncleaved HBEGF DNA (621 bp) cut to shorter cleavage fragments (311 bp and 310 bp) are demonstrated. For (**A**), (**B**) and (**C**), lane 1: no Cas9 control; lane 2 contains original sgRNA; lanes 3-9 contain designer sgRNAs harboring different MBL-binding units; lane 10: DNA marker (GeneRuler 100-bp DNA Ladder).

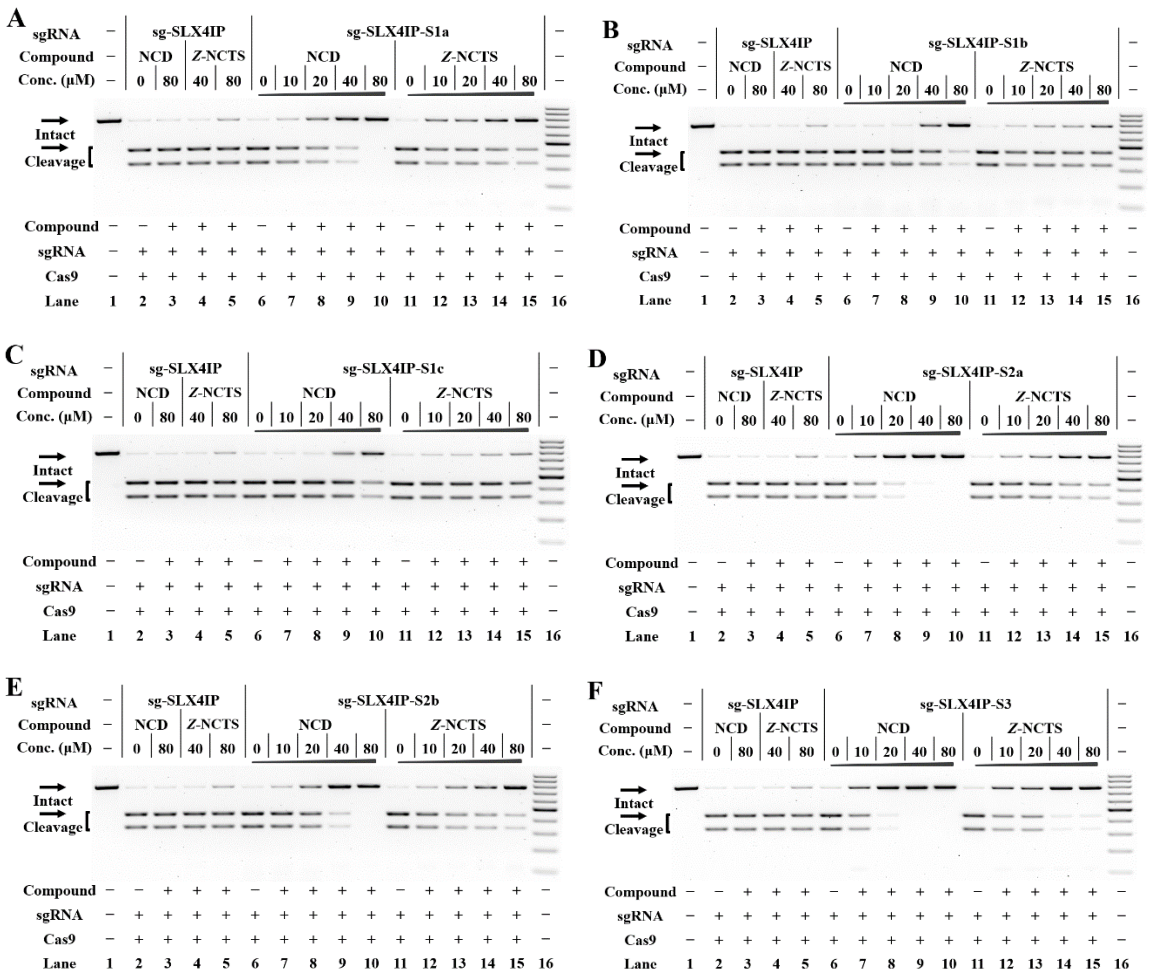

Figure S9. Responsiveness of sequence-modified sg-SLX4IP to different MBLs.

Reactions were performed as described in the Experimental Section. Uncleaved SLX4IP DNA (773 bp) cut to shorter cleavage fragments (441 bp and 332 bp) are demonstrated. All samples were tested in three biological replicates. Image of representative data is shown here. A 2-fold increase in concentration for NCD and *Z*-NCTS showed significant differences in switching CRISPR/Cas9. (**A**)-(**F**): Responsiveness of sg-SLX4IP-S1a (**A**), sg-SLX4IP-S1b (**B**), sg-SLX4IP-S1c (**C**), sg-SLX4IP-S2a (**D**), sg-SLX4IP-S2b (**E**), sg-SLX4IP-S3 (**F**) to each MBL. For (**A**)-(**F**), lane 1: no Cas9 control; lanes 2-5 contain original sg-SLX4IP; lanes 6-10, 11-15 contain designer sgRNAs harboring MBL-binding units; lane 16: DNA marker (GeneRuler 100-bp DNA Ladder).

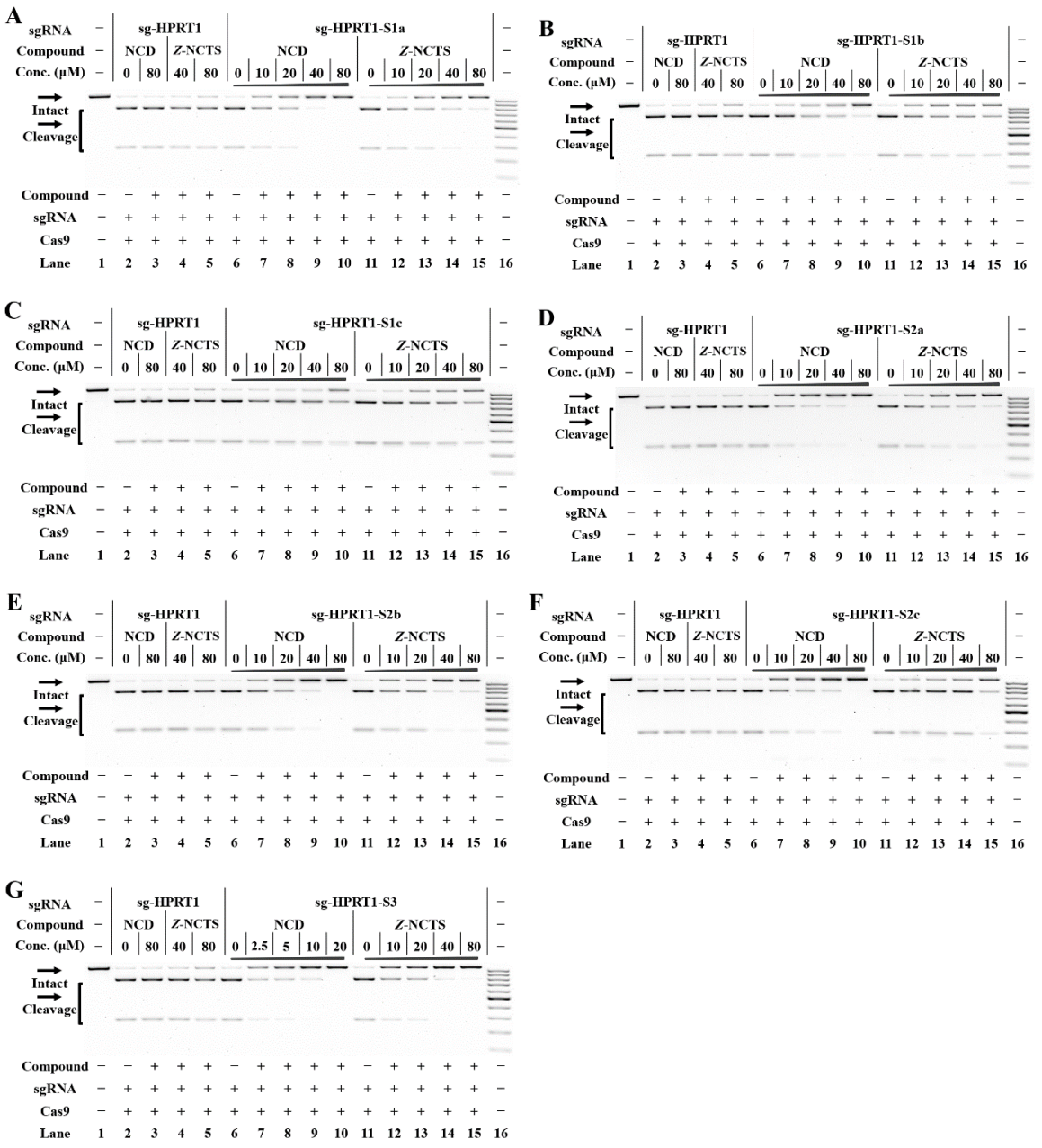

Figure S10. Responsiveness of sequence-modified sg-HPRT1 to different MBLs.

Reactions were performed as described in the Experimental Section. Uncleaved HPRT1 DNA (1083 bp) cut to shorter cleavage fragments (803 bp and 280 bp) are demonstrated. All samples were tested in three biological replicates. Image of representative data is shown here. A 2-fold increase in concentration for NCD and *Z*-NCTS showed significant differences in switching CRISPR/Cas9. (**A**)-(**G**): Responsiveness of sg-HPRT1-S1a (**A**), sg-HPRT1-S1b (**B**), sg-HPRT1-S1c (**C**), sg-HPRT1-S2a (**D**), sg-HPRT1-S2b (**E**), sg-HPRT1-S2c (**F**), sg-HPRT1-S3 (**G**) to each MBL. For (**A**)-(**G**), lane 1: no Cas9 control; lanes 2-5 contain original sg-HPRT1; lanes 6-10, 11-15 contain designer sgRNAs harboring MBL-binding units; lane 16: DNA marker (GeneRuler 100-bp DNA Ladder).

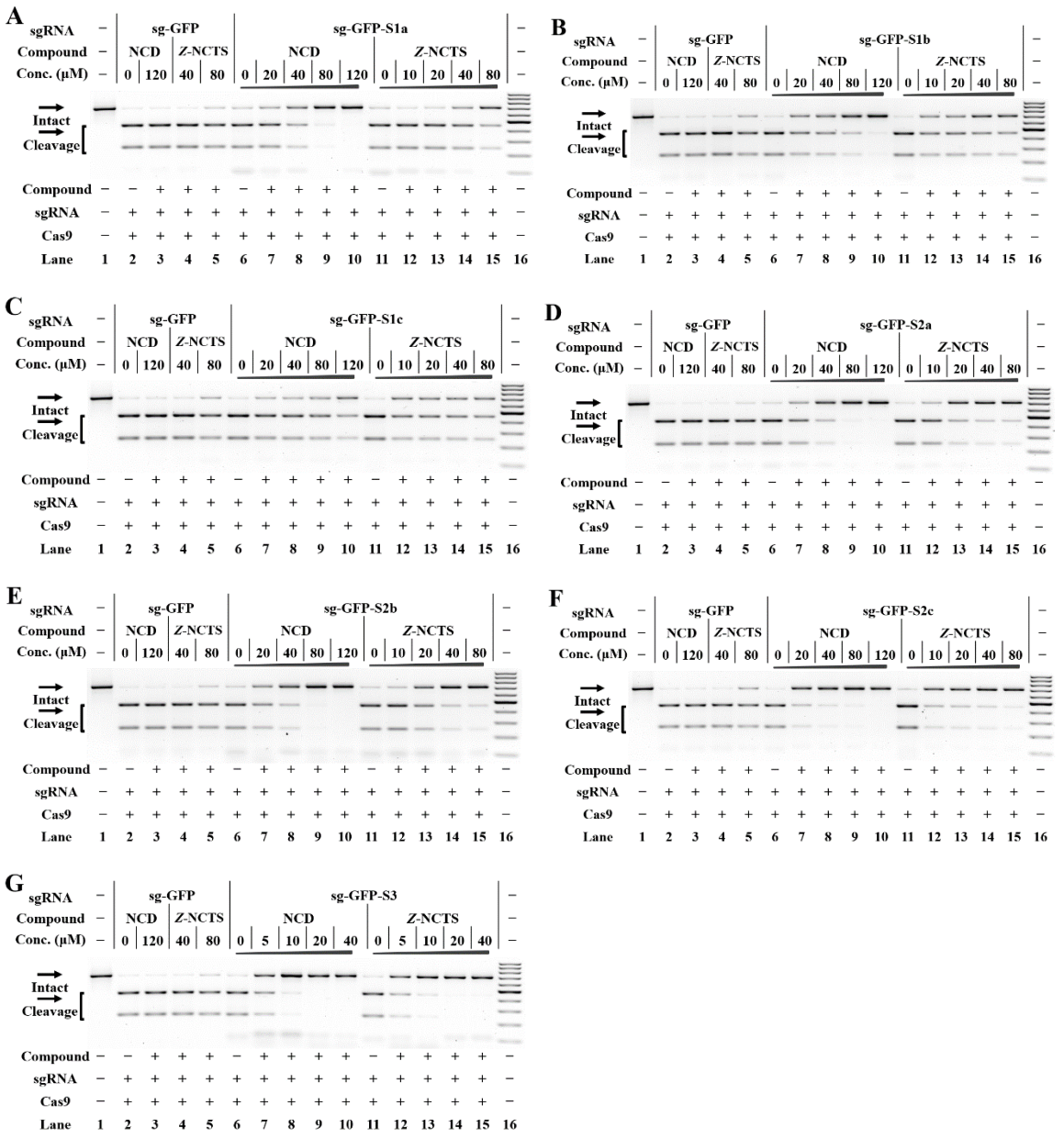

Figure S11. Responsiveness of sequence-modified sg-GFP to different MBLs.

Reactions were performed as described in the Experimental Section. Uncleaved GFP DNA (702 bp) cut to shorter cleavage fragments (469 bp and 233 bp) are demonstrated. All samples were tested in three biological replicates. Image of representative data is shown here. A 2-fold increase in concentration for NCD and *Z*-NCTS showed significant differences in switching CRISPR/Cas9. (**A**)-(**G**): Responsiveness of sg-GFP-S1a (**A**), sg-GFP-S1b (**B**), sg-GFP-S1c (**C**), sg-GFP-S2a (**D**), sg-GFP-S2b (**E**), sg-GFP-S2c (**F**) and sg-GFP-S3 (**G**) to each MBL. For (**A**)-(**G**), lane 1: no Cas9 control; lanes 2-5 contain original sg-GFP; lanes 6-10, 11-15 contain designer sgRNAs harboring MBL-binding units; lane 16: DNA marker (GeneRuler 100-bp DNA Ladder).

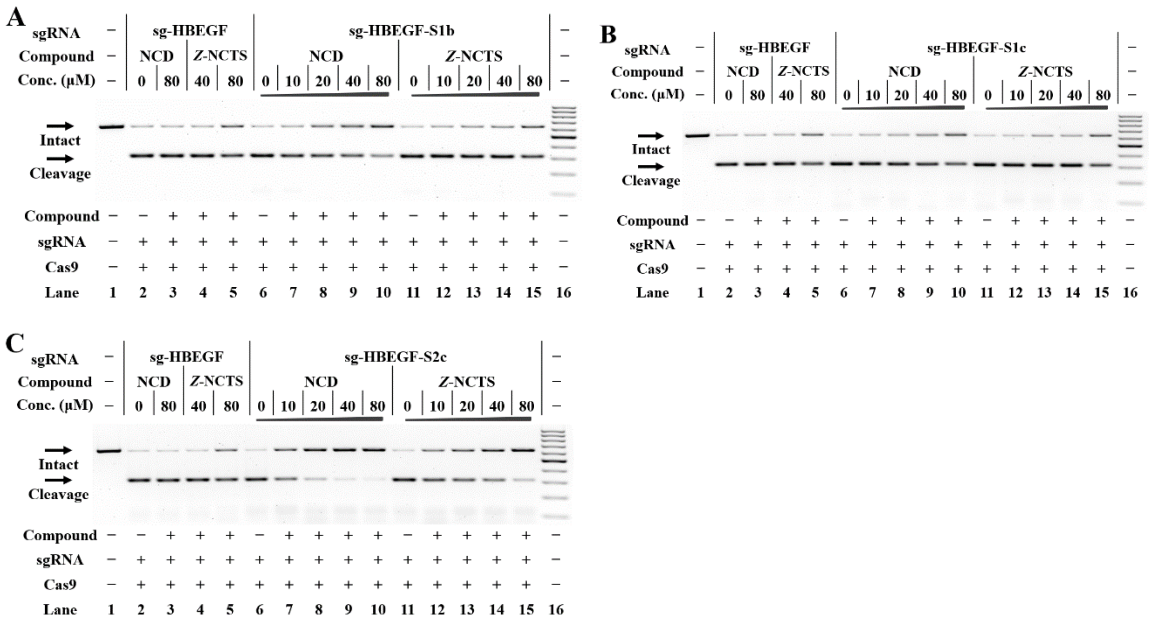

Figure S12. Responsiveness of sequence-modified sg-HBEGF to different MBLs.

Reactions were performed as described in the Experimental Section. Uncleaved HBEGF DNA (621 bp) cut to shorter cleavage fragments (311 bp and 310 bp) were demonstrated. All samples were tested in three biological replicates. Image of representative data is shown here. A 2-fold increase in concentration for NCD and *Z*-NCTS showed significant differences in switching CRISPR/Cas9. (**A**)-(**C**): Responsiveness of sg-GFP-S1b (**A**), sg-GFP-S1c (**B**) and sg-GFP-S2c (**C**) to each MBL. For (**A**)-(**C**), lane 1: no Cas9 control; lanes 2-5 contain original sg-HBEGF; lanes 6-10, 11-15 contain designer sgRNAs harboring MBL-binding units; lane 16: DNA marker (GeneRuler 100-bp DNA Ladder).

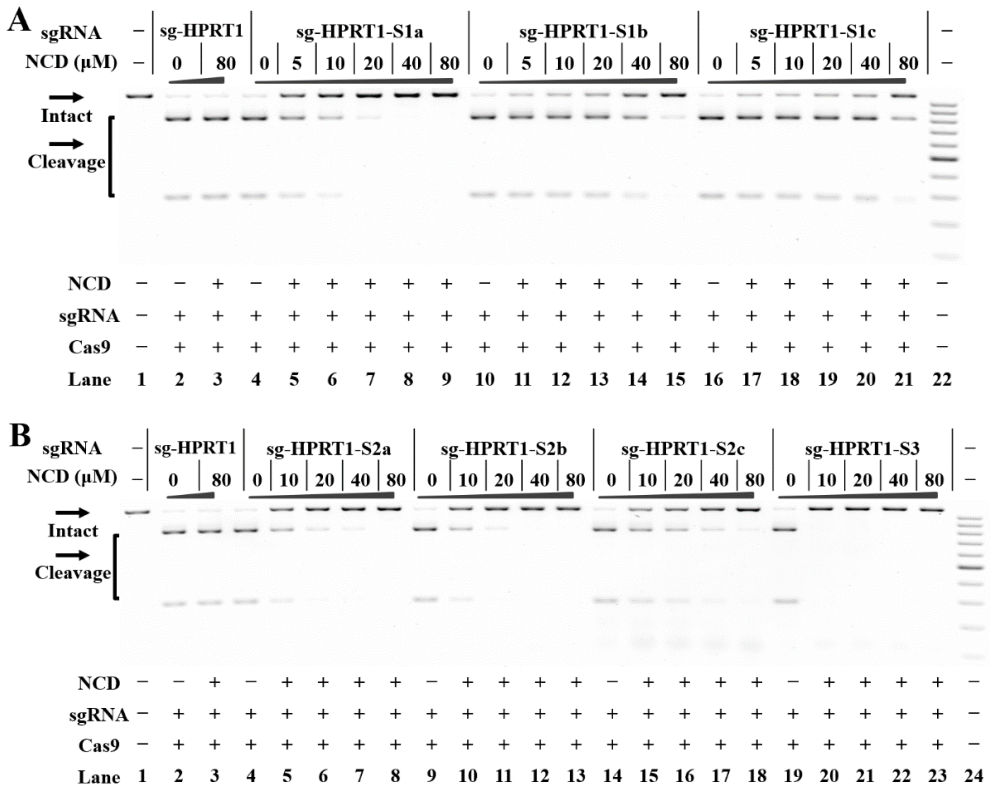

Figure S13. Ligand control of sequence-modified sg-HPRT1 for switching CRISPR/Cas9.

Reactions were performed as described in the Experimental Section. Uncleaved HPRT1 DNA (1083 bp) cut to shorter cleavage fragments (803 bp and 280 bp) are demonstrated. All samples were tested in three biological replicates. Image of representative data is shown here. (**A**) The NCD-dependent inhibition of CRISPR/Cas9 with single-site variants. Lane 1: no Cas9 control; lanes 2-3 contain original sg-HPRT1; lanes 4-9 contain sg-HPRT1-S1a; lanes 10-15 contain sg-HPRT1-S1b; lanes 16-21 contain sg-HPRT1-S1c; lane 22: DNA marker (GeneRuler 100-bp DNA Ladder). (**B**) The NCD-dependent inhibition of CRISPR/Cas9 with multi-nucleotide variants. Lane 1: no Cas9 control; lanes 2-3 contain original sg-HPRT1; lanes 4-8 contain sg-HPRT1-S2a; lanes 9-13 contain sg-HPRT1-S2b; lanes 14-18 contain sg-HPRT1-S2c; lanes 19-23 contain sg-HPRT1-S3; lane 24: DNA marker.

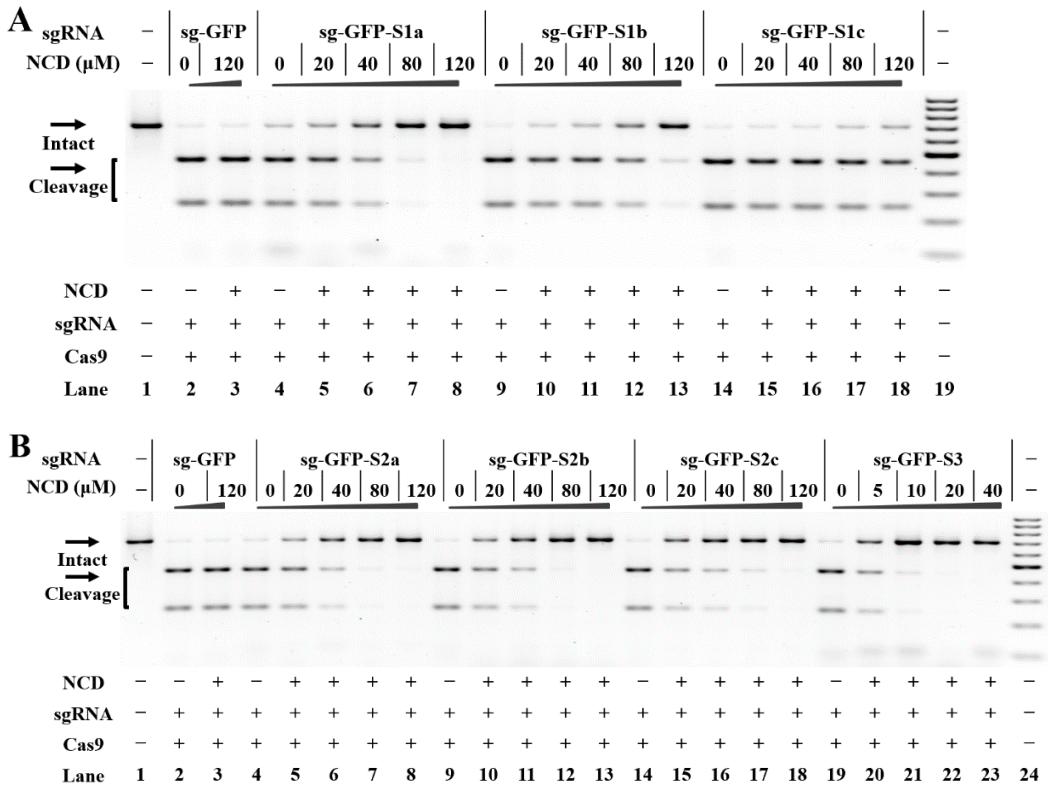

Figure S14. Ligand control of sequence-modified sg-GFP for switching CRISPR/Cas9.

Reactions were performed as described in the Experimental Section. Uncleaved GFP DNA (702 bp) cut to shorter cleavage fragments (469 bp and 233 bp) are demonstrated. All samples were tested in three biological replicates. Image of representative data is shown here. (**A**) The NCD-dependent inhibition of CRISPR/Cas9 with single-site variants. Lane 1: no Cas9 control; lanes 2-3 contain original sg-GFP; lanes 4-8 contain sg-GFP-S1a; lanes 9-13 contain sg-GFP-S1b; lanes 14-18 contain sg-GFP-S1c; lane 19: DNA marker (GeneRuler 100-bp DNA Ladder). (**B**) The NCD-dependent inhibition of CRISPR/Cas9 with multi-nucleotide variants. Lane 1: no Cas9 control; lanes 2-3 contain original sg-GFP; lanes 4-8 contain sg-GFP-S2a; lanes 9-13 contain sg-GFP-S2b; lanes 14-18 contain sg-GFP-S2c; lanes 19-23 contain sg-GFP-S3; lane 24: DNA marker.

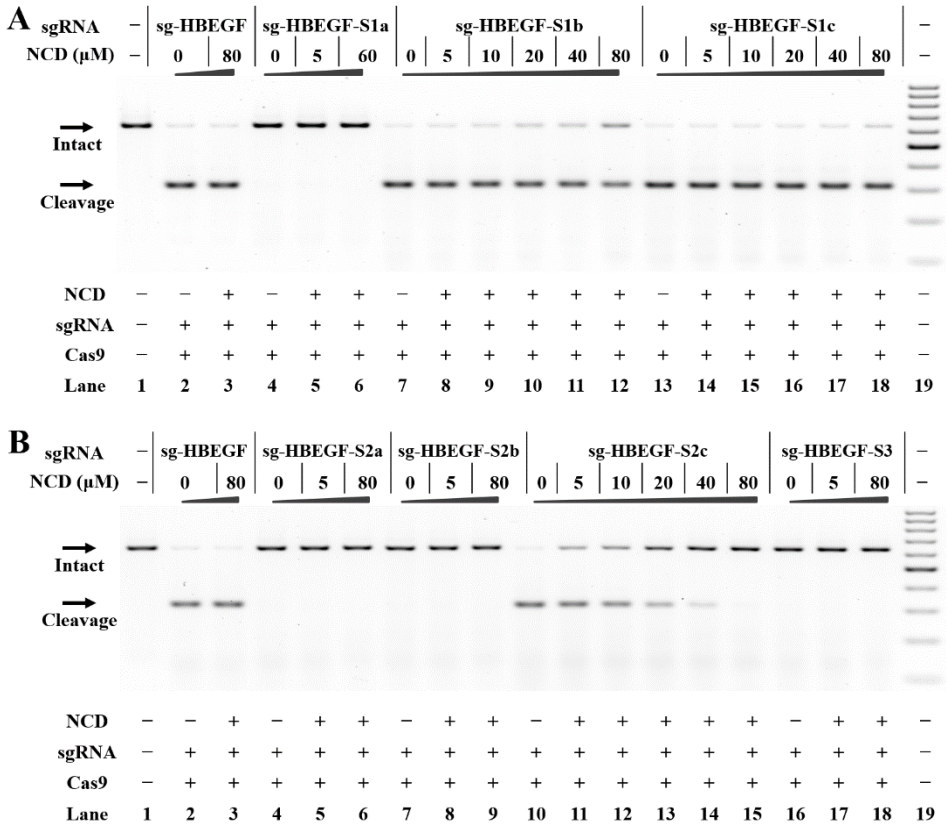

Figure S15. Ligand control of sequence-modified sg-HBEGF for switching CRISPR/Cas9

Reactions were performed as described in the Experimental Section. Uncleaved HBEGF DNA (621 bp) cut to shorter cleavage fragments (311 bp and 310 bp) were demonstrated. All samples were tested in three biological replicates. Image of representative data is shown here. (**A**) The NCD-dependent inhibition CRISPR/Cas9 with single-site variants. Lane 1: no Cas9 control; lanes 2-3 contain original sg-HBEGF; lanes 4-6 contain sg-HBEGF-S1a; lanes 7-12 contain sg-HBEGF-S1b; lanes 13-18 contain sg-HBEGF-S1c; lane 19: DNA marker (GeneRuler 100-bp DNA Ladder). (**B**) The NCD-dependent inhibition of CRISPR/Cas9 with multi-nucleotide variants. Lane 1: no Cas9 control; lanes 2-3 contain original sg-HBEGF; lanes 4-6 contain sg-HBEGF-S2a; lanes 7-9 contain sg-HBEGF-S2b; lanes 10-15 contain sg-HBEGF-S2c; lanes 16-18 contain sg-HBEGF-S3; lane 19: DNA marker.

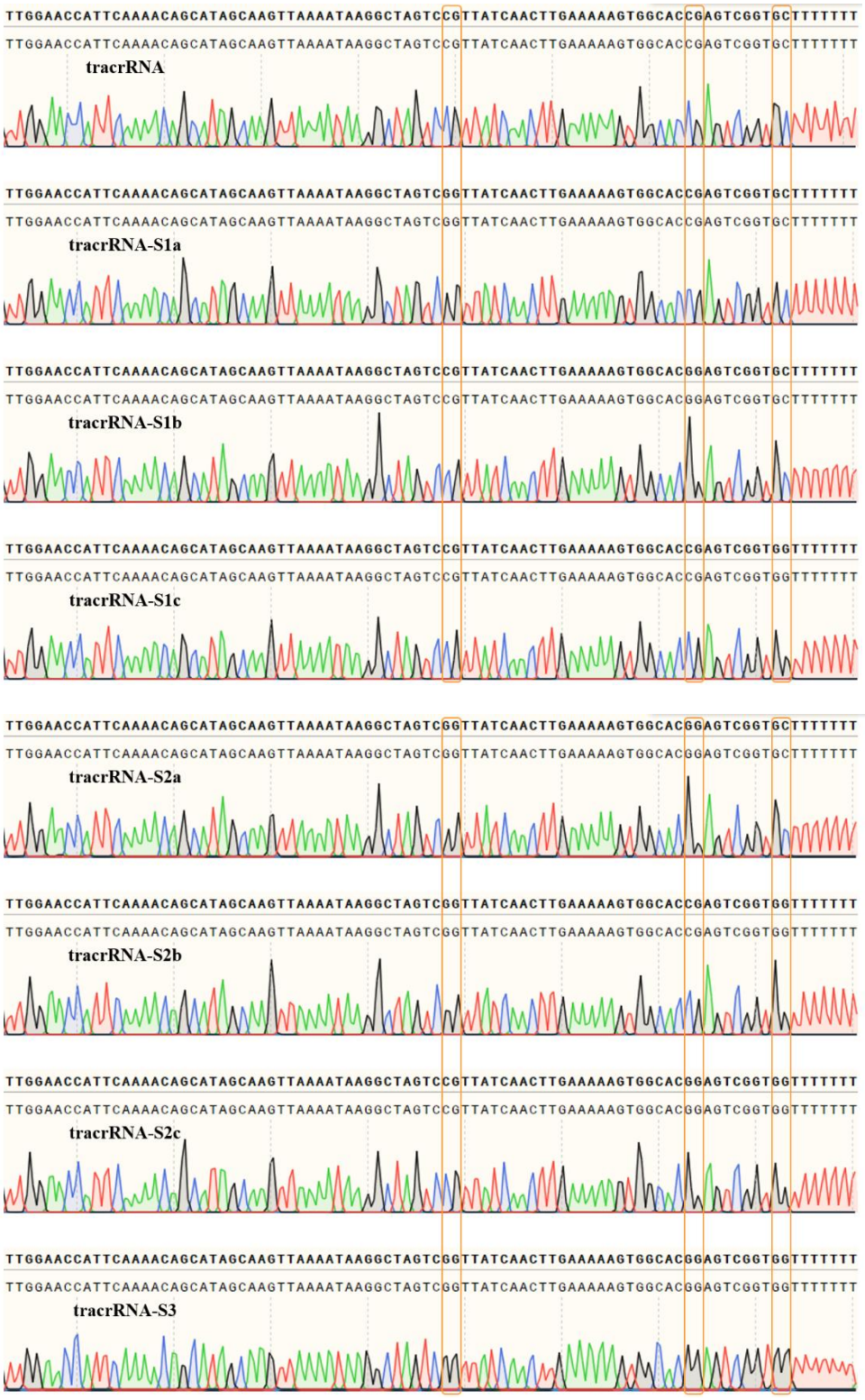

Figure S16. Sanger sequencing analysis of each designer tracrRNA.
The sites for engineering are indicated.

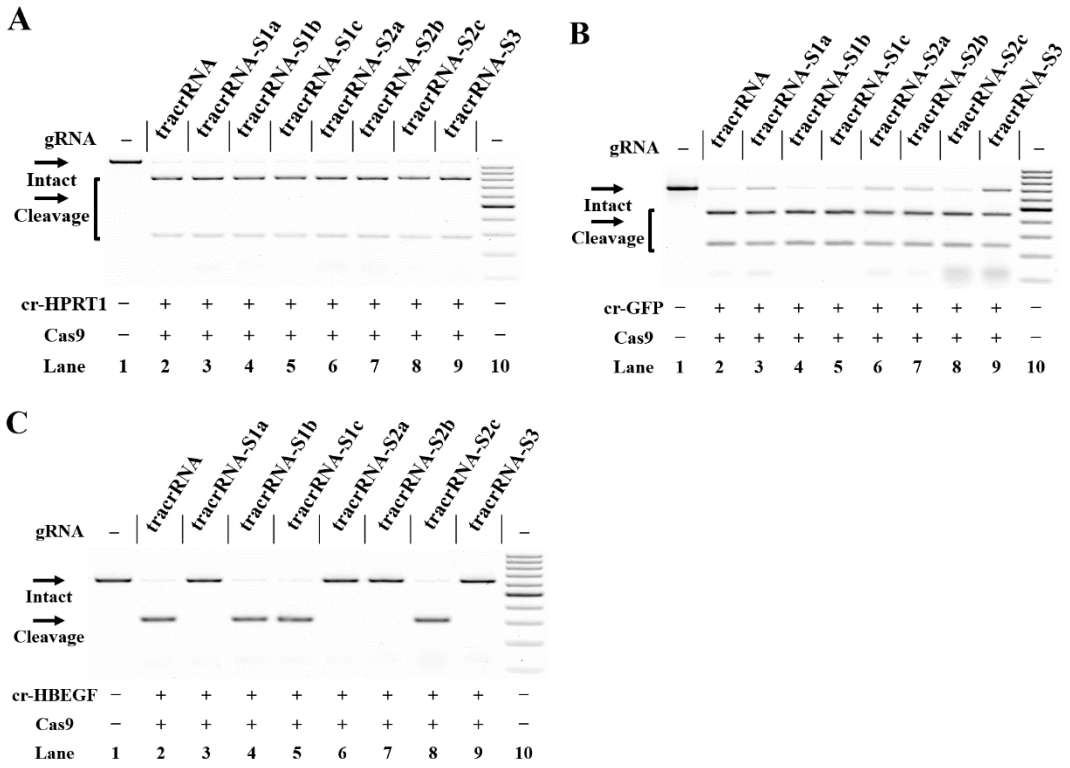

Figure S17. The tolerance of Cas9 to each designer tracrRNA.

Reactions were performed as described in the Experimental Section. All samples were tested in three biological replicates. Image of representative data is shown here. (**A**) Uncleaved HPRT1 DNA (1083 bp) cut to shorter cleavage fragments (803 bp and 280 bp) are demonstrated. Lane 1: no Cas9 control; lane 2 contains cr-HPRT1 and original tracrRNA; lanes 3-9 contain cr-HPRT1 and designer tracrRNAs harboring different MBL-binding units; lane 10: DNA marker (GeneRuler 100-bp DNA Ladder). (**B**) Uncleaved GFP DNA (702 bp) cut to shorter cleavage fragments (469 bp and 233 bp) are demonstrated. Lane 1: no Cas9 control; lane 2 contains cr-GFP and original tracrRNA; lanes 3-9 contain cr-GFP and designer tracrRNAs harboring different MBL-binding units; lane 10: DNA marker. (**C**) Uncleaved HBEGF DNA (621 bp) cut to shorter cleavage fragments (311 bp and 310 bp) are demonstrated. Lane 1: no Cas9 control; lane 2 contains cr-HBEGF and original tracrRNA; lanes 3-9 contain cr-HBEGF and designer tracrRNAs harboring different MBL-binding units; lane 10: DNA marker.

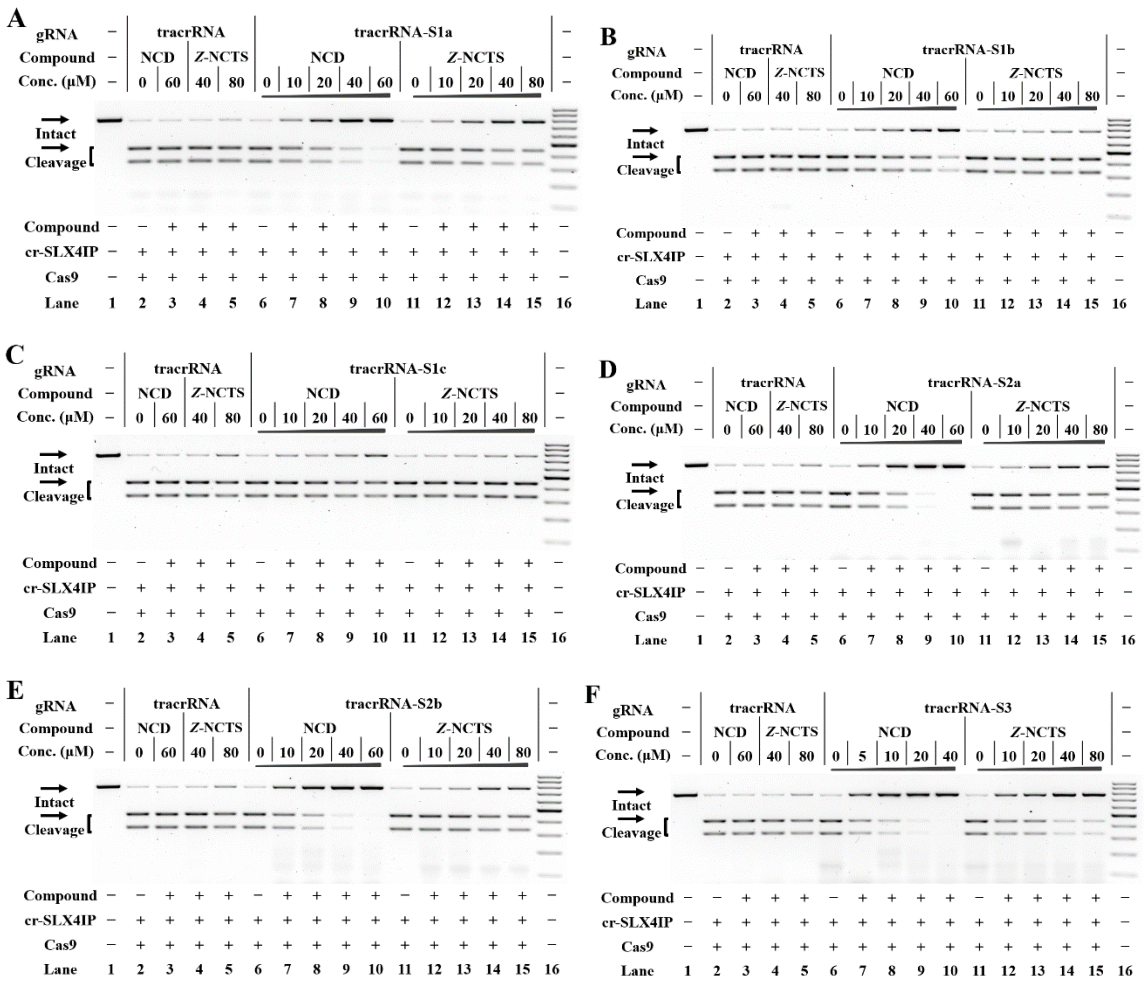

Figure S18. Responsiveness of CRISPR/Cas9 with cr-SLX4IP and designer tracrRNAs to different MBLs.

Reactions were performed as described in the Experimental Section. Uncleaved SLX4IP DNA (773 bp) cut to shorter cleavage fragments (441 bp and 332 bp) are demonstrated. All samples were tested in three biological replicates. Image of representative data is shown here. A 2-fold increase in concentration for NCD and *Z*-NCTS showed significant differences in switching CRISPR/Cas9. (**A**)-(**F**): Responsiveness of tracrRNA-S1a (**A**), tracrRNA-S1b (**B**), tracrRNA-S1c (**C**), tracrRNA-S2a (**D**), tracrRNA-S2b (**E**), tracrRNA-S3 (**F**) to each MBL. For (**A**)-(**F**), lane 1: no Cas9 control; lanes 2-5 contain cr-SLX4IP and original tracrRNA; lanes 6-10, 11-15 contain cr-SLX4IP and designer tracrRNAs harboring MBL-binding units; lane 16: DNA marker (GeneRuler 100-bp DNA Ladder).

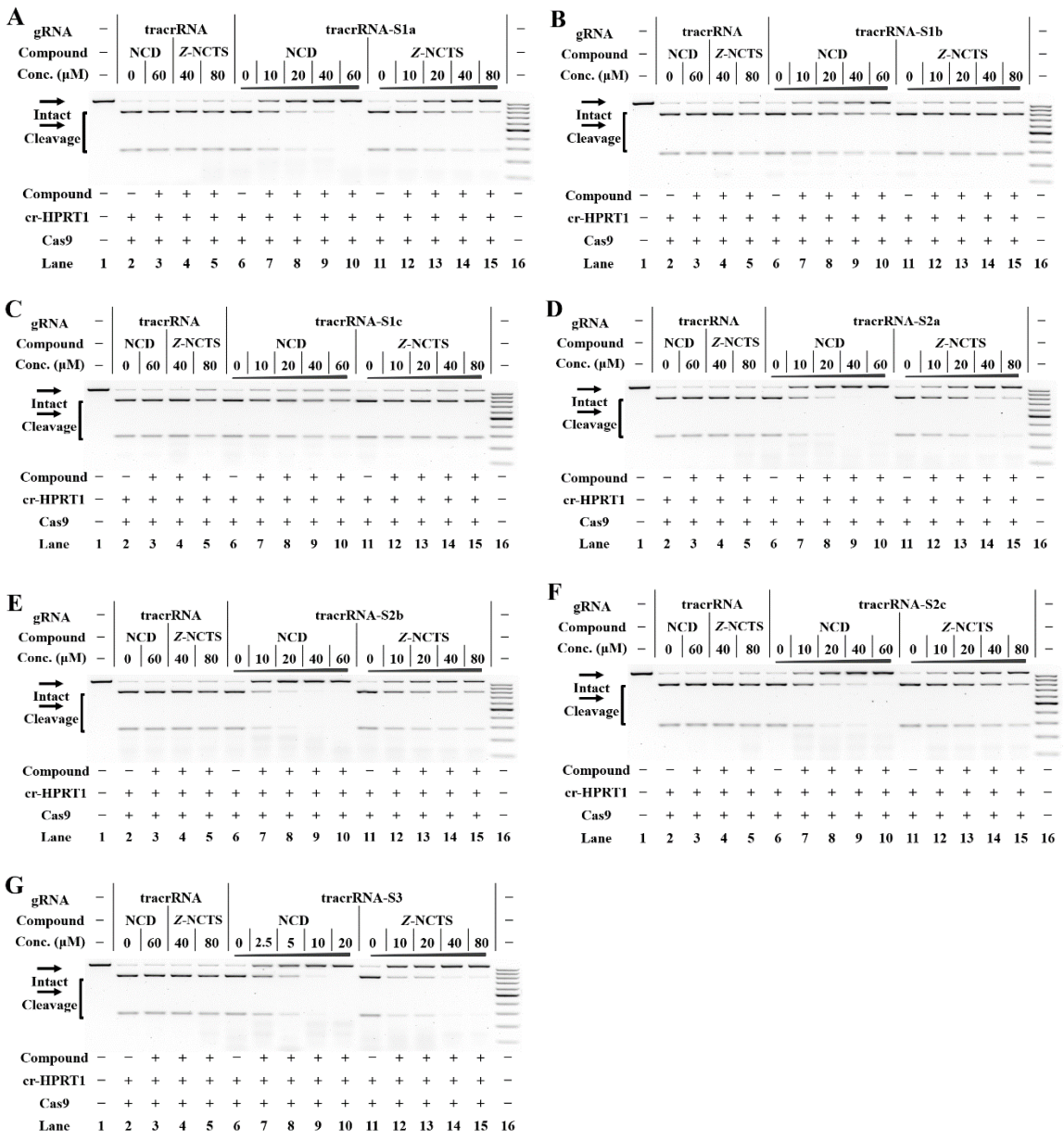

Figure S19. Responsiveness of CRISPR/Cas9 with cr-HPRT1 and designer tracrRNAs.

Reactions were performed as described in the Experimental Section. Uncleaved HPRT1 DNA (1083 bp) cut to shorter cleavage fragments (803 bp and 280 bp) are demonstrated. All samples were tested in three biological replicates. Image of representative data is shown here. A 2-fold increase in concentration for NCD and *Z*-NCTS showed significant differences in switching CRISPR/Cas9. (**A**)-(**G**): Responsiveness of tracrRNA-S1a (**A**), tracrRNA-S1b (**B**), tracrRNA-S1c (**C**), tracrRNA-S2a (**D**), tracrRNA-S2b (**E**), tracrRNA-S2c (**F**), tracrRNA-S3 (**G**) to each MBL. For (**A**)-(**G**), lane 1: no Cas9 control; lanes 2-5 contain cr-HPRT1 and original tracrRNA; lanes 6-10, 11-15 contain cr-HPRT1 and designer tracrRNAs harboring MBL-binding units; lane 16: DNA marker (GeneRuler 100-bp DNA Ladder).

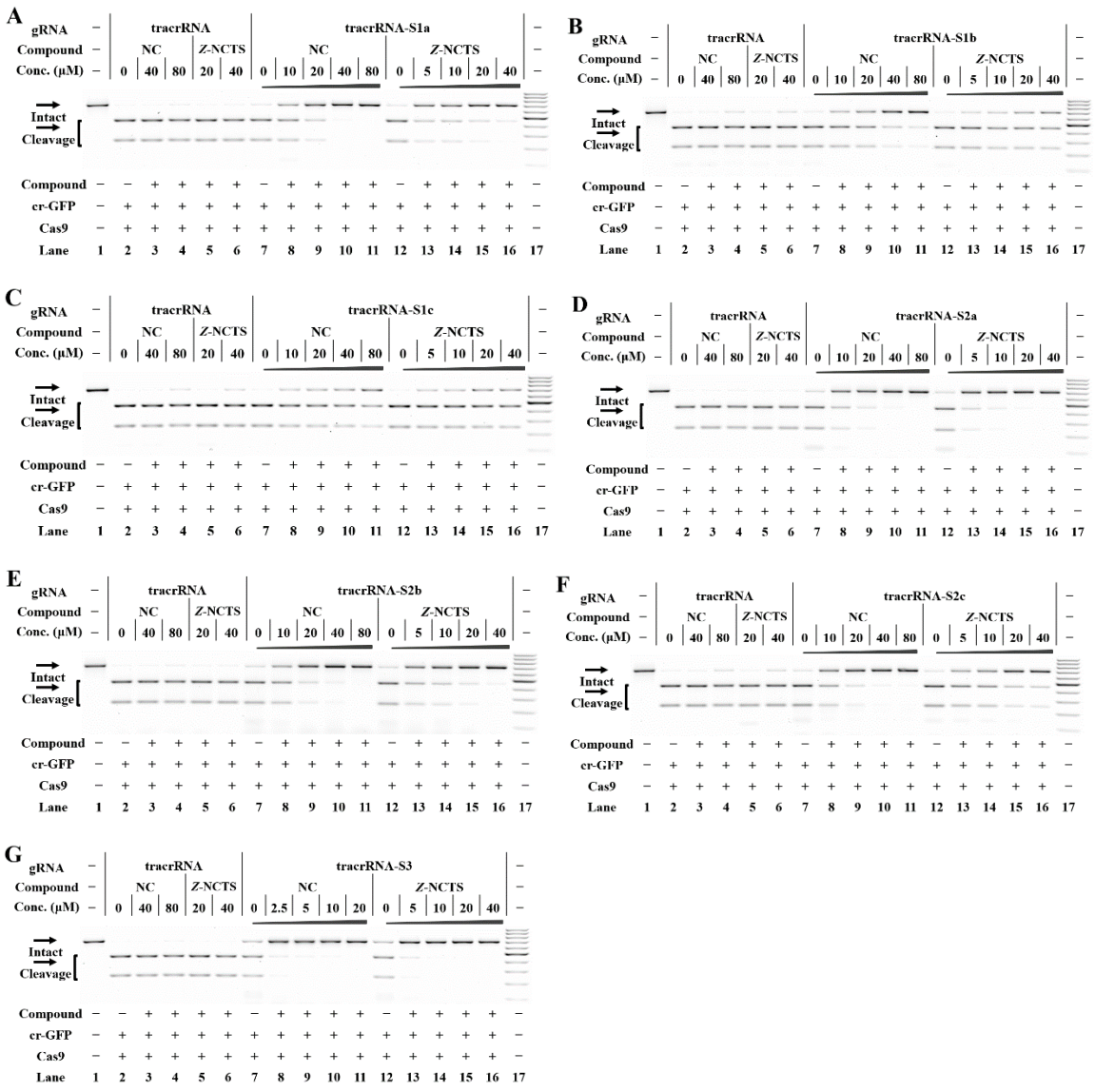

Figure S20. Responsiveness of CRISPR/Cas9 with cr-GFP and designer tracrRNAs.

Reactions were performed as described in the Experimental Section. Uncleaved GFP DNA (702 bp) cut to shorter cleavage fragments (469 bp and 233 bp) are demonstrated. All samples were tested in three biological replicates. Image of representative data is shown here. A 2-fold increase in concentration for NCD and *Z*-NCTS showed significant differences in switching CRISPR/Cas9. (**A**)-(**G**): Responsiveness of tracrRNA-S1a (**A**), tracrRNA-S1b (**B**), tracrRNA-S1c (**C**), tracrRNA-S2a (**D**), tracrRNA-S2b (**E**), tracrRNA-S2c (**F**), tracrRNA-S3 (**G**) to each MBL. For (**A**)-(**G**), lane 1: no Cas9 control; lanes 2-6 contain cr-GFP and original tracrRNA; lanes 7-11, 12-16 contain cr-GFP and designer tracrRNAs harboring MBL-binding units; lane 17: DNA marker (GeneRuler 100-bp DNA Ladder).

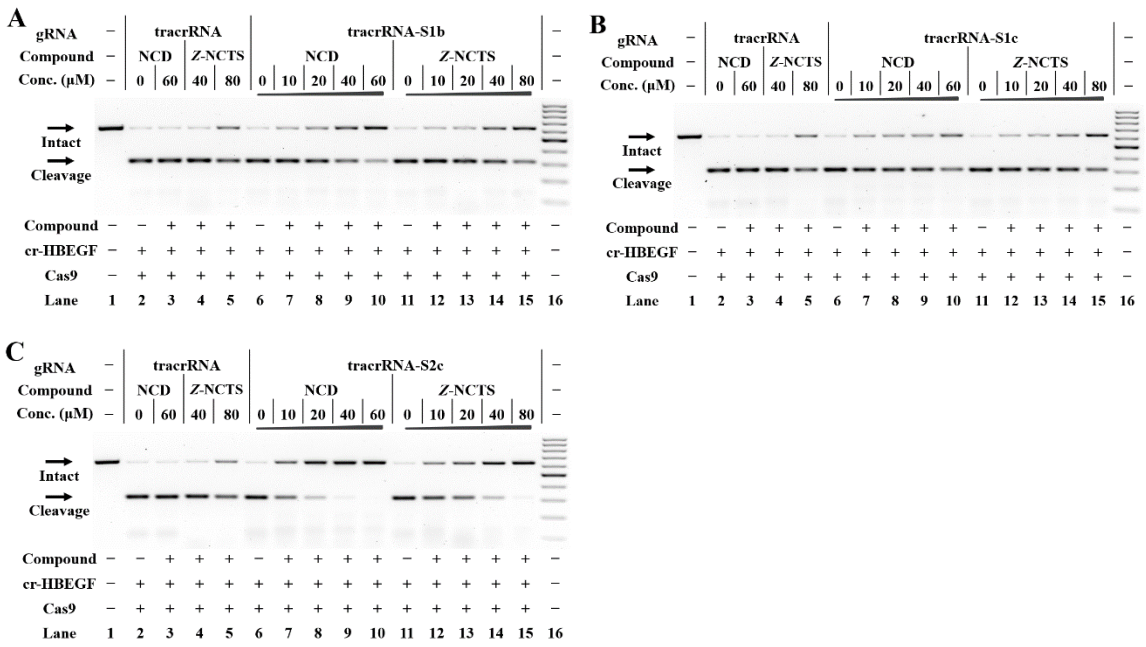

Figure S21. Responsiveness of CRISPR/Cas9 with cr-HBEGF and designer tracrRNAs.

Reactions were performed as described in the Experimental Section. Uncleaved HBEGF DNA (621 bp) cut to shorter cleavage fragments (311 bp and 310 bp) were demonstrated. All samples were tested in three biological replicates. Image of representative data is shown here. A 2-fold increase in concentration for NCD and *Z*-NCTS showed significant differences in switching CRISPR/Cas9. (**A**)-(**C**): Responsiveness of tracrRNA-S1b (**A**), tracrRNA-S1c (**B**) and tracrRNA-S2c (**C**) to each MBL. For (**A**)-(**C**), lane 1: no Cas9 control; lanes 2-5 contain cr-HBEGF and original tracrRNA; lanes 6-10, 11-15 contain cr-HBEGF and designer tracrRNAs harboring MBL-binding units; lane 16: DNA marker (GeneRuler 100-bp DNA Ladder).

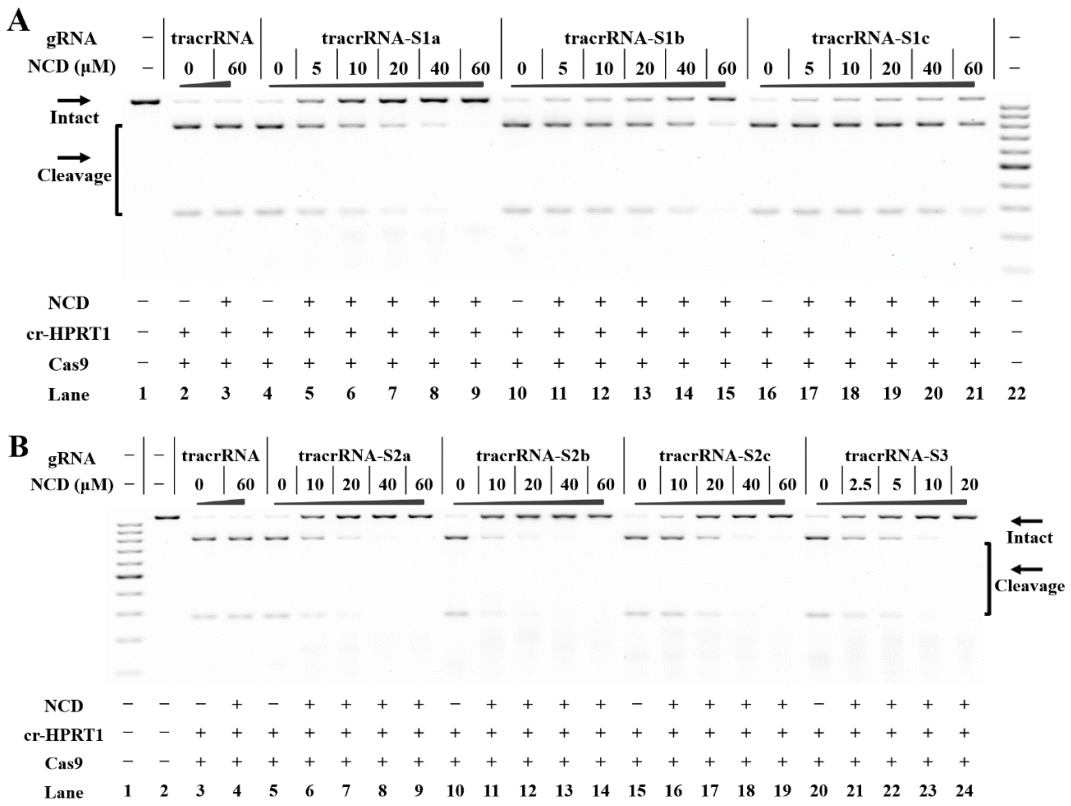

Figure S22. Ligand control of CRISPR/Cas9 with cr-HPRT1 and designer tracrRNAs.

Reactions were performed as described in the Experimental Section. Uncleaved HPRT1 DNA (1083 bp) cut to shorter cleavage fragments (803 bp and 280 bp) are demonstrated. All samples were tested in three biological replicates. Image of representative data is shown here. (**A**) Effects of NCD on the function of tracrRNA and its single-site variants to support Cas9-mediated DNA cleavage. Lane 1: no Cas9 control; lanes 2-3 contain cr-HPRT1 and original tracrRNA; lanes 4-9 contain cr-HPRT1 and tracrRNA-S1a; lanes 10-15 contain cr-HPRT1 and tracrRNA-S1b; lanes 16-21 contain cr-HPRT1 and tracrRNA-S1c; lane 22: DNA marker (GeneRuler 100-bp DNA Ladder). (**B**) Effects of NCD on the function of tracrRNA and its multi-nucleotide variants to support Cas9-mediated DNA cleavage. Lane 1: DNA marker; lane 2: no Cas9 control; lanes 3-4 contain cr-HPRT1 and original tracrRNA; lanes 5-9 contain cr-HPRT1 and tracrRNA-S2a; lanes 10-14 contain cr-HPRT1 and tracrRNA-S2b; lanes 15-19 contain cr-HPRT1 and tracrRNA-S2c; lanes 20-24 contain cr-HPRT1 and tracrRNA-S3.

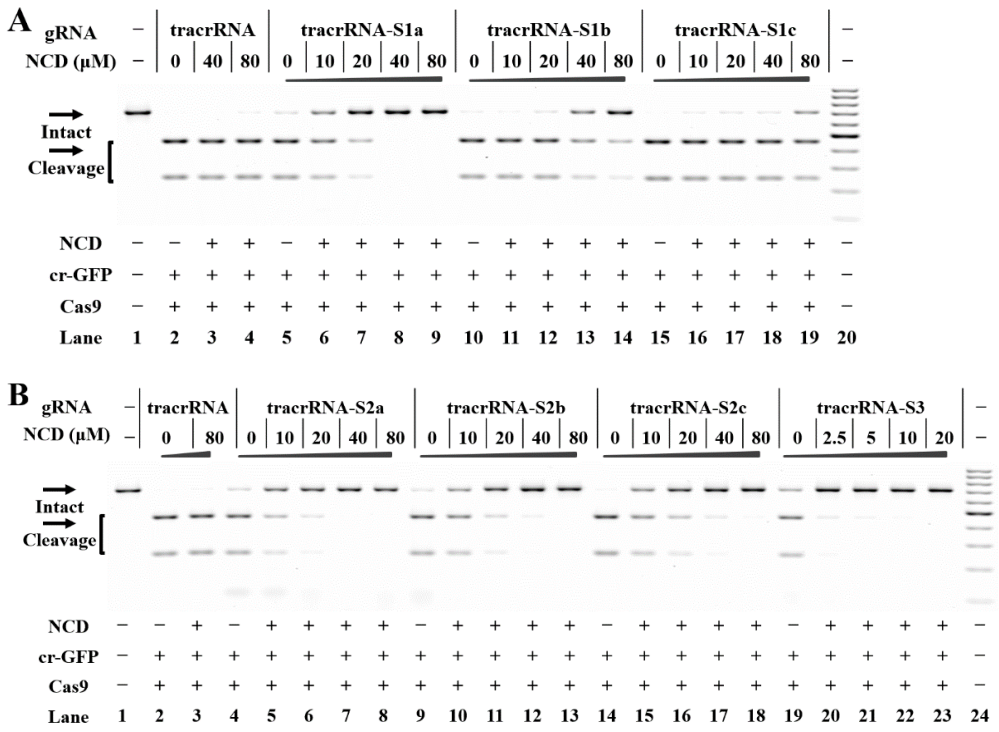

Figure S23. Ligand control of CRISPR/Cas9 with cr-GFP and designer tracrRNAs.

Reactions were performed as described in the Experimental Section. Uncleaved GFP DNA (702 bp) cut to shorter cleavage fragments (469 bp and 233 bp) are demonstrated. All samples were tested in three biological replicates. Image of representative data is shown here. (**A**) Effects of NCD on the function of tracrRNA and its single-site variants to support Cas9-mediated DNA cleavage. Lane 1: no Cas9 control; lanes 2-3 contain cr-GFP and original tracrRNA; lanes 4-9 contain cr-GFP and tracrRNA-S1a; lanes 10-14 contain cr-GFP and tracrRNA-S1b; lanes 15-19 contain cr-GFP and tracrRNA-S1c; lane 20: DNA marker (GeneRuler 100-bp DNA Ladder). (**B**) Effects of NCD on the function of tracrRNA and its multi-nucleotide variants to support Cas9-mediated DNA cleavage. Lane 1: no Cas9 control; lanes 2-3 contain cr-GFP and original tracrRNA; lanes 4-8 contain cr-GFP and tracrRNA-S2a; lanes 9-13 contain cr-GFP and tracrRNA-S2b; lanes 14-18 contain cr-GFP and tracrRNA-S2c; lanes 19-23 contain cr-GFP and tracrRNA-S3; lane 24: DNA marker.

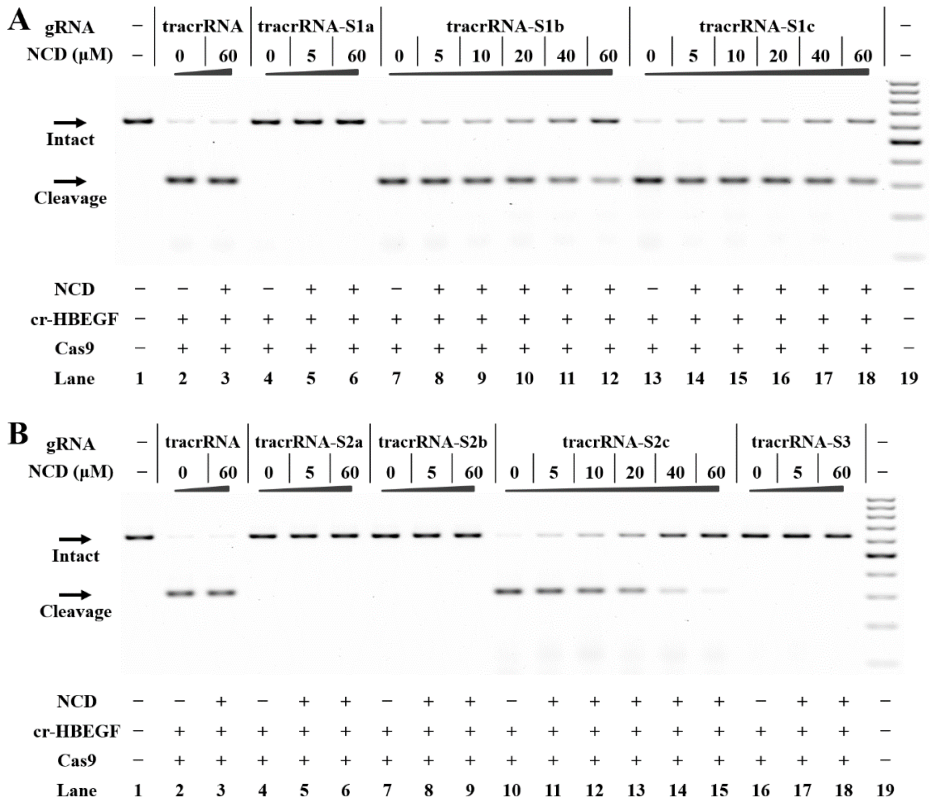

Figure S24. Ligand control of CRISPR/Cas9 with cr-HBEGF and designer tracrRNAs.

Reactions were performed as described in the Experimental Section. Uncleaved HBEGF DNA (621 bp) cut to shorter cleavage fragments (311 bp and 310 bp) were demonstrated. All samples were tested in three biological replicates. Image of representative data is shown here. (**A**) Effects of NCD on the function of tracrRNA and its single-site variants to support Cas9-mediated DNA cleavage. Lane 1: no Cas9 control; lanes 2-3 contain cr-HBEGF and original tracrRNA; lanes 4-6 contain cr-HBEGF and tracrRNA-S1a; lanes 7-12 contain cr-HBEGF and tracrRNA-S1b; lanes 13-18 contain cr-HBEGF and tracrRNA-S1c; lane 19: DNA marker (GeneRuler 100-bp DNA Ladder). (**B**) Effects of NCD on the function of tracrRNA and its multi-nucleotide variants to support Cas9-mediated DNA cleavage. Lane 1: no Cas9 control; lanes 2-3 contain cr-HBEGF and original tracrRNA; lanes 4-6 contain cr-HBEGF and tracrRNA-S2a; lanes 7-9 contain cr-HBEGF and tracrRNA-S2b; lanes 10-15 contain cr-HBEGF and tracrRNA-S2c; lanes 16-18 contain cr-HBEGF and tracrRNA-S3; lane 19: DNA marker.

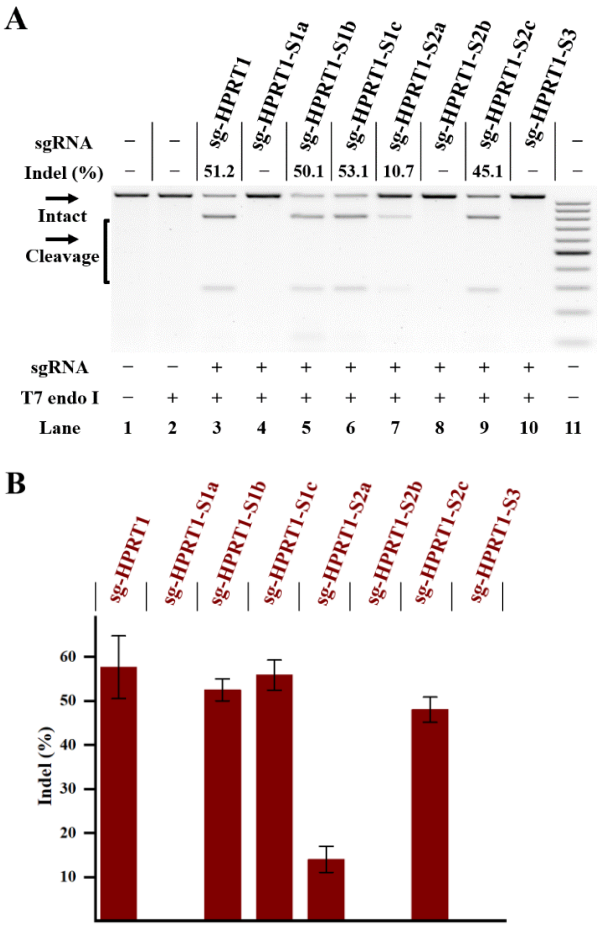

Figure S25. Efficiency of designer sgRNAs targeting the *HPRT1* gene in a stable Cas9-expressing cell line.

Cellular studies were performed using HeLa-OC cells as described in the Experimental Section. The sgRNAs were delivered into HeLa-OC cells using Lipofectamine 3000. The treatment for each sample is indicated by the signs at the bottom of each lane. All samples were tested in three biological replicates. Image of representative data is shown here. (**A**) Editing of *HPRT1* gene in HeLa-OC cells using the indicated sgRNAs. Uncleaved HPRT1 DNA (1083 bp) cut to shorter cleavage fragments (803 bp and 280 bp) are demonstrated. Lane 1: target control; lane 2: no sgRNA control; lane 3 contains original sg-HPRT1; lanes 4-10 contain designer sgRNAs harboring different MBL-binding units; lane 11: DNA marker (GeneRuler 100-bp DNA Ladder). (**B**). The effect of sequence modification on the function of sgRNAs in cells. The data represent the mean of three replicates and were shown as mean ± SEM.

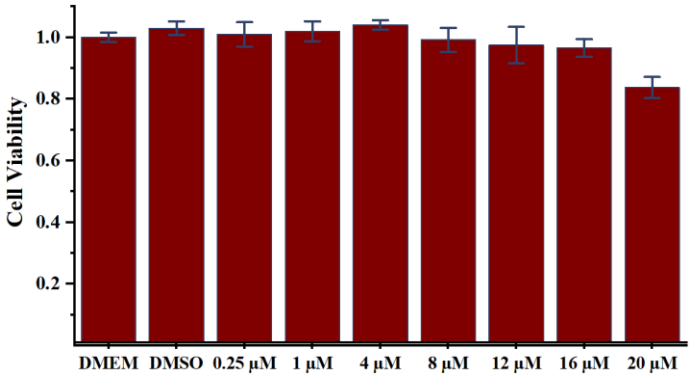

Figure S26. The tolerance of HeLa-OC cells to NCD.

HeLa-OC cells were treated with NCD at different concentrations and toxicity was measured using the the 3-(4,5-dimethylthiazol-2-yl)-2,5-diphenyltetrazolium bromide (MTT) cytotoxicity assay. Values were plotted relative to the mean of DMEM control set to 100% (= relative growth). All data were presented as the means ± SEM from three independent experiments. Error bars: ± SEM. The cytotoxicity threshold for NCD was higher than 16 μM.

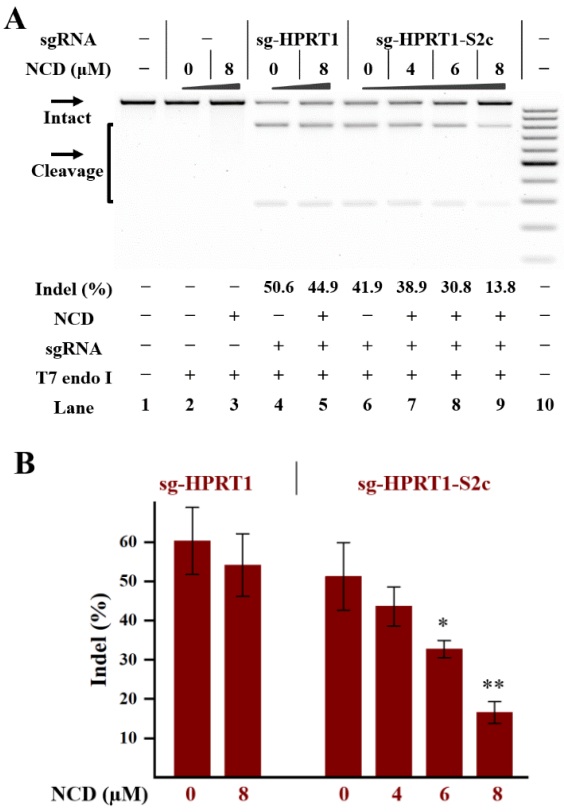

Figure S27. Ligand control of designer sgRNAs in a stable Cas9-expressing cell line.

Cellular studies were performed using HeLa-OC cells as described in the Experimental Section. Hela-OC cells were exposed to the NCD ligand for 24 hr before being harvested for DNA cleaving activity assessments. All samples were tested in three biological replicates. Image of representative data is shown here. (**A**) Ligand control of designer sgRNAs targeting the *HPRT1* gene in HeLa-OC cells. Uncleaved HPRT1 DNA (1083 bp) cut to shorter cleavage fragments (803 bp and 280 bp) are demonstrated. Lane 1: target control; lanes 2-3: no sgRNA control; lanes 4-5 contain original sg-HPRT1; lanes 6-9 contain sg-SLX4IP-S2c; lane 10: DNA marker (GeneRuler 100-bp DNA Ladder). (**B**) Bar graph shows the effect of NCD on the function of sgRNAs in HeLa-OC cells. The data represent the mean of three replicates and are shown as mean ± SEM. In each group, the indel formation of NCD-treated cells were compared to that of mock-treated cells. P values less than 0.05 are given one asterisk, and P values less than 0.01 are given two asterisks.

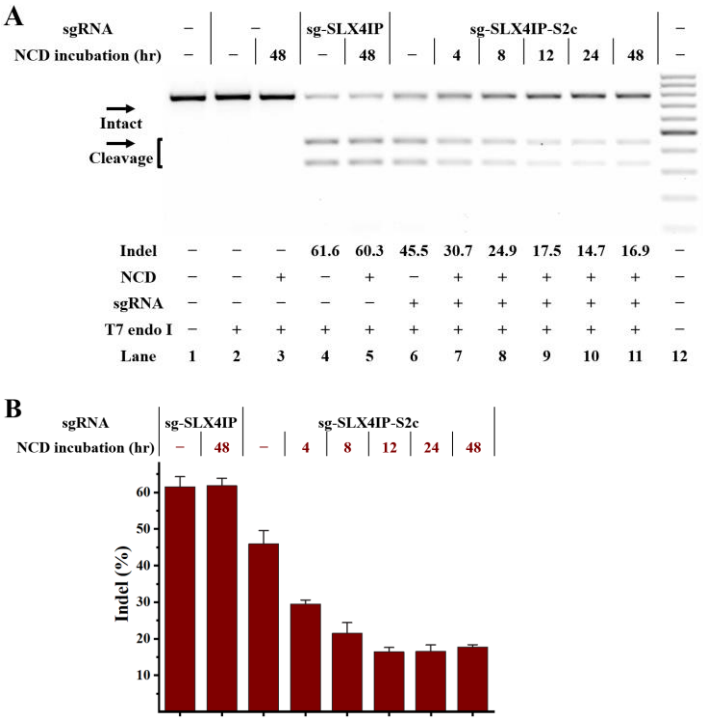

Figure S28. The time-dependent experiment to characterize in cellular potency of NCD.

Cellular studies were performed using HeLa-OC cells. Hela-OC cells were exposed to the NCD ligand for different periods before being harvested for DNA cleaving activity assessments. All samples were tested in three biological replicates. Image of representative data is shown here. (**A**) The time-dependent experiment to characterize in cellular potency of NCD. Uncleaved SLX4IP DNA (773 bp) cut to shorter cleavage fragments (441 bp and 332 bp) are demonstrated. Lane 1: target control; lanes 2-3: no sgRNA control; lanes 4-5 contain original sg-SLX4IP; lanes 6-11 contain sg-SLX4IP-S2c; lane 12: DNA marker (GeneRuler 100-bp DNA Ladder). (**B**) Bar graph shows the effect of NCD on the function of sgRNAs in HeLa-OC cells. The data represent the mean of three replicates and are shown as mean ± SEM.

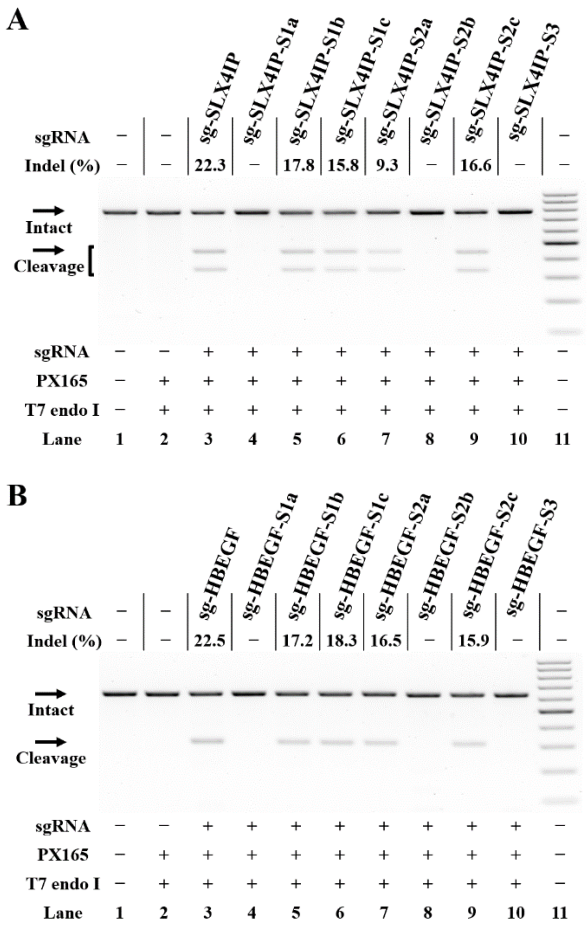

Figure S29. Efficiency of the hybrid system with IVT sgRNAs and Cas9-only plasmids.

Cellular studies were performed as described in the Experimental Section. The sgRNAs and plasmids were delivered into HeLa cells using Lipofectamine 3000. The treatment for each sample is indicated by the signs at the bottom of each lane. All samples were tested in three biological replicates. Image of representative data is shown here. (**A**) Editing of *SLX4IP* gene in HeLa-OC cells using the hybrid system. Uncleaved SLX4IP DNA (773 bp) cut to shorter cleavage fragments (441 bp and 332 bp) are demonstrated. Lane 1: target control; lane 2: no sgRNA control; lane 3 contains PX165 and original sg-SLX4IP; lanes 4-10 contain PX165 and designer sgRNAs harboring different MBL-binding units; lane 11: DNA marker (GeneRuler 100-bp DNA Ladder). (**B**) Editing of *HBEGF* gene in HeLa-OC cells using the hybrid system. Uncleaved HBEGF DNA (621 bp) cut to shorter cleavage fragments (311 bp and 310 bp) were demonstrated. Lane 1: target control; lane 2: no sgRNA control; lane 3 contains PX165 and original sg-HBEGF; lanes 4-10 contain PX165 and designer sgRNAs harboring different MBL-binding units; lane 11: DNA marker.

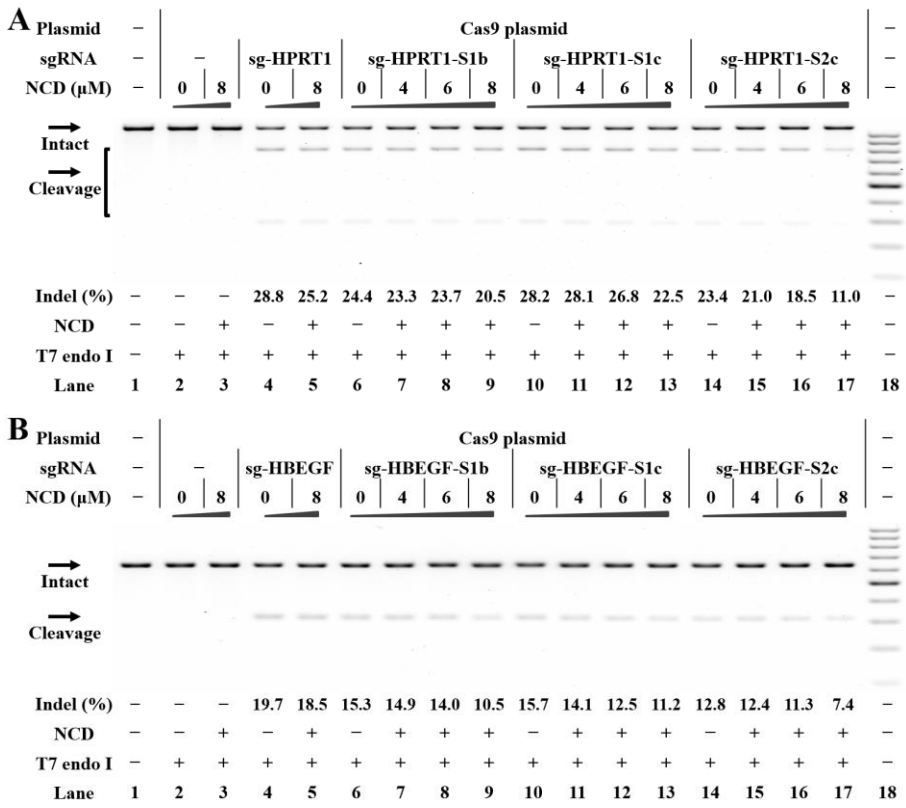

Figure S30. Ligand control of the hybrid system with IVT sgRNAs and Cas9-only plasmids.

Cellular studies were performed as described in the Experimental Section. The plasmids and sgRNAs were delivered into HeLa cells before the treatment with NCD. Hela cells were exposed to the NCD ligand for 24 hr before being harvested for DNA cleaving activity assessments. All samples were tested in three biological replicates. Image of representative data is shown here. (**A**) Ligand control of the hybrid system with PX165 and sgRNA targeting the *HPRT1* gene. Uncleaved HPRT1 DNA (1083 bp) cut to shorter cleavage fragments (803 bp and 280 bp) are demonstrated. Lane 1: target control; lanes 2-3: no sgRNA control; lanes 4-5 contain PX165 and original sg-HPRT1; lanes 6-9 contain PX165 and sg-HPRT1-S1b; lanes 10-13 contain PX165 and sg-HPRT1-S1c; lanes 14-17 contain PX165 and sg-HPRT1-S2c; lane 18: DNA marker (GeneRuler 100-bp DNA Ladder). (**B**) Ligand control of the hybrid system with PX165 and sgRNA targeting the *HBEGF* gene. Uncleaved HBEGF DNA (621 bp) cut to shorter cleavage fragments (311 bp and 310 bp) were demonstrated. Lane 1: target control; lanes 2-3: no sgRNA control; lanes 4-5 contain PX165 and original sg-HBEGF; lanes 6-9 contain PX165 and sg-HBEGF-S1b; lanes 10-13 contain PX165 and sg-HBEGF-S1c; lanes 14-17 contain PX165 and sg-HBEGF-S2c; lane 18: DNA marker.

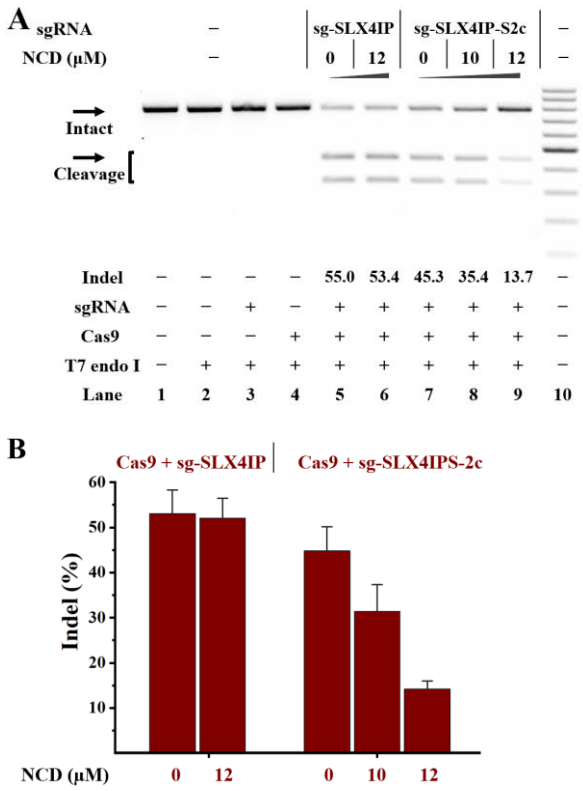

Figure S31. Cas9 RNP study of using Cas9 protein along with different IVT sgRNAs.

30 picomole EnGen Spy Cas9 NLS protein with 45 picomole sgRNAs were electroporated into 8 × 10^5 HeLa cells before the treatment with NCD. The electroporation was performed using a Lonza 4D-Nucleofector X unit in 100 μL SE buffer using SE-CN114 as the program according to the manufacturer's protocol. Cells were further cultured at 37 °C in 5 % CO_2 for an additional 24 hr. The target editing efficiency and inhibition thereof were quantified by T7E1 assay. The treatment for each sample is indicated by the signs at the bottom of each lane. All samples were tested in three biological replicates. Image of representative data is shown here. (**A**) Cas9 RNP study of using Cas9 protein along with different IVT sgRNAs. Uncleaved SLX4IP DNA (773 bp) cut to shorter cleavage fragments (441 bp and 332 bp) are demonstrated. Lane 1: target control; lane 2: T7 endo I control; lane 3: sgRNA-only control; lane 4: Cas9-only control; lanes 5-6 contain Cas9/sg-SLX4IP; lanes 7-9 contain Cas9/sg-SLX4IP-S2c; lane 10: DNA marker (GeneRuler 100-bp DNA Ladder). (**B**) Bar graph shows the effect of NCD on the function of Cas9 RNP in HeLa cells. The data represent the mean of three replicates and are shown as mean ± SEM.

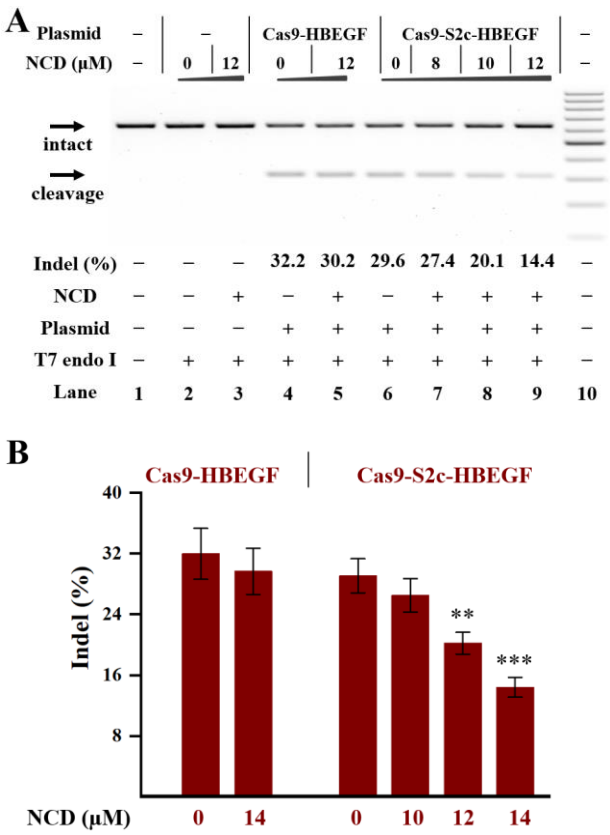

Figure S32. Ligand control of all-in-one plasmids with MBL-binding units.

Cellular studies were performed as described in the Experimental Section. Each complete plasmid was delivered into HeLa cells before the NCD treatment. Hela cells were exposed to the NCD ligand for 24 hr before being harvested for DNA cleaving activity assessments. All samples were tested in three biological replicates. Image of representative data is shown here. (**A**) Ligand control of designer plasmids targeting the *HBEGF* gene. Uncleaved HBEGF DNA (621 bp) cut to shorter cleavage fragments (311 bp and 310 bp) were demonstrated. Lane 1: target control; lanes 2-3: no plasmid control; lanes 4-5 contain PX459-HBEGF; lanes 6-9 contain PX459-S2c-HBEGF; lane 10: DNA marker (GeneRuler 100-bp DNA Ladder). (**B**) Bar graph shows the effect of NCD on the function of all-in-one plasmids. The data are presented as the means ± SEM from three independent experiments. In each group, the indel formation of NCD-treated cells were compared to that of mock-treated cells. P values less than 0.01 are given two asterisks, and P values less than 0.001 are given three asterisks.

Table S1. DNA and RNA sequences used in the current study.

Oligomer	Sequence(from 5'to 3')	Construct
R-SL1	5'-AGGCUAGUCCGU-3'	
R-SL1-S1a	5'-AGGCUAGUCGGU-3'	
R-SL3	5'-UGGCACCGAGUCGGUGCU-3'	
R-SL3-S1b	5'-UGGCACGGAGUCGGUGCU-3'	
R-SL3-S1c	5'-UGGCACCGAGUCGGUGGU-3'	
R-SL3-S2	5'-UGGCACGGAGUCGGUGGU-3'	
sg-HPRT1-F	5'-TCTAATACGACTCACTATAGGGCCCAAGGAAAGACTATGAAAGTTTTAGAGCTAGAAATAGCAAGTTAAAATA-3'	Forward primer for each sg-HPRT1 construct
sg-SLX4IP-F	5'-TCTAATACGACTCACTATAGGGCCACAGCCAGGATTTAAGAGTTTTAGAGCTAGAAATAGCAAGTTAAAATA-3'	Forward primer for each sg-SLX4IP construct
sg-GFP-F	5'-TCTAATACGACTCACTATAGGGATGCCGTTCTTCTGCTTGTGTTTTAGAGCTAGAAATAGCAAGTTAAAATA-3'	Forward primer for each sg-GFP construct
sg-HBEGF-F	5'-TCTAATACGACTCACTATAGGGTTCTCTCGGCACTGGTGACGTTTTAGAGCTAGAAATAGCAAGTTAAAATA-3'	Forward primer for each sg-HBEGF construct
sgRNA-R	5'-AAAAGCACCGACTCGGTGCCACTTTTTCAAGTTGATAACGGACTAGCCTTATTTTAACTTGCTATTTCTA-3'	Reverse primer for each sgRNA construct
sgRNA-S1a-R	5'-AAAAGCACCGACTCGGTGCCACTTTTTCAAGTTGATAACCGACTAGCCTTATTTTAACTTGCTATTTCTA	Reverse primer for each sgRNA-S1a construct
sgRNA-S1b-R	5'-AAAAGCACCGACTCCGTGCCACTTTTTCAAGTTGATAACGGACTAGCCTTATTTTAACTTGCTATTTCTA	Reverse primer for each sgRNA-S1b construct
sgRNA-S1c-R	5'-AAAACCACCGACTCGGTGCCACTTTTTCAAGTTGATAACGGACTAGCCTTATTTTAACTTGCTATTTCTA	Reverse primer for each sgRNA-S1c construct
sgRNA-S2a-R	5'-AAAAGCACCGACTCCGTGCCACTTTTTCAAGTTGATAACCGACTAGCCTTATTTTAACTTGCTATTTCTA	Reverse primer for each sgRNA-S2a construct
sgRNA-S2b-R	AAAACCACCGACTCGGTGCCACTTTTTCAAGTTGATAACCGACTAGCCTTATTTTAACTTGCTATTTCTA	Reverse primer for each sgRNA-S2b construct
sgRNA-S2c-R	5'-AAAACCACCGACTCCGTGCCACTTTTTCAAGTTGATAACGGACTAGCCTTATTTTAACTTGCTATTTCTA	Reverse primer for each sgRNA-S2c construct
sgRNA-S3-R	5'-AAAACCACCGACTCCGTGCCACTTTTTCAAGTTGATAACCGACTAGCCTTATTTTAACTTGCTATTTCTA	Reverse primer for each sgRNA-S3 construct
sg-HPRT1	5'-GGGCCCAAGGAAAGACUAUGAAAGUUUUAGAGCUAGAAAUAGCAAGUUAAAAUAAGGCUAGUCCGUUAUCAACUUGAAAAAGUGGCACCGAGUCGGUGCUUUUU-3'	sgRNA

sg-HPRT1-S1a	5’-GGGCCCAAGGAAAGACUAUGAAAGUUUUAGAGCUAGAAAUAGCAAGUUAAAAUAAGGCUAGUCGGUUAUCAACUUGAAAAAGUGGCACCGAGUCGGUGCUUUUU-3’	designer sgRNA
sg-HPRT1-S1b	5’-GGGCCCAAGGAAAGACUAUGAAAGUUUUAGAGCUAGAAAUAGCAAGUUAAAAUAAGGCUAGUCCGUUAUCAACUUGAAAAAGUGGCACGGAGUCGGUGCUUUUU-3’	designer sgRNA
sg-HPRT1-S1c	5’-GGGCCCAAGGAAAGACUAUGAAAGUUUUAGAGCUAGAAAUAGCAAGUUAAAAUAAGGCUAGUCCGUUAUCAACUUGAAAAAGUGGCACCGAGUCGGUGGUUUUU-3’	designer sgRNA
sg-HPRT1-S2a	5’-GGGCCCAAGGAAAGACUAUGAAAGUUUUAGAGCUAGAAAUAGCAAGUUAAAAUAAGGCUAGUCGGUUAUCAACUUGAAAAAGUGGCACGGAGUCGGUGCUUUU-3’	designer sgRNA
sg-HPRT1-S2b	5’-GGGCCCAAGGAAAGACUAUGAAAGUUUUAGAGCUAGAAAUAGCAAGUUAAAAUAAGGCUAGUCGGUUAUCAACUUGAAAAAGUGGCACCGAGUCGGUGGUUUU-3’	designer sgRNA
sg-HPRT1-S2c	5’-GGGCCCAAGGAAAGACUAUGAAAGUUUUAGAGCUAGAAAUAGCAAGUUAAAAUAAGGCUAGUCCGUUAUCAACUUGAAAAAGUGGCACGGAGUCGGUGGUUUU-3’	designer sgRNA
sg-HPRT1-S3	5’-GGGCCCAAGGAAAGACUAUGAAAGUUUUAGAGCUAGAAAUAGCAAGUUAAAAUAAGGCUAGUCGGUUAUCAACUUGAAAAAGUGGCACGGAGUCGGUGGUUUU-3’	designer sgRNA
sg-SLX4IP	5’-GGGCCACAGCCAGGAUUUAAGAGUUUUAGAGCUAGAAAUAGCAAGUUAAAAUAAGGCUAGUCCGUUAUCAACUUGAAAAAGUGGCACCGAGUCGGUGCUUUU-3’	sgRNA
sg-SLX4IP-S1a	5’-GGGCCACAGCCAGGAUUUAAGAGUUUUAGAGCUAGAAAUAGCAAGUUAAAAUAAGGCUAGUCGGUUAUCAACUUGAAAAAGUGGCACCGAGUCGGUGCUUUU-3’	designer sgRNA
sg-SLX4IP-S1b	5’-GGGCCACAGCCAGGAUUUAAGAGUUUUAGAGCUAGAAAUAGCAAGUUAAAAUAAGGCUAGUCCGUUAUCAACUUGAAAAAGUGGCACGGAGUCGGUGCUUUU-3’	designer sgRNA
sg-SLX4IP-S1c	5’-GGGCCACAGCCAGGAUUUAAGAGUUUUAGAGCUAGAAAUAGCAAGUUAAAAUAAGGCUAGUCCGUUAUCAACUUGAAAAAGUGGCACCGAGUCGGUGGUUUU-3’	designer sgRNA

sg-SLX4IP-S2a	5’-GGGCCACAGCCAGGAUUUAAGAGUUUUAGAGCUAGAAAUAGCAAGUUAAAAUAAGGCUAGUCGGUUAUCAACUUGAAAAAGUGGCACGGAGUCGGUGCUUUU-3’	designer sgRNA
sg-SLX4IP-S2b	5’-GGGCCACAGCCAGGAUUUAAGAGUUUUAGAGCUAGAAAUAGCAAGUUAAAAUAAGGCUAGUCGGUUAUCAACUUGAAAAAGUGGCACCGAGUCGGUGGUUUU-3’	designer sgRNA
sg-SLX4IP-S2c	5’-GGGCCACAGCCAGGAUUUAAGAGUUUUAGAGCUAGAAAUAGCAAGUUAAAAUAAGGCUAGUCCGUUAUCAACUUGAAAAAGUGGCACGGAGUCGGUGGUUUU-3’	designer sgRNA
sg-SLX4IP-S3	5’-GGGCCACAGCCAGGAUUUAAGAGUUUUAGAGCUAGAAAUAGCAAGUUAAAAUAAGGCUAGUCGGUUAUCAACUUGAAAAAGUGGCACGGAGUCGGUGGUUUU-3’	designer sgRNA
sg-HBEGF	5’-GGGUUCUCUCGGCACUGGUGACGUUUUAGAGCUAGAAAUAGCAAGUUAAAAUAAGGCUAGUCCGUUAUCAACUUGAAAAAGUGGCACCGAGUCGGUGCUUUU-3’	sgRNA
sg-HBEGF-S1a	5’-GGGUUCUCUCGGCACUGGUGACGUUUUAGAGCUAGAAAUAGCAAGUUAAAAUAAGGCUAGUCGGUUAUCAACUUGAAAAAGUGGCACCGAGUCGGUGCUUUU-3’	designer sgRNA
sg-HBEGF-S1b	5’-GGGUUCUCUCGGCACUGGUGACGUUUUAGAGCUAGAAAUAGCAAGUUAAAAUAAGGCUAGUCCGUUAUCAACUUGAAAAAGUGGCACGGAGUCGGUGCUUUU-3’	designer sgRNA
sg-HBEGF-S1c	5’-GGGUUCUCUCGGCACUGGUGACGUUUUAGAGCUAGAAAUAGCAAGUUAAAAUAAGGCUAGUCCGUUAUCAACUUGAAAAAGUGGCACCGAGUCGGUGGUUUU-3’	designer sgRNA
sg-HBEGF-S2a	5’-GGGUUCUCUCGGCACUGGUGACGUUUUAGAGCUAGAAAUAGCAAGUUAAAAUAAGGCUAGUCGGUUAUCAACUUGAAAAAGUGGCACGGAGUCGGUGCUUUU-3’	designer sgRNA
sg-HBEGF-S2b	5’-GGGUUCUCUCGGCACUGGUGACGUUUUAGAGCUAGAAAUAGCAAGUUAAAAUAAGGCUAGUCGGUUAUCAACUUGAAAAAGUGGCACCGAGUCGGUGGUUUU-3’	designer sgRNA
sg-HBEGF-S2c	5’-GGGUUCUCUCGGCACUGGUGACGUUUUAGAGCUAGAAAUAGCAAGUUAAAAUAAGGCUAGUCCGUUAUCAACUUGAAAAAGUGGCACGGAGUCGGUGGUUUU-3’	designer sgRNA

sg-HBEGF-S3	5’-GGGUUCUCUCGGCACUGGUGACGUUUUAGAGCUAGAAAUAGCAAGUUAAAAUAAGGCUAGUCGGUUAUCAACUUGAAAAAGUGGCACGGAGUCGGUGGUUUU-3’	designer sgRNA
sg-GFP	5’-GGGAUGCCGUUCUUCUGCUUGUGUUUUAGAGCUAGAAAUAGCAAGUUAAAAUAAGGCUAGUCCGUUAUCAACUUGAAAAAGUGGCACCGAGUCGGUGCUUUU-3’	sgRNA
sg-GFP-S1a	5’-GGGAUGCCGUUCUUCUGCUUGUGUUUUAGAGCUAGAAAUAGCAAGUUAAAAUAAGGCUAGUCGGUUAUCAACUUGAAAAAGUGGCACCGAGUCGGUGCUUUU-3’	designer sgRNA
sg-GFP-S1b	5’-GGGAUGCCGUUCUUCUGCUUGUGUUUUAGAGCUAGAAAUAGCAAGUUAAAAUAAGGCUAGUCCGUUAUCAACUUGAAAAAGUGGCACGGAGUCGGUGCUUUU-3’	designer sgRNA
sg-GFP-S1c	5’-GGGAUGCCGUUCUUCUGCUUGUGUUUUAGAGCUAGAAAUAGCAAGUUAAAAUAAGGCUAGUCCGUUAUCAACUUGAAAAAGUGGCACCGAGUCGGUGGUUUU-3’	designer sgRNA
sg-GFP-S2a	5’-GGGAUGCCGUUCUUCUGCUUGUGUUUUAGAGCUAGAAAUAGCAAGUUAAAAUAAGGCUAGUCGGUUAUCAACUUGAAAAAGUGGCACGGAGUCGGUGCUUUU-3’	designer sgRNA
sg-GFP-S2b	5’-GGGAUGCCGUUCUUCUGCUUGUGUUUUAGAGCUAGAAAUAGCAAGUUAAAAUAAGGCUAGUCGGUUAUCAACUUGAAAAAGUGGCACCGAGUCGGUGGUUUU-3’	designer sgRNA
sg-GFP-S2c	5’-GGGAUGCCGUUCUUCUGCUUGUGUUUUAGAGCUAGAAAUAGCAAGUUAAAAUAAGGCUAGUCCGUUAUCAACUUGAAAAAGUGGCACGGAGUCGGUGGUUUU-3’	designer sgRNA
sg-GFP-S3	5’-GGGAUGCCGUUCUUCUGCUUGUGUUUUAGAGCUAGAAAUAGCAAGUUAAAAUAAGGCUAGUCGGUUAUCAACUUGAAAAAGUGGCACGGAGUCGGUGGUUUU-3’	designer sgRNA
tracrRNA-F	5’-TCTAATACGACTCACTATAGGGTTGGAACCATTCAAAACAGCATAGCAAGTTAAAATAAGGCTAG-3’	Forward primer for each tracrRNA construct
tracrRNA-R	5’-AAAAAAAGCACCGACTCGGTGCCACTTTTTCAAGTTGATAACGGACTAGCCTTATTTTAACTTGCT-3’	Reverse primer for original tracrRNA construct

tracrRNA-S1a-R	5’-AAAAAAAGCACCGACTCGGTGCCACTTTTTCAAGTTGATAACCGACTAGCCTTATTTTAACTTGCT-3’	Reverse primer for tracrRNA-S1a construct
tracrRNA-S1b-R	5’-AAAAAAAGCACCGACTCCGTGCCACTTTTTCAAGTTGATAACGGACTAGCCTTATTTTAACTTGCT-3’	Reverse primer for tracrRNA-S1b construct
tracrRNA-S1c-R	5’-AAAAAAACCACCGACTCGGTGCCACTTTTTCAAGTTGATAACGGACTAGCCTTATTTTAACTTGCT-3’	Reverse primer for tracrRNA-S1c construct
tracrRNA-S2a-R	5’-AAAAAAAGCACCGACTCCGTGCCACTTTTTCAAGTTGATAACCGACTAGCCTTATTTTAACTTGCT-3’	Reverse primer for tracrRNA-S2a construct
tracrRNA-S2b-R	5’-AAAAAAACCACCGACTCGGTGCCACTTTTTCAAGTTGATAACCGACTAGCCTTATTTTAACTTGCT-3’	Reverse primer for tracrRNA-S2b construct
tracrRNA-S2c-R	5’-AAAAAAACCACCGACTCCGTGCCACTTTTTCAAGTTGATAACGGACTAGCCTTATTTTAACTTGCT-3’	Reverse primer for tracrRNA-S2c construct
tracrRNA-S3-R	5’-AAAAAAACCACCGACTCCGTGCCACTTTTTCAAGTTGATAACCGACTAGCCTTATTTTAACTTGCT-3’	Reverse primer for tracrRNA-S3 construct
tracrRNA	5’-GGGUUGGAACCAUUCAAAACAGCAUAGCAAGUUAAAAUAAGGCUAGUCCGUUAUCAACUUGAAAAAGUGGCACCGAGUCGGUGCUUUUUUU-3’	original tracrRNA
tracrRNA-S1a	5’-GGGUUGGAACCAUUCAAAACAGCAUAGCAAGUUAAAAUAAGGCUAGUCGGUUAUCAACUUGAAAAAGUGGCACCGAGUCGGUGCUUUUUUU-3’	designer tracrRNA
tracrRNA-S1b	5’-GGGUUGGAACCAUUCAAAACAGCAUAGCAAGUUAAAAUAAGGCUAGUCCGUUAUCAACUUGAAAAAGUGGCACGGAGUCGGUGCUUUUUUU-3’	designer tracrRNA
tracrRNA-S1c	5’-GGGUUGGAACCAUUCAAAACAGCAUAGCAAGUUAAAAUAAGGCUAGUCCGUUAUCAACUUGAAAAAGUGGCACCGAGUCGGUGGUUUUUUU-3’	designer tracrRNA
tracrRNA-S2a	5’-GGGUUGGAACCAUUCAAAACAGCAUAGCAAGUUAAAAUAAGGCUAGUCGGUUAUCAACUUGAAAAAGUGGCACGGAGUCGGUGCUUUUUUU-3’	designer tracrRNA
tracrRNA-S2b	5’-GGGUUGGAACCAUUCAAAACAGCAUAGCAAGUUAAAAUAAGGCUAGUCGGUUAUCAACUUGAAAAAGUGGCACCGAGUCGGUGGUUUUUUU-3’	designer tracrRNA
tracrRNA-S2c	5’-GGGUUGGAACCAUUCAAAACAGCAUAGCAAGUUAAAAUAAGGCUAGUCCGUUAUCAACUUGAAAAAGUGGCACGGAGUCGGUGGUUUUUUU-3’	designer tracrRNA
tracrRNA-S3	5’-GGGUUGGAACCAUUCAAAACAGCAUAGCAAGUUAAAAUAAGGCUAGUCGGUUAUCAACUUGAAAAAGUGGCACGGAGUCGGUGGUUUUUUU-3’	designer tracrRNA

crSLX4IP	5’-GGGCCACAGCCAGGAUUUAAGAGUUUUAGAGCUAUGCUGUUUUG-3’	crRNA
crHPRT1	5’-GGGCCCAAGGAAAGACUAUGAAAGUUUUAGAGCUAUGCUGUUUUG-3’	crRNA
crGFP	5’-GGGAUGCCGUUCUUCUGCUUGUGUUUUAGAGCUAUGCUGUUUUG-3’	crRNA
crHBEGF	5’-GGGUUCUCUCGGCACUGGUGACGUUUUAGAGCUAUGCUGUUUUG-3’	crRNA
S2c-up-F	5’-CTTTTGCTGGCCTTTTGCTCA-3’	For preparation of designer plasmid with MBL-binding units
S2c-up-R	5’-CAAAAAACCACCGACTCCGTGCCACTTTTTCAAGTTGATAACG-3’	
S2c-down-F	5’-AAAAAGTGGCACGGAGTCGGTGGTTTTTTGTTTTAGAGCTAG-3’	
S2c-down-R	5’-TGGTAATAGCGATGACTAATAC-3’	
t-HPRT1-F	5’-GTTGTGATAAAAGGTGATGCTC-3’	For PCR of t-HPRT1
t-HPRT1-R	5’-TCATAAACACATCCATGGGAC-3’	
t-SLX4IP-F	5’-TTATCCGGCACTGTGAAAGCT-3’	For PCR of t-SLX4IP
t-SLX4IP-R	5’-CCTGATGTTTAGCAACTTTTTGG-3’	
t-GFP-F	5’-GAGGAGCTGTTCACCGGG-3’	For PCR of t-GFP
t-GFP-R	5’-CTTGTACAGCTCGTCCATGC-3’	
t-HBEGF-F	5’-GCCGCTTCGAAAGTGACTGG-3’	For PCR of t-HBEGF
t-HBEGF-R	5’-GATCCCCCAGTGCCCATCAG-3’	
oligo-SLX4IP-F	5’-CACCGCCACAGCCAGGATTTAAGA-3’	target sequences used in the all-in-one plasmid assay
oligo-SLX4IP-R	5’-AAACTCTTAAATCCTGGCTGTGGC-3’	
oligo-HBEGF-F	5’-CACCGTTCTCTCGGCACTGGTGAC-3’	target sequences used in the all-in-one plasmid assay
oligo-HBEGF-R	5’-AAACGTCACCAGTGCCGAGAGAAC-3’	

Appendix A: NMR spectra copies of the selected synthesized compounds

This section contains the NMR spectra of the selected synthesized compounds. For each compound, the spectra are shown in the following order: ^{1}H NMR and ^{13}C NMR. The chemical structure of the compound is drawn on each spectrum.

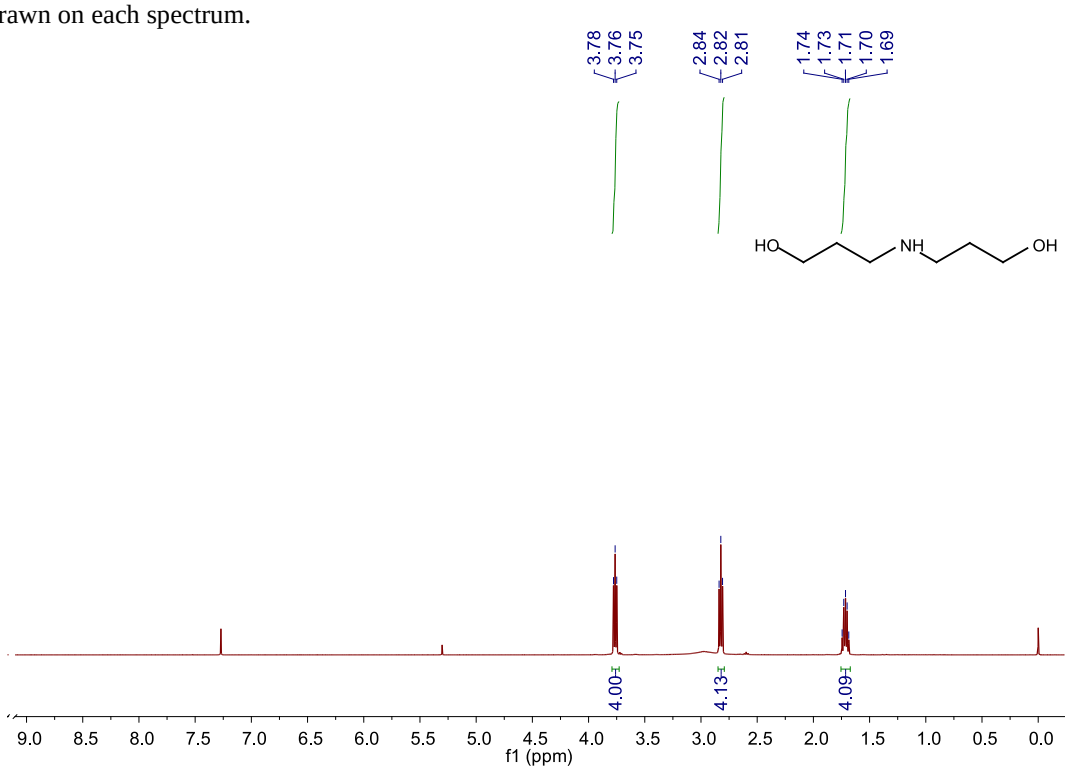

^{1}H NMR spectrum of compound **2** in $CDCl_3$

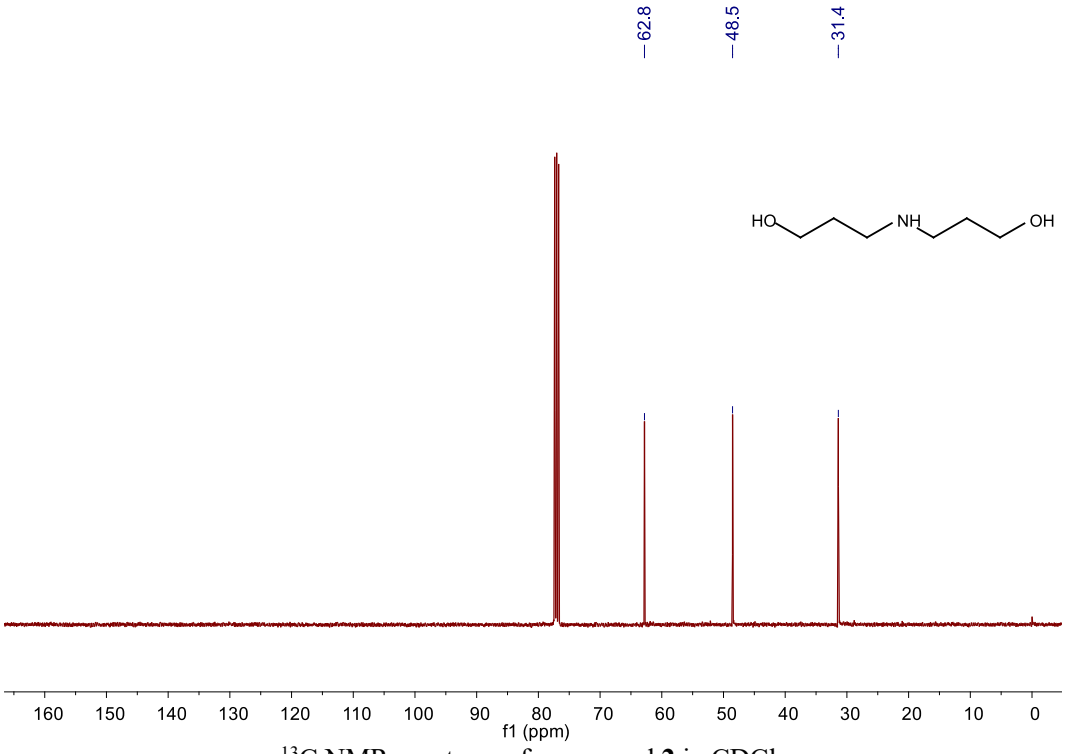

^{13}C NMR spectrum of compound **2** in $CDCl_3$

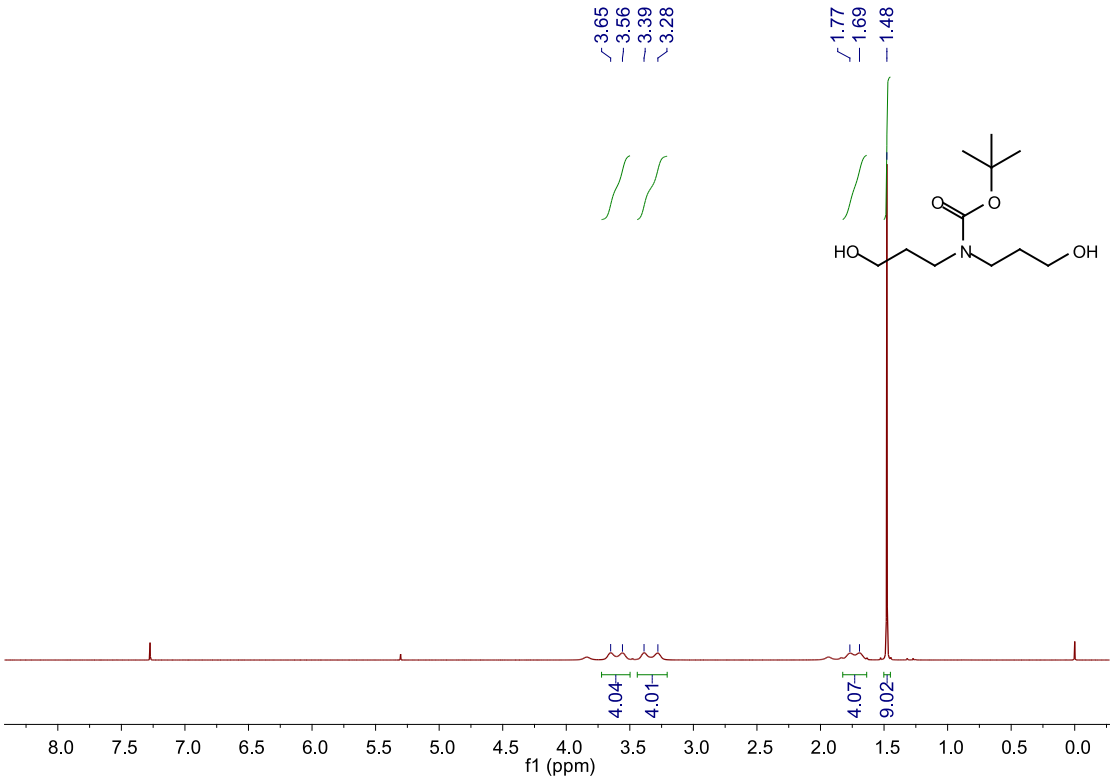

^{1}H NMR spectrum of compound **3** in $CDCl_3$

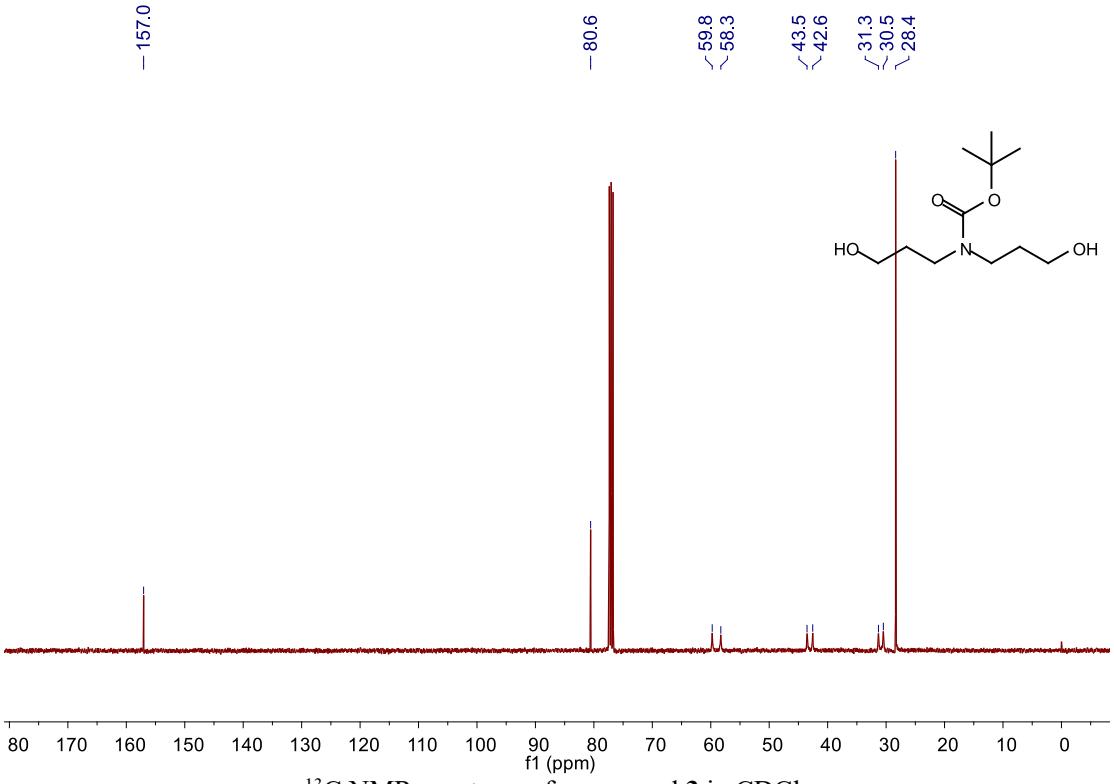

^{13}C NMR spectrum of compound **3** in $CDCl_3$

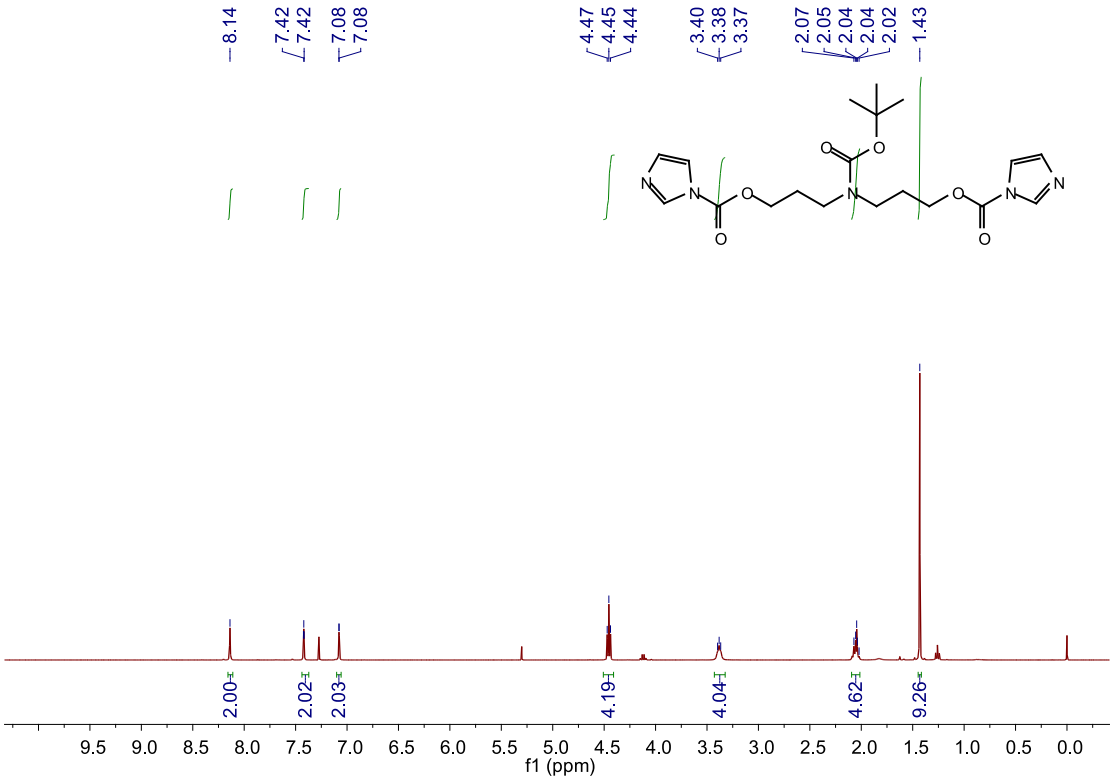

^{1}H NMR spectrum of compound **4** in $CDCl_3$

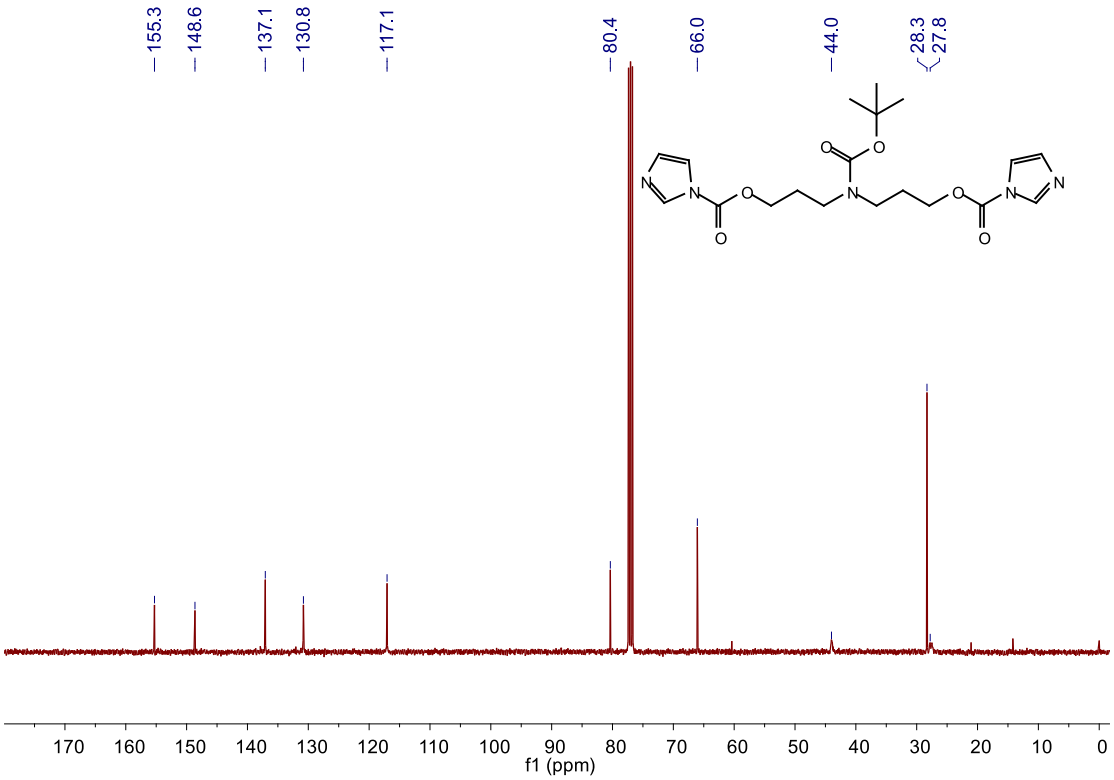

^{13}C NMR spectrum of compound **4** in $CDCl_3$

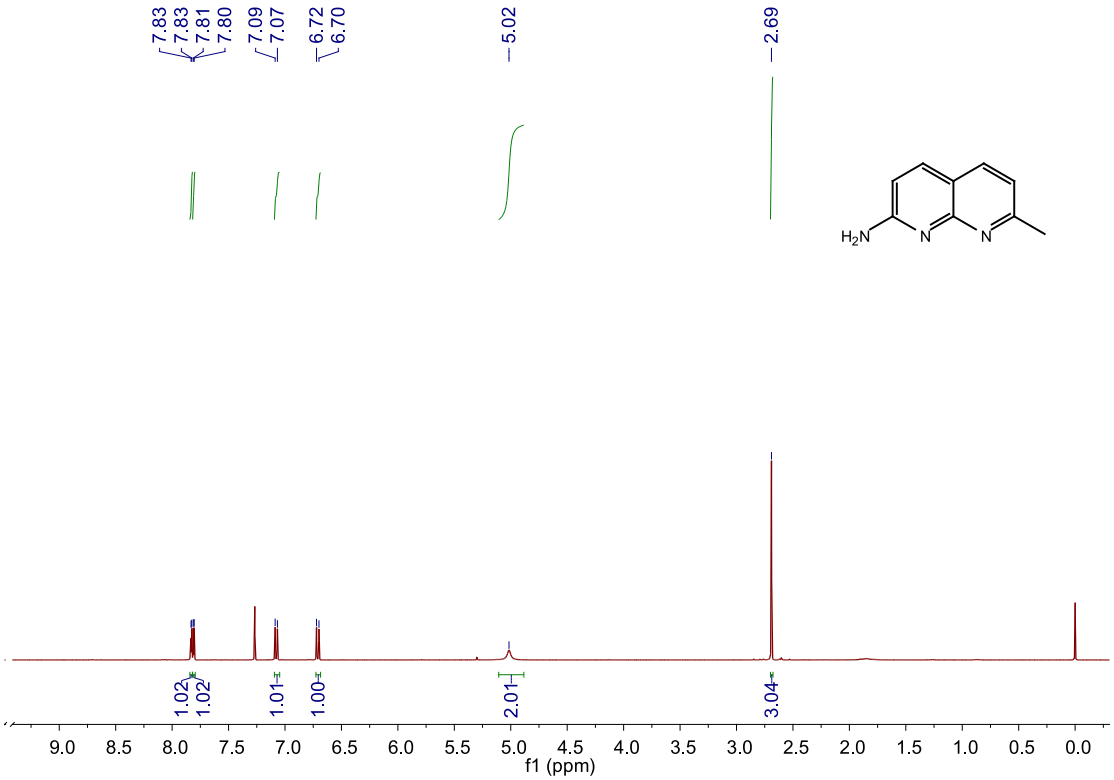

^{1}H NMR spectrum of compound **6** in $CDCl_3$

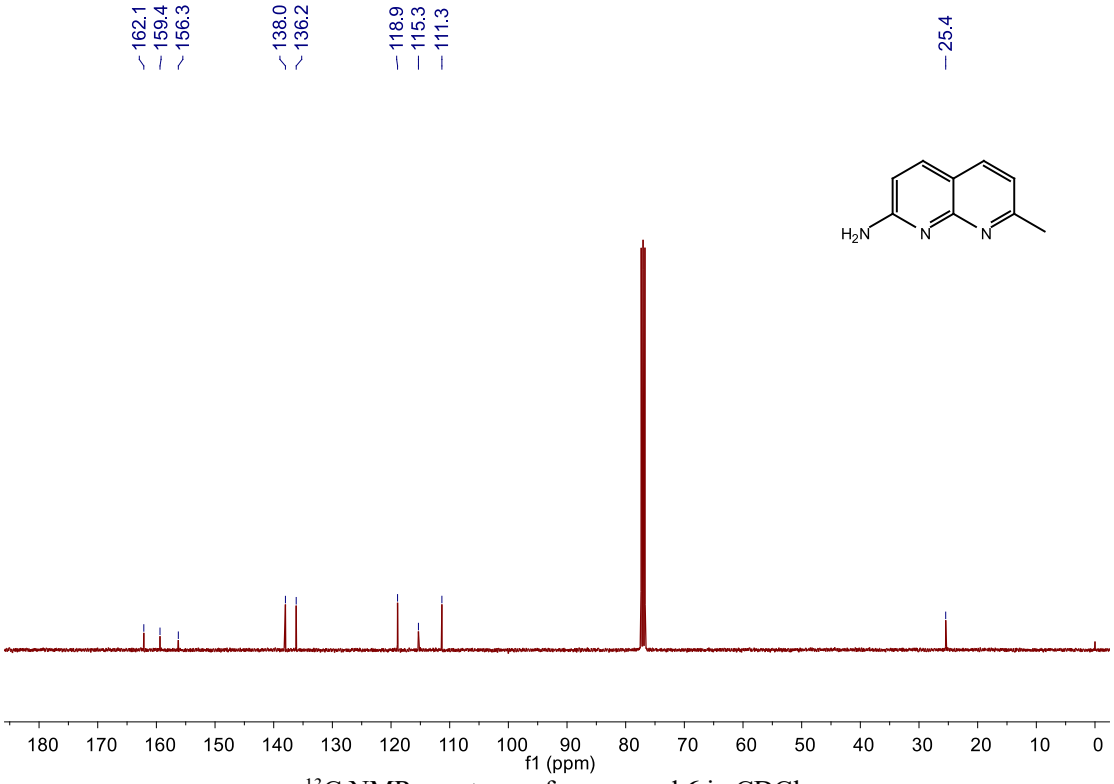

^{13}C NMR spectrum of compound **6** in $CDCl_3$

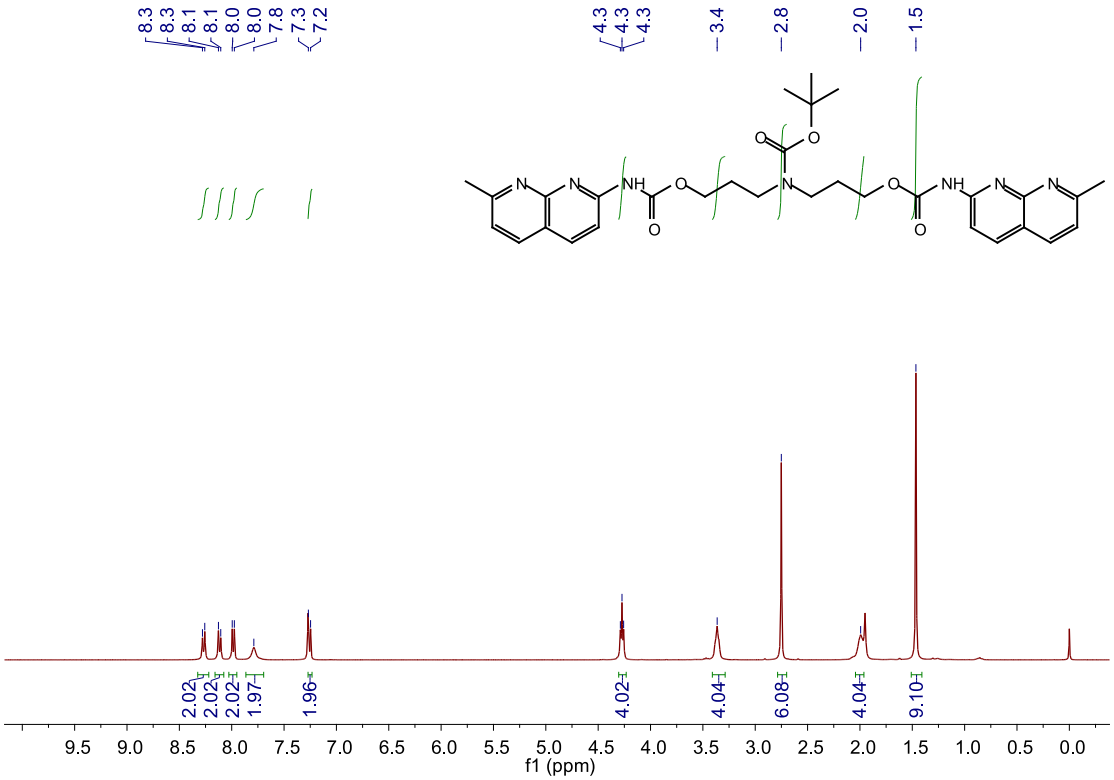

^{1}H NMR spectrum of compound **7** in $CDCl_3$

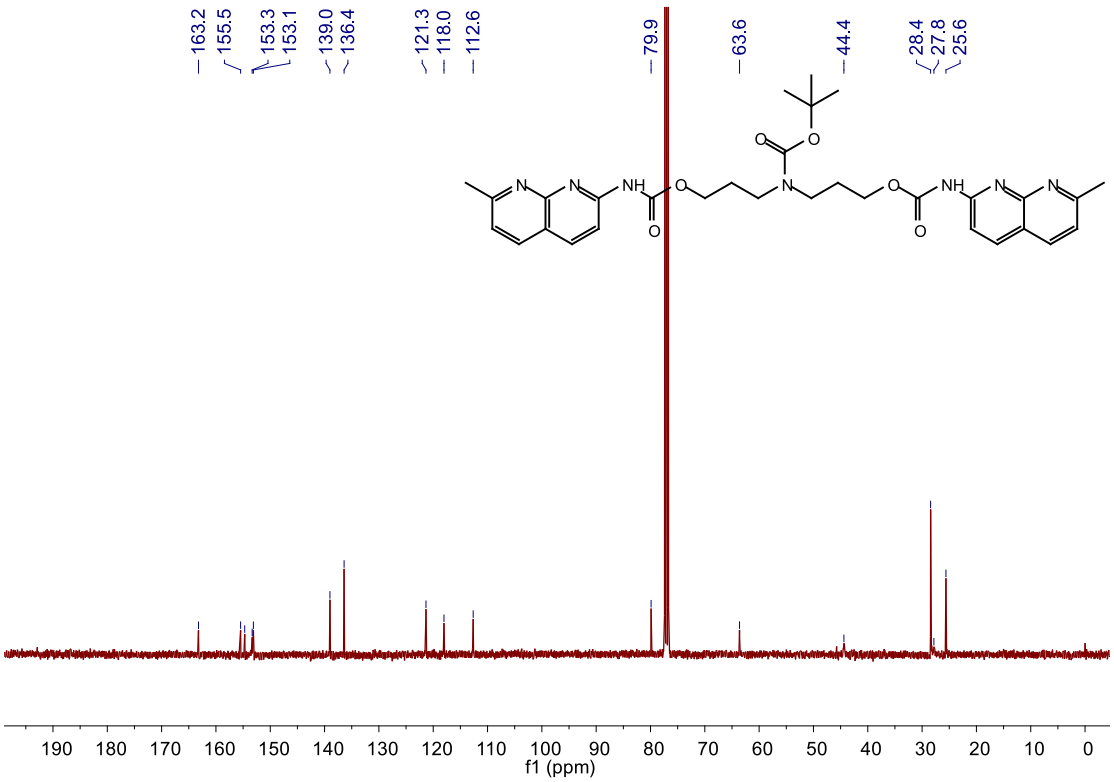

^{13}C NMR spectrum of compound **7** in $CDCl_3$

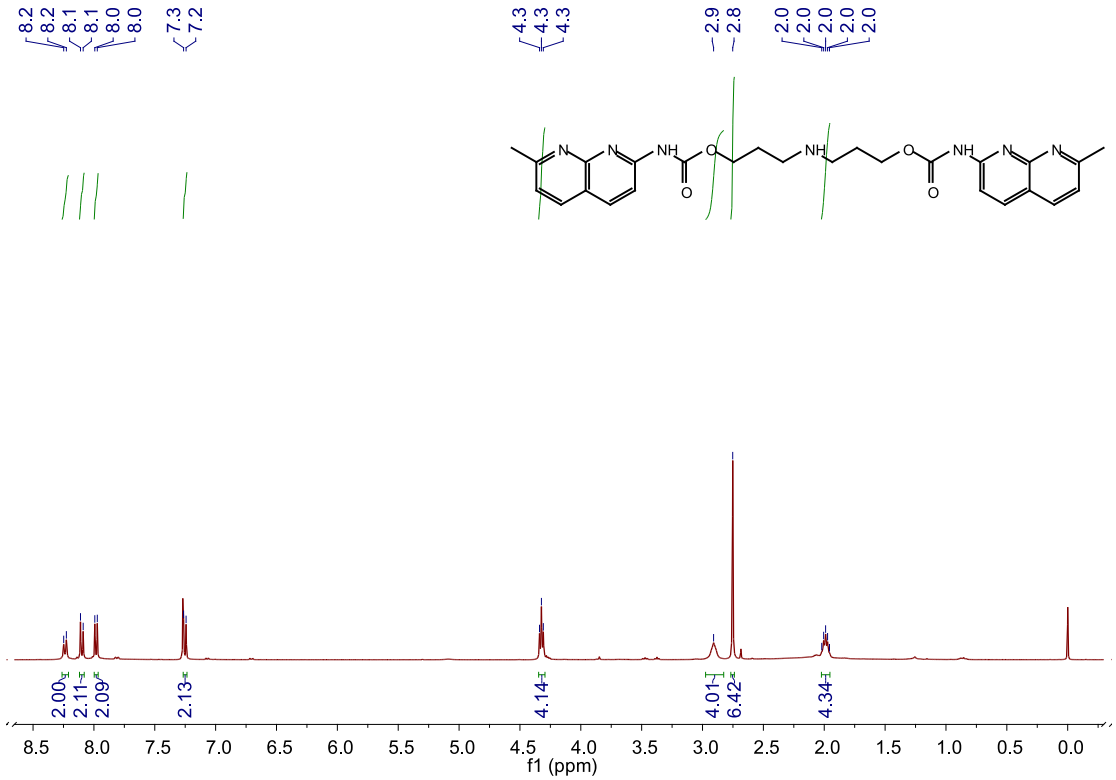

^{1}H NMR spectrum of **NCD** in $CDCl_3$

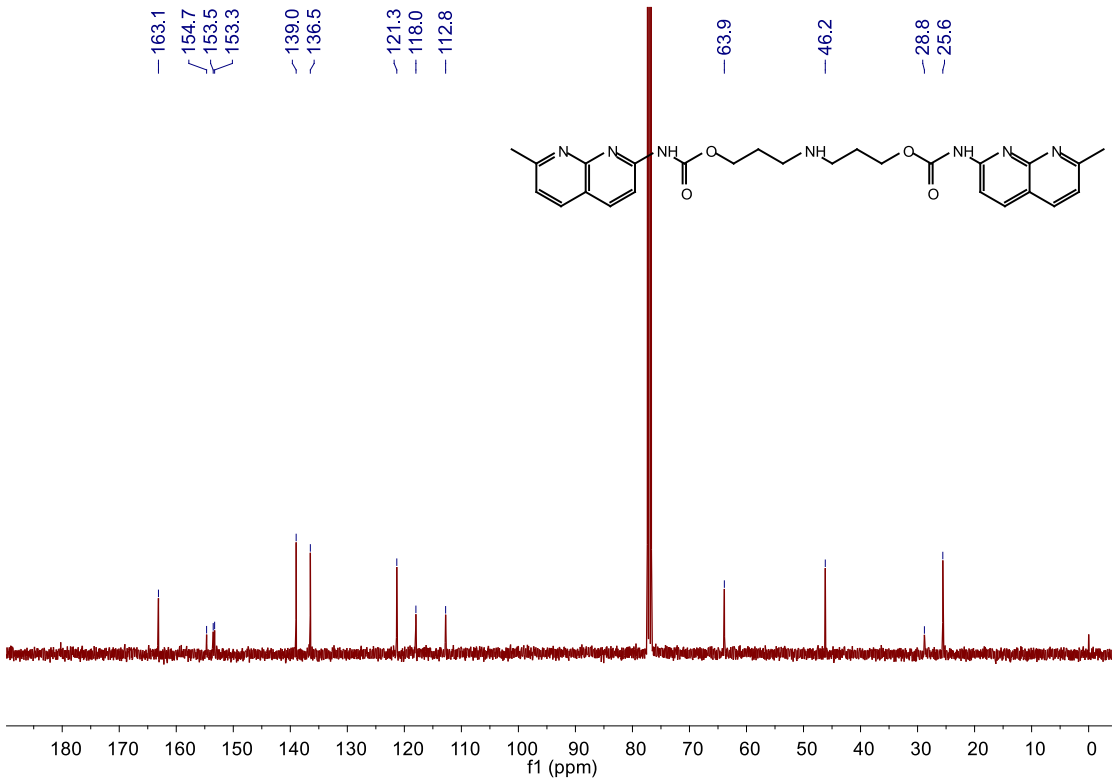

^{13}C NMR spectrum of **NCD** in $CDCl_3$

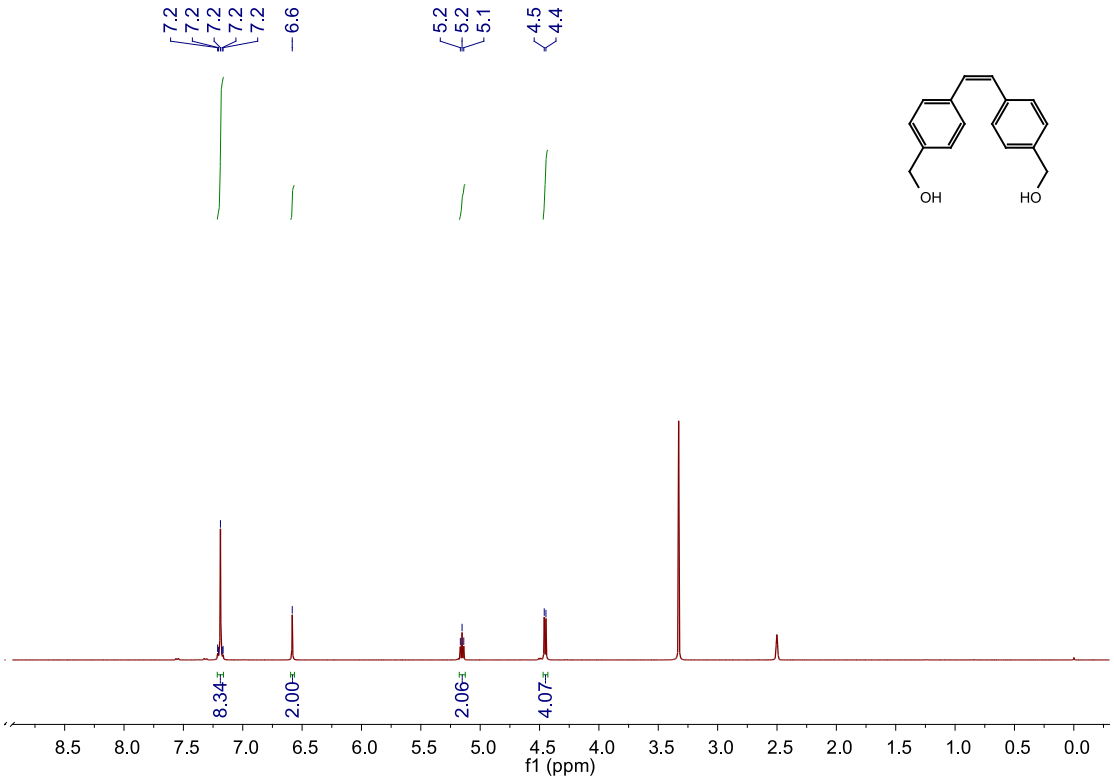

^{1}H NMR spectrum of compound **9** in $CDCl_3$

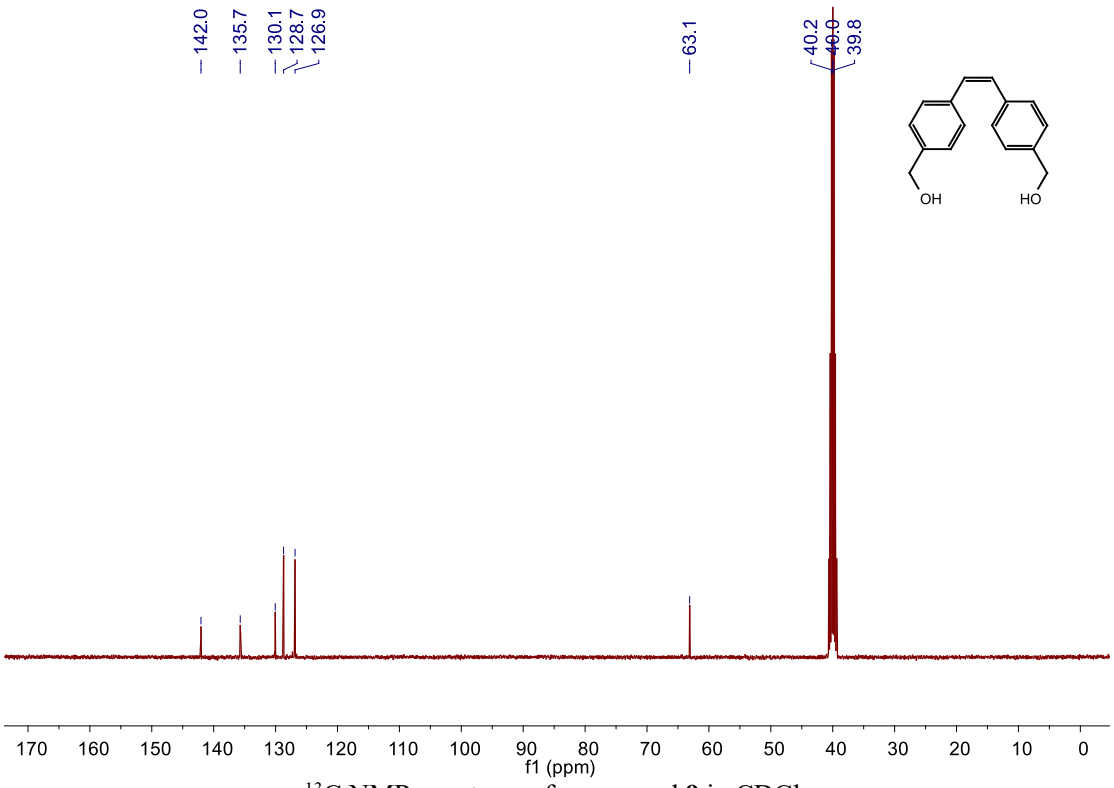

^{13}C NMR spectrum of compound **9** in $CDCl_3$

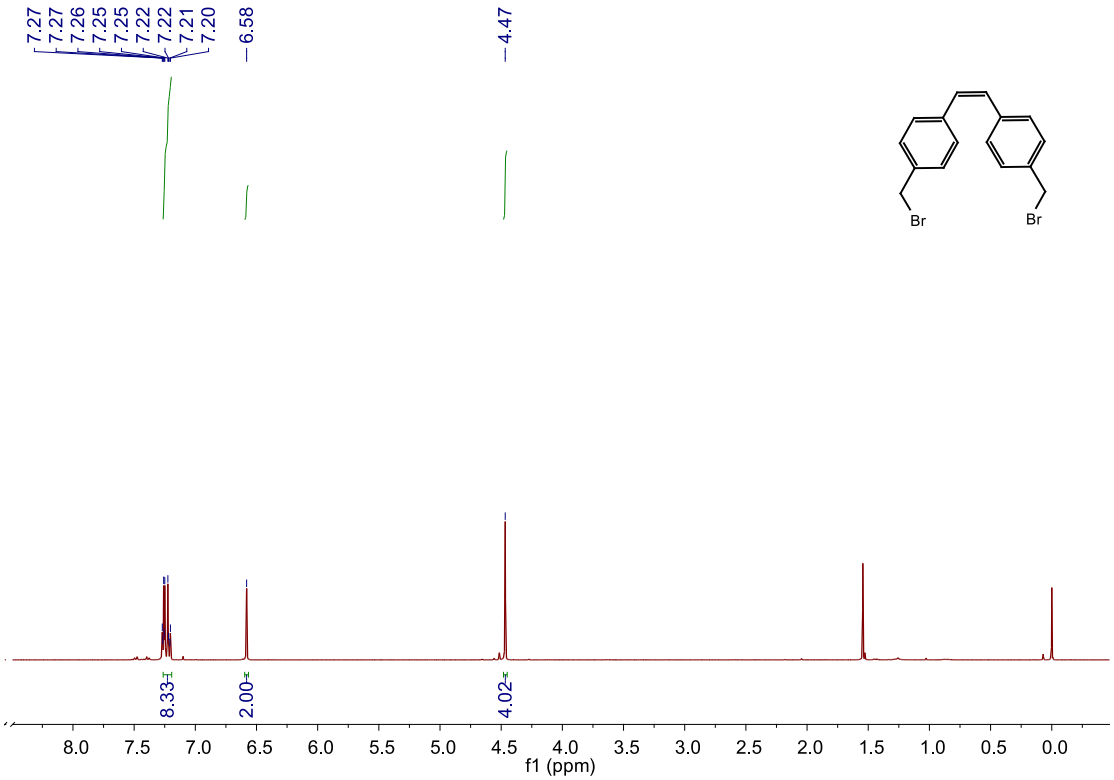

^{1}H NMR spectrum of compound **10** in $CDCl_3$

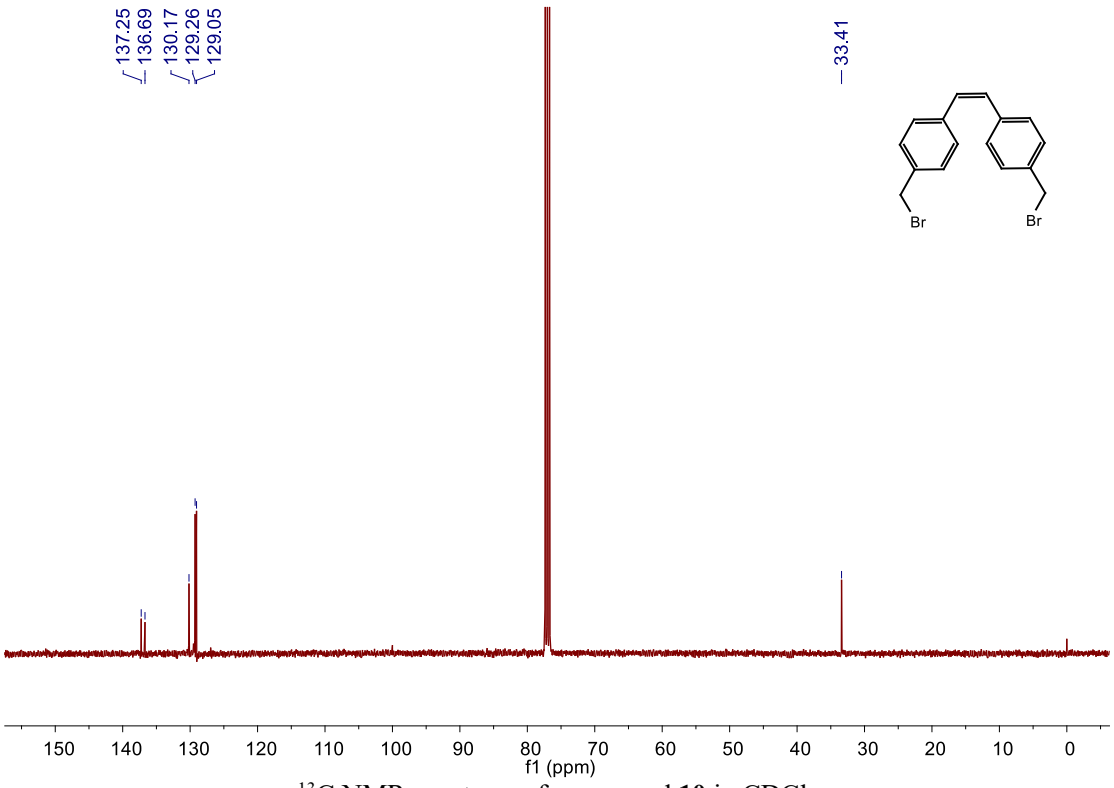

^{13}C NMR spectrum of compound **10** in $CDCl_3$

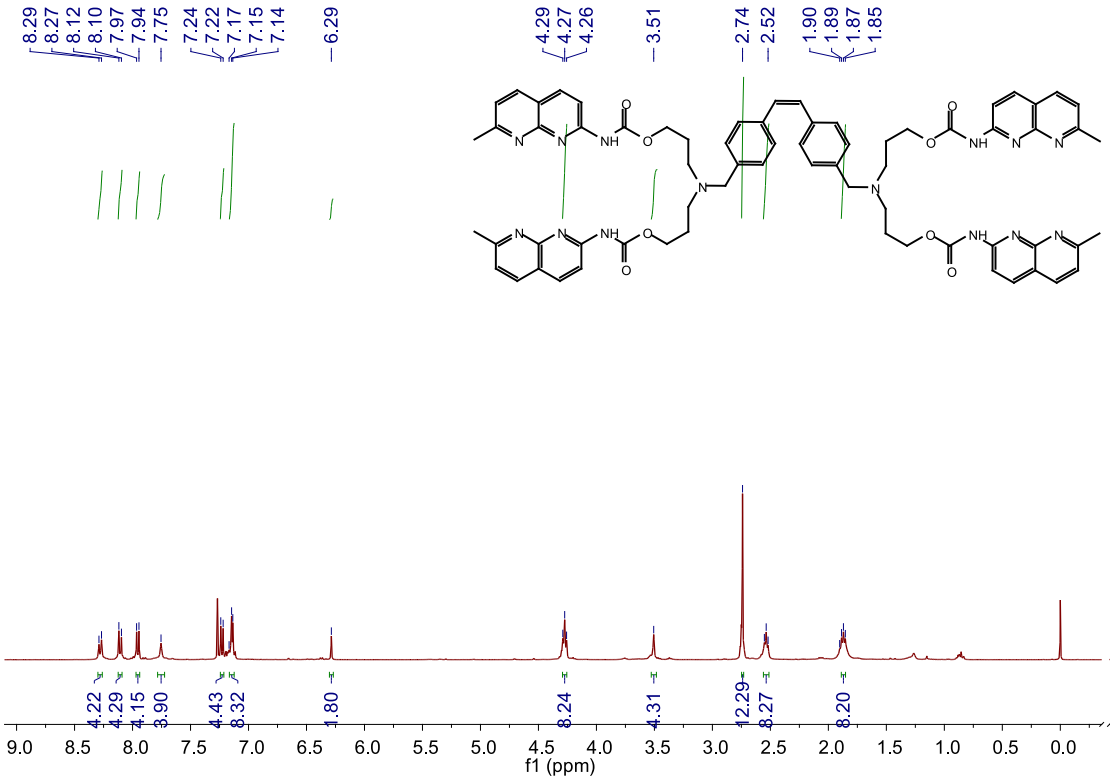

^{1}H NMR spectrum of ***Z*-NCTS** in $CDCl_3$

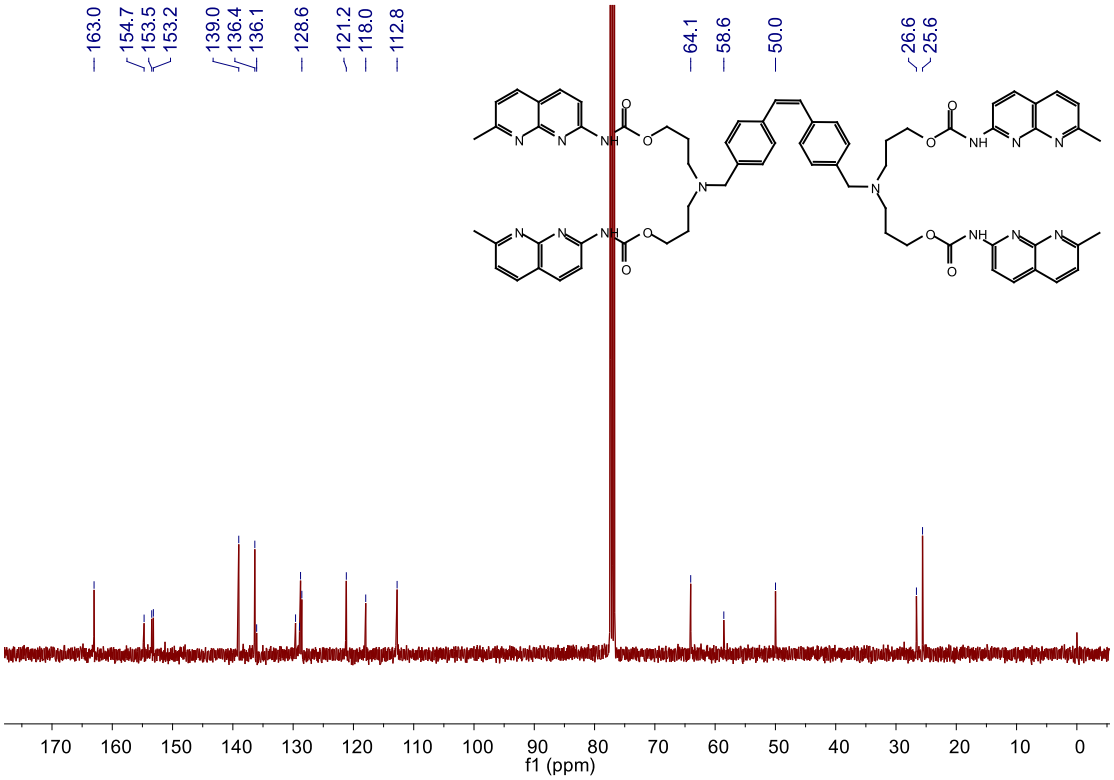

^{13}C NMR spectrum of ***Z*-NCTS** in $CDCl_3$

Appendix B: HRMS spectral copies of the used compounds in the current study

This section contains the HRMS spectra of the used compounds in this study. The chemical structure of the compound is drawn on each spectrum.

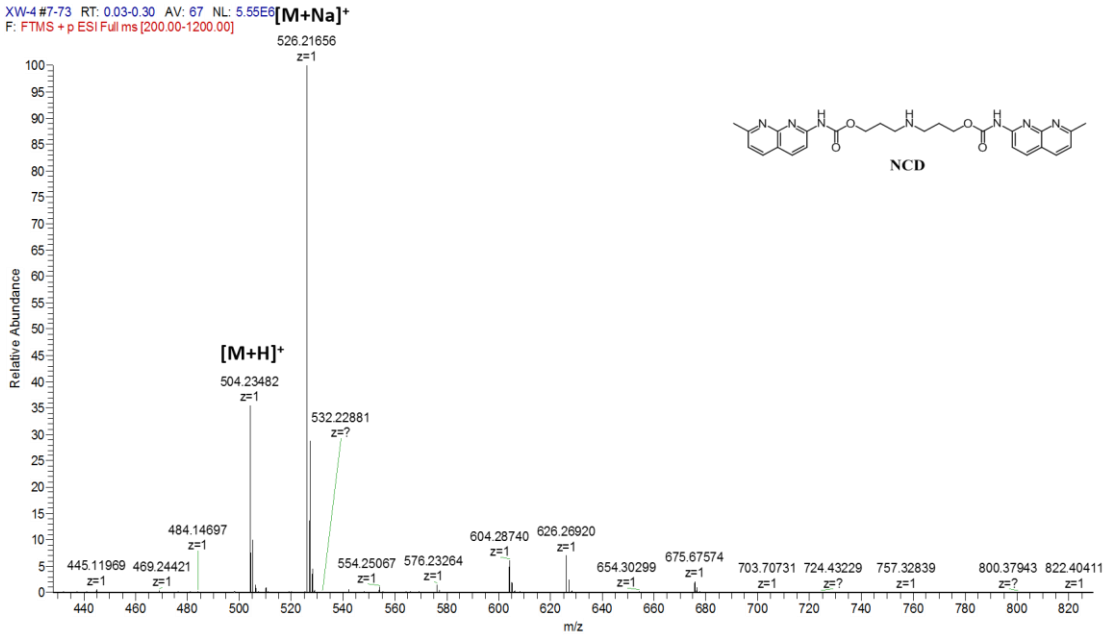

HRMS spectrum of **NCD**

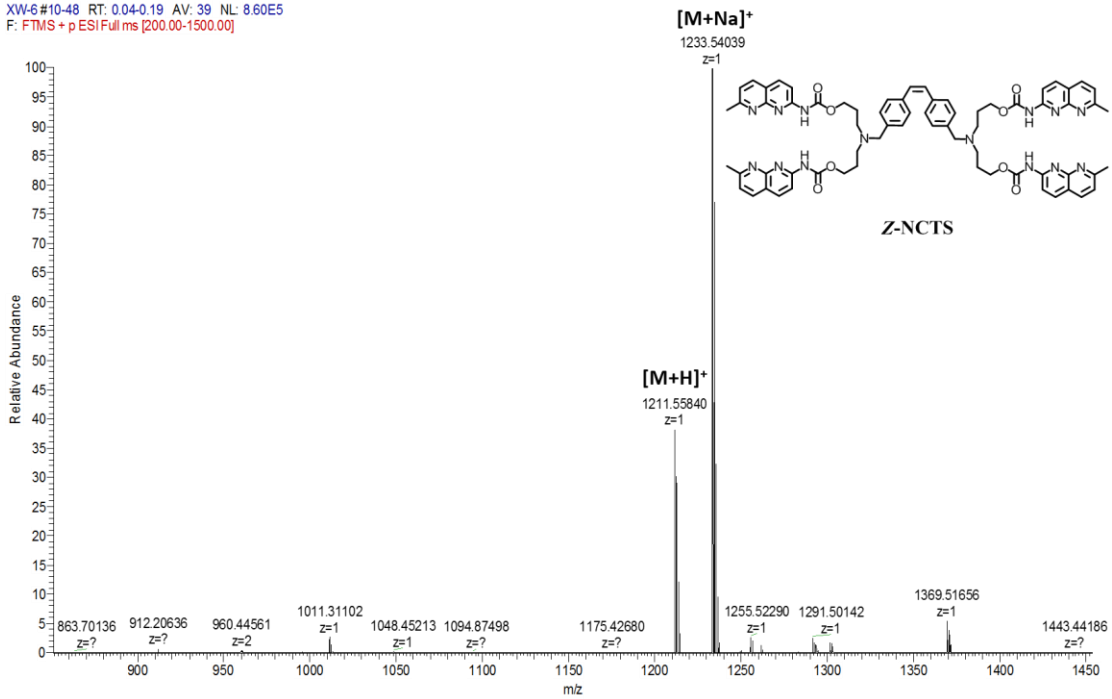

HRMS spectrum of ***Z*-NCTS**

SI References

1. Chen, S., *et al.* Dithiol amino acids can structurally shape and enhance the ligand-binding properties of polypeptides. *Nat Chem* **6**, 1009-1016 (2014).
2. Berbeci, L.S., Wang, W. & Kaifer, A.E. Drastically decreased reactivity of thiols and disulfides complexed by cucurbit[6]uril. *Org Lett* **10**, 3721-3724 (2008).
3. Pellizzaro, M.L., *et al.* Conformer-independent ureidoimidazole motifs--tools to probe conformational and tautomeric effects on the molecular recognition of triply hydrogen-bonded heterodimers. *Chemistry* **17**, 14508-14517 (2011).
4. Xu, Y., Smith, M.D., Krause, J.A. & Shimizu, L.S. Control of the intramolecular [2+2] photocycloaddition in a bis-stilbene macrocycle. *J Org Chem* **74**, 4874-4877 (2009).
5. Dohno, C., Kohyama, I., Hong, C. & Nakatani, K. Naphthyridine tetramer with a pre-organized structure for 1:1 binding to a CGG/CGG sequence. *Nucleic Acids Res* **40**, 2771-2781 (2012).
6. Zhou, Y., *et al.* High-throughput screening of a CRISPR/Cas9 library for functional genomics in human cells. *Nature* **509**, 487-491 (2014).